Fisheries Centre Research Reports

2008 Volume 16 Number 3

Modelling Present and Climate-Shifted Distribution of Marine Fishes and Invertebrates

Fisheries Centre, University of British Columbia, Canada

Modelling Present and Climate-Shifted Distribution of Marine Fishes and Invertebrates

edited by
William W. L. Cheung, Vicky W.Y. Lam and Daniel Pauly

MODELLING PRESENT AND CLIMATE-SHIFTED DISTRIBUTION OF MARINE FISHES AND INVERTEBRATES

edited by
William W. L. Cheung, Vicky W.Y. Lam and Daniel Pauly

CONTENTS

Page

CHAPTER 3   **ASYMMETRY IN LATITUDINAL, LONGITUDINAL AND BATHYMETRIC DISTRIBUTION OF MARINE FISHES AND INVERTEBRATES**

Daniel Pauly, William W. L. Cheung, Chris Close, Sally Hodgson, Vicky W.Y. Lam and Reg Watson

DIRECTOR'S FOREWORD

This report is the first publication of the *Sea Around Us* Project focusing on global warming and its effects on marine fisheries. It is therefore a report on methodology: we had to first develop methodological approaches before results could be presented.

The first contribution in this report describes a new approach and software for simulating the widely documented poleward movement of marine fishes and invertebrates in response to warming oceans. The software for simulating these movements implements a model, largely driven by the temperature changes predicted for the next decades by coupled atmosphere-ocean models, which considers a moderately large number of processes (reproduction, survival, migration, etc.) and features of the organisms in question (affinities to certain habitats, depth ranges, etc.). However, the model was designed such that it would be straightforward to parameterize, at least for 1,500+ species and higher taxa used by the Food and Agriculture Organization of the United Nations (FAO) to reports on global marine fisheries statistics, and for all of which the *Sea Around Us* Project has basic information, including detailed distribution range maps.

Thus, the first paper in this report will serve a starting point for several planned articles on global warming effects on marine communities and fisheries, with the model at its core being gradually modified and improved as applications are completed.

The second and third contributions in this report deal with the distribution range maps of marine taxa used by the model in the first. Thus, they propose a number of simple adjustments which help take seasonality and other modifying factors into account, both when generating present distribution range maps, and when shifting them poleward using the model mentioned above.

The projections that we hope to generate, using these data and models, will obviously not be the last word on the poleward migration of marine fishes and invertebrates. However, because they cover a set of globally important species, they will enable the *Sea Around Us* Project to contribute in a major way to debates on the possible impacts of global warming on marine fisheries and biodiversity, a key environmental issue for the next decades.

Daniel Pauly
Director, UBC Fisheries Centre
4 January 2008

ACKNOWLEDGEMENTS

LIST OF ACRONYMS

Acronym or variable	Definition or description (dimension)
A_i	Relative abundance in cell i
a	Southern boundary of the annual and winter distribution range (coordinate)
AS	Actual shift in the distribution range
$AvgS$	Latitudinal shift of centroid in summer (distance)
$AvgS'$	Latitudinal shift of centroid in winter (distance)
b	Southern boundary of the summer distribution range (coordinate)
c'	Constant for calculating the intrinsic rate of population increase
c	Centroid of the annual distribution range (coordinate)
C (Annual)	Latitudinal position of the centroid of species' annual average relative distribution (coordinate)
$CA_{i,t}$	Absolute coral abundance at grid cell (30' x 30') i and time (year) t (Area)
CM2.1	Coupled Model, version 2.1
C_s'	Latitudinal position of the centroid of species' summer distribution (coordinate)
C_w'	Latitudinal position of the centroid of species' winter distribution (coordinate)
CS'	Actual shift in centroid of the distribution range (distance)
CS_s'	Maximum potential shift in centroid's latitudinal positions in summer (distance)
CS_w'	Maximum potential shift in centroid's latitudinal positions in winter (distance)
D	Diffusion coefficient
d	Northern boundary of the winter distribution range (coordinate)
DS	Ratio of future to current habitat suitability
Dep	Depth (length)
$Dist_{ij}$	Distance between two adjacent cells (length)
DM	The Developmental type of larvae
e	Northern boundary of the annual and summer distribution range (coordinate)
E	Emigration of animals from a cell (relative abundance)
Er	Radius of the Earth (length)
G	Intrinsic population growth (time^{-1})
GFDL	Geophysical Fluid Dynamics Laboratory
GR	Minimum grid resolution (length)
H	Habitat types
I	Net adult migration (relative abundance)
Ice	Sea ice coverage (Area)
I_{ji}	Net migrated adults at cell i from surrounding cells j (relative abundance)
K	Von Bertalanffy growth parameter (time^{-1})
k	Scaling factor representing the sensitivity of the calculated emigration rate to changes in environmental suitability
KC_i	Population carrying capacity at cell i (relative abundance)
KR	Carrying capacity ratio of the destination cell
Lat	Latitude (coordinate)
Lav	Larval abundance (relative abundance)
LC	Latitude at the centre of the grid cell i where the specific area of coral occurs (coordinate)
L	Settled larvae at cell i from surrounding cells j (relative abundance)
L^U	Upper latitudinal limit (coordinate)
L^L	Lower latitudinal limit (coordinate)
Lon	Longitude (coordinate)
M	Natural mortality rate (time^{-1})
m_i	The instantaneous movement rate for randomly moving organisms to emigrate across each cell boundary (time^{-1})

LIST OF ACRONYMS (CON'T)

Acronym or variable	Definition or description (dimension)
$m_i^{(base)}$	Movement rate in the absence of any gradient (time^{-1})
MGSVA	Mariano Global Surface Velocity Analysis
MI	Motility Index
MP (Annual)	Latitudinal position of the mid-point of the annual distribution (coordinate)
MP_S	Mid-point between the centroid and the southern bound of the annual distribution (coordinate)
MP_W	Mid-point between the centroid and the northern bound of the annual distribution (coordinate)
MP_S'	Latitudinal position of the mid-point in summer (coordinate)
MP_W'	Latitudinal position of the mid-point in winter (coordinate)
$Mort_{i,t}$	Dispersed animals that die at cell i and time step t (relative abundance)
MS'	Actual shift in the latitudinal position of the mid-point (distance)
MS_s'	Maximum potential shift in the latitudinal position of the mid-point in summer (distance)
MS_w'	Maximum potential shift in the latitudinal position of the mid-point in winter
N or n	Number of spatial cells where the species occurs (count)
NL'	Latitude of the northern bound in winter (coordinate)
NL	Latitude of the original northern bound (coordinate)
NOAA	National Oceanic and Atmospheric Administration
P	Habitat suitability
PLD	Pelagic larval dispersal (time)
r	Intrinsic rate of population increase (time^{-1})
R	Rate of larval production (time^{-1})
RE	Rate of the re-entrance of the emigrated animals to the source cells (time^{-1})
S	Larval settlement rate (time^{-1})
Skew	Degree of skewness
SL'	Latitude of the southern bound in summer (coordinate)
SL	Latitude of the original southern bound (coordinate)
SST	Sea Surface Temperature (temperature)
T	Average water temperature in the animal's range (temperature)
TG	Function to calculate the temperature-gradient index at the upper and lower latitudinal limits
Ta	Optimal preferred temperature of a species (temperature)
TPP	Temperature Preference Profile
u	East-west current velocity (length time^{-1})
v	North-south current velocity (length time^{-1})
V_i	Adult dispersal rate (time^{-1})
W_{inf}	Asymptotic weight (weight)
x	Length of a cell (length)
δ^2	Standard deviation of the normal distribution function f
λ	Instantaneous rate of larval mortality and settlement (time^{-1})

CHAPTER 1

DYNAMIC BIOCLIMATE ENVELOPE MODEL TO PREDICT CLIMATE-INDUCED CHANGES IN DISTRIBUTION OF MARINE FISHES AND INVERTEBRATES[1]

William W. L. Cheung, Vicky W.Y. Lam and Daniel Pauly

Sea Around Us Project, Fisheries Centre, Aquatic Ecosystems Research Laboratory, 2202 Main Mall, The University of British Columbia, Vancouver, British Columbia, Canada. V6T 1Z4.

ABSTRACT

Global climate change is recognized as an important determining factor for the future distributions of marine organisms, notably fishes and invertebrates. Shifting of distribution range may affect global marine fisheries and have large socio-economic implications. However, global-scale evaluation of the impact of climate change on marine species is lacking. In this paper, we develop a dynamic bioclimate envelope model to predict the effect of climate change on the distributions of marine species with emphasis on commercially exploited fishes and invertebrates. First, the model infers, for various species, bioclimate envelopes based on their current distribution. Bioclimate envelopes are defined by sea water temperature, bathymetry, habitats and distance from sea ice. Secondly, the model predicts the shifting of the bioclimate envelopes induced by changes in climate variables. Simultaneously, following the shifting of the bioclimate envelopes, the model simulates movement of relative abundance through changes in population growth, mortality, larval dispersal and adult movement. We test the model with several commercially exploited fish species with widely different biogeography. The model provides reasonable and robust predictions of future distribution ranges of the four species under different scenarios of sea water warming. Moreover, the predictions are robust to major model assumptions and parameter uncertainty. Using realistic climate change predictions from the NOAA/GFDL Coupled Model, this model will be used to evaluate impacts of climate change on global marine fisheries.

INTRODUCTION

There is ample evidence from empirical observations and climate models indicating that mean global temperatures have been increasing over the last 100 years (IPCC 2007). Global temperature has increased by over 0.6 °C since 1900 and it may continue to increase at a rate of around 0.2 °C per decade (IPCC 2007). Biological responses to this change have been observed in both terrestrial and marine biomes (Murawski 1993; Hughes 2000; McCarty 2001; Parmesan & Yohe 2003; Perry *et al.* 2005; Hobday *et al.* 2006). The responses include changes in physiology (e.g. productivity), geographic range and phenology at population, species, community and ecosystem levels (Hughes 2000; McCarty 2001). For instance, nearly two-thirds of marine fishes in the North Sea shifted in mean latitude or depth or both over 25 years as sea temperature increased (Perry *et al.* 2005). During the last century, annual growth rates for the juveniles of eight long-lived fish species in the southwest Pacific increased in shallow waters and decreased in deep waters where ocean warming and cooling occurred, respectively (Thresher *et al* 2007). This agrees with the quantitative model of fish physiology, which predicts increasing growth performance and fecundity in higher latitude and the converse in lower latitude as sea

temperature increases (Pörtner *et al.* 2001). Moreover, global warming may increase extinction/extirpation risk of some populations and species (Pounds 2001; Thomas *et al.* 2004). It may also have large implications for communities and industries that depend on these marine species for food and income (Roessig 2004). Thus, predicting effects of climate change on marine species is important in understanding the overall impacts of such global changes on human society and ecosystem.

Bioclimate envelope model has been widely used to predict the effects of climate change on the distribution range of terrestrial species (Pearson & Dawson 2003). A bioclimate envelope can be defined as a set of physical and biological conditions that are suitable to a given species. Such a bioclimate envelope is generally identified by studying the relationships between current species occurrences and biogeographical attributes using statistical methods (e.g. generalized additive model, Luoto *et al.* 2005) or artificial intelligence models (e.g. artificial neural network, Pearson *et al.* 2002). Thus, shifts in species distributions can be predicted by evaluating changes in bioclimate envelope under climate change scenarios. For instance, a bioclimate envelope model based on a genetic algorithm and museum specimens was used to predict distributional shifts of Mexican terrestrial faunas under global climate change scenarios (Peterson *et al.* 2002).

Bioclimate envelope models are important tools to provide guidance for policy making (Hannah *et al.* 2002) although predictions from such models may be uncertain (Peason & Dawson 2003; Araújo *et al.* 2005; Araújo & New 2006; Lawler *et al.* 2006). Critiques of bioclimatic modelling are detailed by Pearson & Dawson (2003); they include the lack of consideration of biotic interactions, evolutionary change and species dispersal. Understanding these processes is important to a comprehensive evaluation of impacts of climate change on the marine ecosystem (Harley *et al.* 2006). However, bioclimate envelope models are among the best tools available to predict large scale potential ecological changes under climate change scenarios. Their applications are particularly appropriate at large spatial scale, as will be presented below. Also, model uncertainty can be reduced by examining results from multiple alternative models (Pearson & Dawson 2003). Thus, predictions from such models are useful in generating hypotheses of possible ecological impacts from climate change.

Two global databases, i.e., that compiled by the *Sea Around Us* Project (Watson *et al.* 2004), and FishBase (Froese & Pauly 2007) provide most of the information needed for the development of a global bioclimate envelope model for commercially exploited marine species. This is important as predicting future responses to climate change in marine biomes lags behind those for terrestrial species. Specifically, application of a bioclimate envelope model to large marine ecosystem is limited. This is partly because of the general lack of large-scale biological, ecological and biogeographical data for most marine species. However, such data are made available from the aforementioned global databases. For instance, distributions of relative abundance of all commercially exploited marine species are available from the *Sea Around Us* Project (Close *et al.* 2006). Combining such data with physical attributes such as global ocean temperature, bioclimate envelopes of the marine species could be inferred. These make it possible to construct bioclimate envelope models to predict impacts of climate change on all exploited marine species.

This contribution documents a bioclimate envelope model that aims to predict the effects of global climate change on marine fishes and invertebrates. A major advance of the bioclimate envelope model presented in this contribution is the incorporation of population and dispersal dynamics for predicting impacts of climate change on distribution range. Such dynamics are important factors in determining biogeography of marine system under climate change scenarios (Pearson & Dawson 2003; Harley *et al.* 2006). Although our model does not explicitly deal with the effects of biological interactions and evolutionary changes (Pearson & Dawson 2003), we discuss the implications of these factors for the uncertainty of our model predictions. For the time being, we evaluate the performance of our model by using hypothetically generated climate data, as a first step to quantitatively evaluate the impacts of climate change on marine fishes and invertebrates. We then discuss how this approach will be applied to the study of likely effects of global changes to fisheries at a global scale.

METHODS

We developed a simulation model to predict changes in global distributions of commercial species under different climate change scenarios. This model is essentially a bioclimate envelope model combined with dynamic dispersals of animals. The *Sea Around Us* Project uses the distribution of commercial species (fishes and invertebrates) to map marine fisheries (Watson *et al.* 2004). The distributions have all been recently improved by Close *et al.* (2006), Lam *et al.* (this vol.) and Pauly *et al.* (this vol.). The future distributions of these species were assumed to be predictable from changes in ocean temperature, ocean advections and habitats (coral and sea ice coverage). Details of the model are described in the following.

Current species distributions

Descriptions of current distribution of marine species are fundamental to predicting changes in species distributions. The *Sea Around Us* Project produced distribution maps of over 1,200 commercially exploited fishes and invertebrates (www.seaaroundus.org). Each species' distribution map is presented as potential relative abundance in 30' latitude x 30' longitude cells of the world ocean. The map was generated by a bio-climate model that predicts the suitability of each 30' lat. x 30 long. cell to the studied species. Boundaries of each species' distribution were delineated by the following information: (1) latitudinal range; (2) depth range; (3) affinity to certain habitats; (4) known distribution boundaries from published literature or experts' knowledge, e.g., presence in a United Nations Food and Agriculture Organization (FAO) statistical area. Realistic assumptions were made on distributions of relative abundance within the above ecological limits. For instance, an 'equatorial submergence' filter was used to account for the tendency of demersal species to inhabit shallower waters in higher latitude (Ekman 1957; Close *et al.* 2006). It is emphasized that the *Sea Around Us* Project does not explicitly use temperature and primary production for any of the procedures discussed above. A description of the procedures to predict current species distributions are documented in Close *et al.* (2006). Lam *et al.* (this vol.) and Pauly *et al.* (this vol.) present the modifications required to represent the distribution of seasonally migrating fishes and latitudinal and longitudinal distribution asymmetry, respectively.

Predicted current distributions of seven species: Nassau grouper (*Epinephelus striatus*, Epinephelidae), Small yellow croaker (*Larimichthys polyactis*, Sciaenidae), Polar cod (*Boreogadus saida*, Gadidae), Atlantic cod (*Gadus morhua*, Gadidae), Western Australian rock lobster (*Panulirus Cygnus*, Palinuridae), Antarctic toothfish (*Dissostichus mawsoni*, Nototheniidae), and summer and winter distributions of Australian ruff (*Arripis georgianus*, Australian ruff) were shown here as examples (Figure 1). These examples represent species with different life history and ecology, and from different geographic areas. We used these examples to illustrate the models described in this paper.
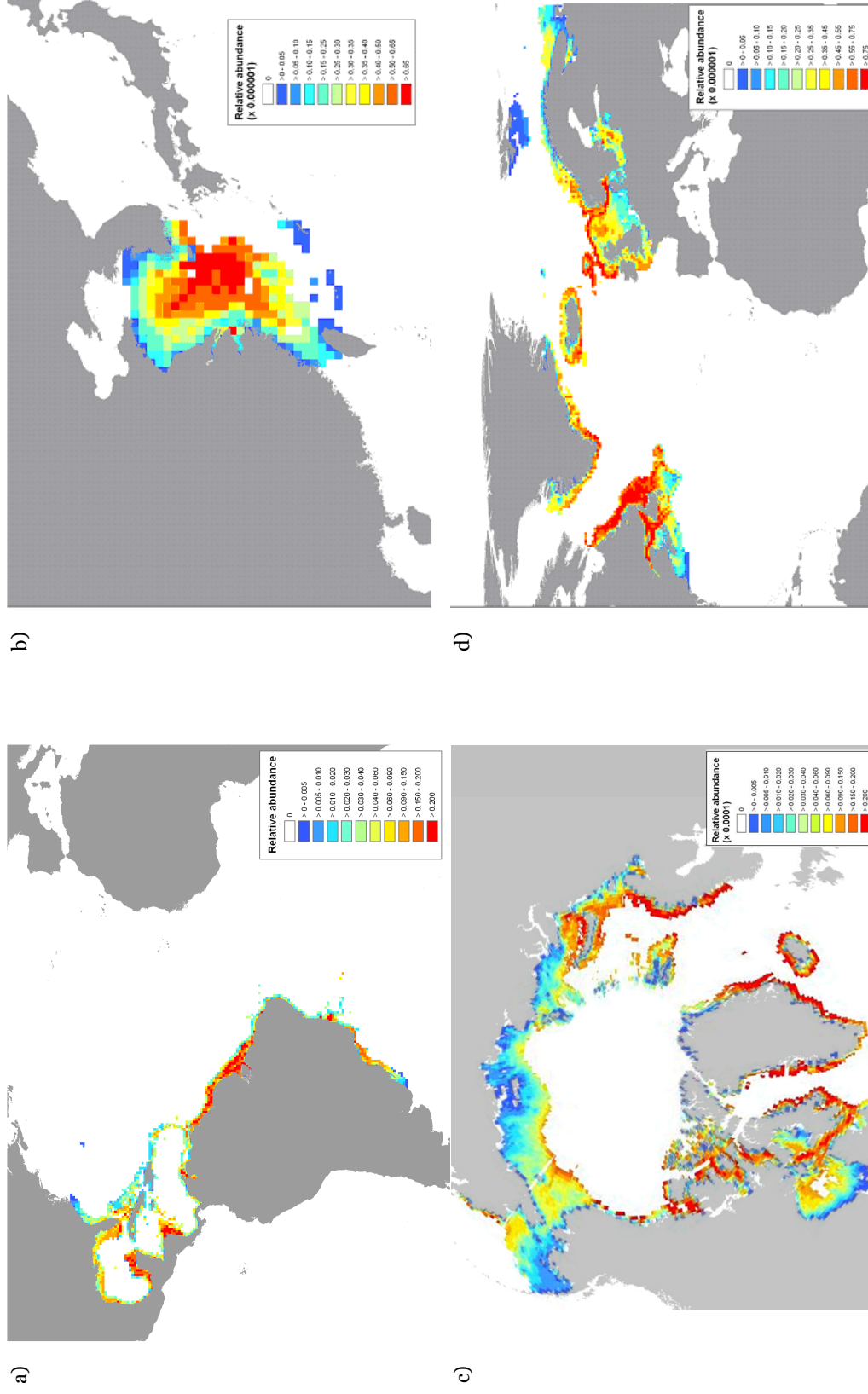
Figure 1. Predicted current distributions of (a) Nassau grouper (*Epinephelus striatus*), (b) Small yellow croaker (*Larimichthys polyactis*), (c) Polar cod (*Boreogadus saida*) and (d) Atlantic cod (*Gadus morhua*) generated from the methodology described in Close *et al.* (2006).

e)

f)

g)

h)

Relative abundance (x 0.00000001)

0
> 0 - 0.010
> 0.010 - 0.040
> 0.040 - 0.060
> 0.060 - 0.080
> 0.080 - 0.100
> 0.100 - 0.125
> 0.125 - 0.150
> 0.150 - 0.180
> 0.180 - 0.300
> 0.300

Relative abundance (x 0.0000001)

0
> 0 - 0.05
> 0.05 - 0.10
> 0.10 - 0.15
> 0.15 - 0.25
> 0.25 - 0.30
> 0.30 - 0.35
> 0.35 - 0.40
> 0.40 - 0.50
> 0.50 - 0.65
> 0.65

Relative Abundance

0
> 0 - 0.003
> 0.003 - 0.007
> 0.007 - 0.012
> 0.012 - 0.020
> 0.020 - 0.030
> 0.030 - 0.040
> 0.040 - 0.060
> 0.060 - 0.080
> 0.080 - 0.150
> 0.150

Relative Abundance

0
> 0 - 0.003
> 0.003 - 0.007
> 0.007 - 0.012
> 0.012 - 0.020
> 0.020 - 0.030
> 0.030 - 0.040
> 0.040 - 0.060
> 0.060 - 0.080
> 0.080 - 0.150
> 0.150

Figure 1. Predicted current distributions of (e) Western Australian rock lobster (*Panulirus cygnus*), (f) Antarctic toothfish (*Dissostichus mawsoni*, Nototheniidae), and (g) summer and (h) winter distributions of Australian ruff (*Arripis georgianus*) generated from the methodology described in Close *et al.* (2006) and Lam *et al.* (2007, this vol.).

Model algorithms

Calculating environmental preferences

Profiles of affinity to environmental and climatic attributes (i.e., seawater temperature, depth, habitat-associations and distance from edge of sea ice) for each species were based on current distribution maps generated by the *Sea Around Us* Project using the methodology documented in Close *et al.* (2006). We assume that the predicted current distributions realistically depict the bioclimate envelopes preferred by the species. In this paper, bio-climate envelopes are defined by (a) sea water temperature; (b) bathymetry; (c) habitats and (d) distance from sea ice. For each of these four bioclimate attributes, we expressed a species' preference to different attribute values by its relative abundance.

a. *Sea water temperature*

Distributions of marine ectothermic animals are strongly dependent on temperature, as these animals are limited by their insufficient capacity of circulation and ventilation under low and high temperature (Pörtner 2001). Physiological performance of marine invertebrates and fishes changes continuously from optimum level to outside their thermal tolerance limits (Frederich & Pörtner 2000; Pörtner 2001). Also, foraging theory predicts that animals will select areas where, eventually, their growth rates can be maximized (Stephens & Krebs 1986). As growth is strongly dependent on physiological performance (Pauly 1980; Elliott 1982; Regier *et al.* 1990), it is reasonable to assume that ectothermic animals tend to inhabit area within their optimal temperature range (Hughes & Grand 2000). Thus, current distributions of marine animals should depict, at least roughly, their temperature preference.

We calculated the temperature preference profile (TPP) of each species by combining current sea temperature with species' predicted distribution ranges, the latter being determined by the *Sea Around Us* Project algorithm (Close *et al.* 2006). We define TPP as the probability of occurrence of a species at different sea water temperatures. To infer TPP from the predicted distribution maps, firstly we converted the observed sea temperature data obtained from Met Office Hadley Centre observations datasets (http://hadobs.metoffice.com/hadisst/) to the 30' x 30' resolution of the *Sea Around Us* Project distribution maps. We overlaid the sea temperature over current distribution maps and calculated species' relative abundance in different temperatures. We assume that relative abundances of demersal and benthopelagic species (e.g., Atlantic cod) depend mainly on annual sea bottom temperature while pelagic species (e.g. Atlantic herring) depend on seasonally-averaged (summer and winter) sea surface temperature (see Lam *et al.* this vol.). We examined the TPP of the studied species to ensure that temperature preference by each species is reasonable. Criteria for judging the acceptability of the temperature profiles include (1) whether the profile is approximately unimodal; and (2) the coefficient of variation of preferred temperature is less than 50%. Distribution maps that resulted in clearly multi-modal temperature profiles or a wide range of preferred temperature might be predicted inaccurately and were reviewed. Also, we assume a linear change in species preference (relative abundance) to water temperature between consecutive temperature classes (Figure 2).

In some cases, sea-water temperature preference by a species is not uni-modal, i.e., there is more than one distinct peak of relative abundance in different temperatures (e.g., Atlantic cod and Western Australian rock lobster, Figure 2d and 2e). Physiological performance of marine ectotherms generally peaks at certain optimum temperature from where it declines to their thermal tolerance limits (Frederich & Pörtner 2000; Pörtner 2001). As we assume that each species distribution represents a single uniform distribution, we consider the multi-modal temperature preference distributions as artifacts which resulted from uncertainties of the original species distribution. As this may lead to unrealistic predictions of species' responses to changes in sea temperature, we smoothed the TPP with running-mean to ensure that the distributions were generally uni-modal. To minimize distortion to the original temperature preference distribution, the number of temperature class averaged in the running mean calculation was increased from 3 until a uni-modal distribution was obtained. In the case of Western Australian rock lobster, a 3-temperature-classes running-mean is required to change the original bi-modal distribution to uni-modal (Figure 3).
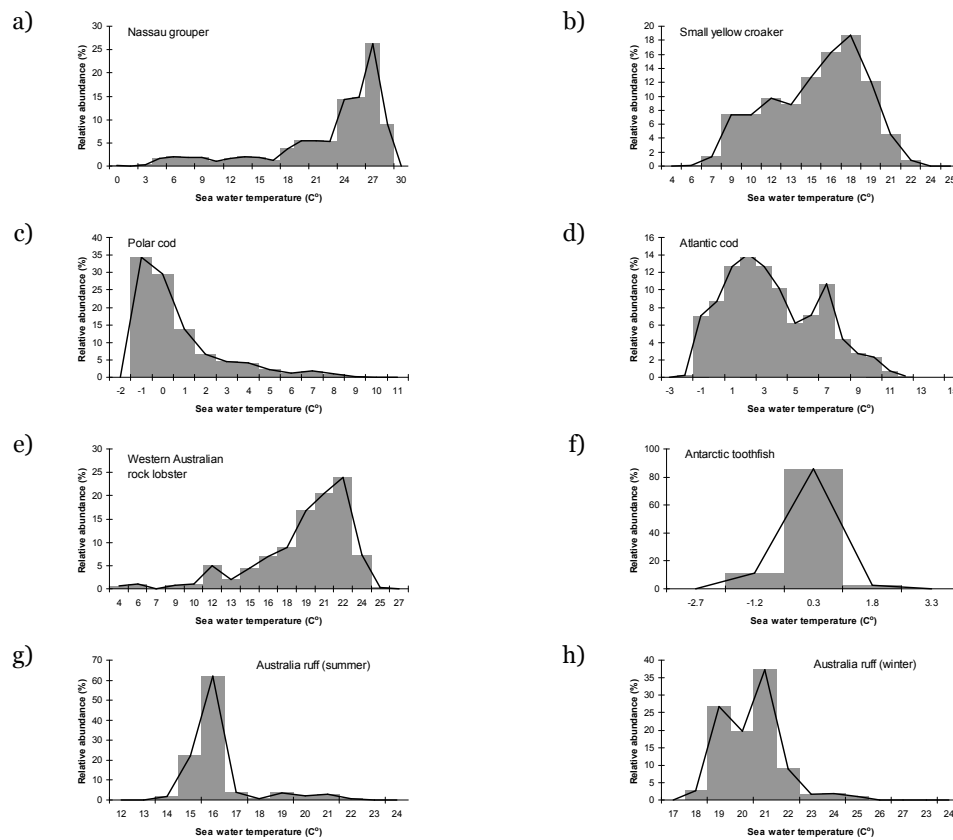
Figure 2. Temperature Preference Profile (TPP) expressed as relative abundance in areas with different sea temperature of: (a) Nassau grouper, (b) Small yellow croaker, (c) Polar cod, (d) Atlantic cod, (e) Western Australian rock lobster, (f) Antarctic toothfish, (g) and (h) summer and winter distributions of Australian ruff. We assume linear changes in a species' preference to sea water temperature between consecutive temperature classes (lines).
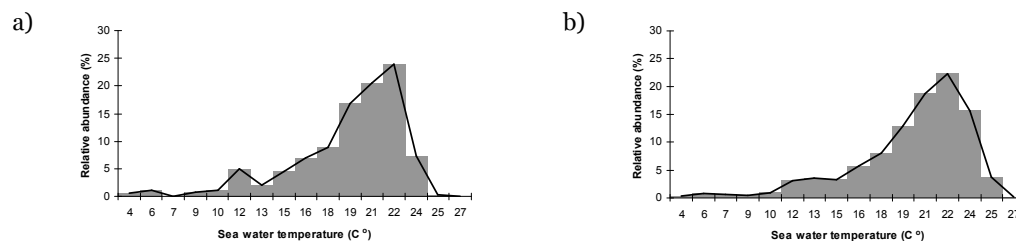
Figure 3. Temperature Preference Profile of Western Australian rock lobster: (a) original distribution, (b) smoothing by 3 temperature classes.

b. Depth limits

We assume that a species' distribution is also limited indirectly by depth. Thus, there are lower and upper limits of water depth outside of which a species does not occur. Different levels of temperature, oxygen concentration, food availability and predation pressure exist at different water depths. Vertical distributions of marine fishes and invertebrates were suggested to be limited partly by these factors in both freshwater and marine environments (Matthews *et al.* 1985; Pihl *et al.* 1991; Orlowski 1999). Also, animals inhabiting extreme depth generally develop special morphological and physiological adaptations (Helfman *et al.* 1997). Thus, species that are adapted to surface waters cannot occur in deep water and conversely. These create limits to the range of water depth where different species occur.

We estimate lower and upper depth limits from species' current distribution. The *Sea Around Us* Project algorithm uses depth limits as criteria to predict a species' distribution. However, because of other physiological or ecological limitations (e.g., temperature) that restrict the distribution of the species, the current species distribution predicted by the *Sea Around Us* Project algorithm (Close *et al.* 2006) may not depict the extreme bathymetric limits of the species. Also, depth limits used by Close *et al.* (2006) were imprecise in most cases. Therefore, we accounted for the high uncertainty of the depth limits by widening them in the current species distribution by 100%. For instance, the original depth limits of Small yellow croaker used by Close *et al.* (2006) is 1 – 105 m, but wider limits of 0.5 – 210 m were used in our model. We assume that a species would maintain its depth limits when its distribution changes as a result of global climate change.

c. Habitats

Each species is assigned an index of association to one or more of the four habitat types: coral reefs, estuaries, seamounts and other habitats. The index represents relative density of a species in the particular habitat. It was assigned based on qualitative descriptions of the ecology of the species from FishBase or other publications and literature (Close *et al.* 2006; Cheung *et al.* 2007). Distribution of relative abundance obtained from the *Sea Around Us* Project algorithm had been adjusted based on the habitat-association index and global distributions of the four habitat types (Close *et al.* 2006, Table 1).

Table 1. Habitat categories for which global maps are available in the *Sea Around Us* Project.

Categories	Origin of global map	Terms often used to describe these categories
Estuary	Alder (2003)	Estuaries, mangroves, river mouth.
Coral	UNEP World Conservation Monitoring Centre (2005)	Coral reef, coral, atoll, reef slope.
Seamounts	Kitchingman and Lai (2004)	Seamounts.
Other habitats	---	Muddy/sandy/rocky bottom.

d. Distance from sea ice

Polar ecosystems, and distributions of their associated species, are largely shaped by the dynamics of sea ice (Longhurst 1981). In both the Arctic and Antarctic, primary productivity under and around sea ice is generally high. For instance, in the Antarctic, phytoplankton growth is enhanced by dynamics of mixed-layer of water affected by influx of lower salinity water from ice-melting. Sea ice cover also provides a habitat that allows for maximum utilization of sunlight and thus enhances primary production (Eicken 1992). Zooplankton such as krill (*Euphasia superba*) forage and take refuge under sea ice (Daly & Macaulay 1988; Brierley *et al.* 2002). The zooplanktons, in turn, form the basis of the foodweb which support fishes and mammals in polar ecosystems (Eicken 1992; Legendre *et al.* 1992; Longhurst 1981). Thus, polar fishes such as Arctic cod and Antarctic toothfish are physiologically adapted to polar environments (Farrell & Steffensen 2005) and generally range close to sea ice (Legendre *et al.* 1992; Fuiman *et al.* 2002).

It is therefore reasonable to assume that polar species are partly dependent on the presence of sea ice at least at a certain distance. To be consistent with the current species distributions, which represent annual average (except for pelagic fishes), annual average sea ice distribution was used. In this study, we used average monthly ice extent (19179-1999) with its border defined by a minimum of 50% sea ice coverage. The sea ice data were obtained from the US National Snow & Ice Data Centre web site (http://nsidc.org/data/smmr_ssmi_ancillary/trends.html#gis) and processed by Kaschner (2004). We calculated the distance between the nearest sea ice and the centre of each 30' lat. x 30' long. cell. Overlaying species' distribution from the *Sea Around Us* Project algorithm on maps of nearest distance from sea ice, we calculated polar species' relative abundance at different distances from sea ice.

In this study, we used a biogeographical definition of polar species (Møller *et al.* 2005), i.e., species that range mostly (≥ 75% of their relative abundance) within the Arctic or Antarctic were categorized as polar. Maps of the Arctic and Antarctic from Møller *et al.* (2005) were employed (Figure 4). A list of exploited polar fishes and invertebrates is shown in Appendix 1.
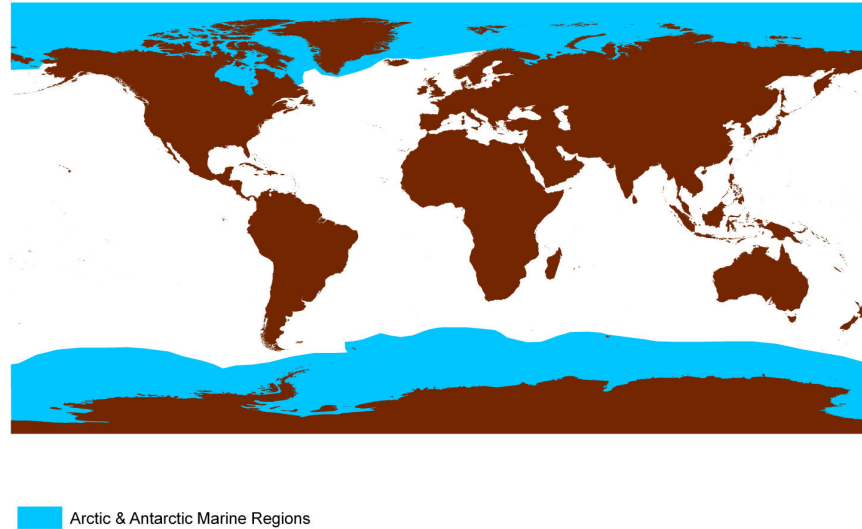
Figure 4. Map of the Arctic and Antarctic (in grey), based on Møller *et al.* (2005).

Dynamics of climate change-induced range shift

We developed a model to predict climate change-induced shift in species distributions. Spatial and temporal dynamics of populations are assumed to be determined by larval and adult dispersals, immigration, intrinsic population growth and extirpation. The rates of these processes are dependent on the 'carrying capacity' in each area (30' lat. x 30 long. cell). Here, carrying capacity is defined as the maximum relative abundance of a species in a cell. It is largely dependent on the environmental suitability of the cell to the species. All these processes are incorporated into the model. Since the model aims to predict changes in relative species distributions while accurate predictions of absolute changes in abundance are not necessary, we simplified the population dynamic models to reduce the number of required parameters that are otherwise unavailable for most of the studied species. Details of the population dynamic model, along with all the assumptions and simplifications, are reported in the following.

Changes in relative abundance of a species in each 30' lat. x 30' long. cell (*i*) at each time step *t* can be expressed as:

$$\frac{dA_i}{dt} = \sum_{j=1}^{N} G_i + L_{ji} + I_{ji} \qquad \dots 1)$$

where A_i is the relative abundance of cell *i*, *G* is the intrinsic population growth, and L_{ji} and I_{ji} are settled larvae and net migrated adults from surrounding cells *j*, respectively.

Growth (G)
We modelled intrinsic population growth through a logistic growth function (Hilborn & Walters 1992):

$$G_i = r \cdot A_i \cdot (1 - \frac{A_i}{KC_i}) \qquad \dots 2)$$

where *r* is intrinsic rate of population increase, A_i and KC_i are the relative abundance and population carrying capacity at cell *i*, respectively. A major assumption of our model is that current species distributions calculated from the algorithm of Close *et al.* (2006) as modified by

Pauly *et al.* (this vol.) and Lam *et al.* (this vol.) are in equilibrium, and every spatial cell at time-step (t) 0 is at its carrying capacity, i.e., $KC_{i,t=0} = A_{i,t=0}$ and, therefore, $G_{i,\,t=0} = 0$.

We used an indirect method to approximately estimate intrinsic rate of population increase (r). Empirically estimated intrinsic rates of increase of most exploited marine species were not available because of a lack of time-series population data (e.g., abundance, catch rate). Therefore, we calculated r based on the estimated natural mortality rate (M):

$$r = c' \cdot M \qquad \qquad \dots 3)$$

where c' is a constant that commonly ranges between 1 and 3. Natural mortality rate was estimated from an empirical equation (Pauly 1980):

$$M = -0.4851 - 0.0824 \cdot \log(W_{\text{inf}}) + 0.6757 \cdot \log(K) + 0.4687 \cdot \log(T) \qquad \dots 4)$$

where W_{inf} is asymptotic weight, K is the von Bertalanffy growth parameter and T is the average water temperature in the animal's range. Acknowledging the high uncertainty of r estimated from this method, we compared the simulation results obtained from a range of r to evaluate the sensitivity of our model to the uncertainty of the population growth rate.

The carrying capacity of a cell varies positively with the habitat suitability to the studied species. As habitat in a cell (defined here by temperature, bathymetry, habitat types and ice-coverage) becomes more suitable for the animal, carrying capacity should also increase. Thus, in our model, carrying capacity KC in cell i is modified according to the change in habitat suitability (P) between time (t), i.e.,

$$KC_{t+1} = KC_t \cdot \frac{P_{t+1}}{P_t} \qquad \qquad \dots 5)$$

and

$$P = P(T) \cdot P(Dep) \cdot P(H) \cdot P(Ice) \qquad \qquad \dots 6)$$

where T, Dep, H and Ice refer to temperature, bathymetry, habitat types and sea ice coverage, respectively.

If an initially unoccupied spatial cell ($A_0 = KC_0 = 0$) or a cell without suitable habitat becomes suitable for the survival of a species as global climate changes, its new carrying capacity is assumed to be the average carrying capacity of other 'occupied' cells with similar habitat suitability.

Spawning and larval dispersal (L)
Immigration consists of two components: larval dispersal and migration of adults. We assume larval production (Lav) to be directly proportional to the relative abundance in a cell (i):

$$Lav_i = R \cdot A_i \qquad \qquad \dots 7)$$

where R is an assumed rate of larval production. Our model does not have an explicit stock-recruitment relationship. The main focus of the model is to simulate changes in cells' carrying capacity and extent of dispersal by the species. The absolute amount of larval production affects only the rate at which carrying capacity level in a cell is being approached, and should not affect the general prediction by the model. On the other hand, we tested the sensitivity of the model outputs to this simplification by comparing model results obtained from a range of larval production rate (R).

Our model calculates dispersal of larvae through ocean current and diffusion. We assume that pelagic larvae disperse passively from surrounding 'source' areas through ocean surface current

and diffusion. Thus, the magnitude of larval recruitment is dependent on pelagic larval duration (*PLD*), strength and direction of ocean currents and diffusivity. *PLD*, expressed in days, can be calculated from an empirical equation established from a meta-analysis of *PLD* from 72 species of fish and invertebrates (O'Connor *et al.* 2007):

$$\ln(PLD) = \beta_0 - 1368 \cdot (\ln(T/T_c)) - 0.283_2 \cdot (\ln(T/T_c))^2 \qquad \ldots 8a)$$

$$\beta_0 = 0.739 + 0.739 \cdot (\overline{\ln(T)} + 0.714 \cdot (DM) \qquad \ldots 8b)$$

$$\overline{\ln(T)} = \frac{\sum_{i=1}^{N} \ln(T_i)}{N} \qquad \ldots 8c)$$

where *T* is sea surface temperature, T_c =15 °C, *N* is the number of spatial cells (*i*) where the species occurs. *DM* is the developmental type of larvae. *DM* is 0 or 1 for lecithotrophic (non-feeding development) or planktotrophic (feeding development) larvae, respectively (O'Connor *et al.* 2007). Thus, *PLD* is shorter in areas where the sea water temperature is higher. On the other hand, *PLD* is longer when the average temperature over the entire occurrence range of a species is higher, reflecting its evolutionary adaptation to higher environmental temperature (O'Connor *et al.* 2007).

Based on the calculated *PLD* and ocean current velocity data, the model calculates dispersal of pelagic larvae over time through diffusion and advection. Diffusion and advection of ocean current are important factors determining dispersal of pelagic larvae of marine organisms (Possingham & Roughgarden 1990; Gaylord & Gaines 2000; Bradbury & Snelgrove 2001; Gaines *et al.* 2003). The temporal and spatial patterns of pelagic larval dispersal were modelled by a two-dimensional advection-diffusion equation (e.g., Sibert *et al.* 1999; Gaylord & Gaines 2000; Hundsdorfer & Verwer 2003):

$$\frac{\partial Lav}{\partial t} = \frac{\partial}{\partial x}\left(D \frac{\partial Lav}{\partial x} \right) + \frac{\partial}{\partial y}\left(D \frac{\partial Lav}{\partial y} \right) - \frac{\partial}{\partial x}(u \cdot Lav) - \frac{\partial}{\partial y}(v \cdot N) - \lambda \cdot Lav \qquad \ldots 9)$$

where change in relative larvae abundance over time ($\partial Lav/\partial t$) is determined by diffusion (i.e., the first two terms on the right-hand side of eq. 9) and current-driven movements (i.e., the third and fourth terms of eq. 9). Diffusion is characterized by a diffusion parameter *D*, while advection is characterized by the two current velocity parameters (*u, v*) which describe the east-west and north-south current movement. Diffusion coefficient, expressed in m² s⁻¹, is assumed to be a function of length scale of the spatial grid: $D = (1.1 \times 10^{-4}) \cdot GR^{1.33}$ where *GR* is the minimum grid resolution (Nahas *et al.* 2003).

Annual average current fields were obtained from the NOAA/GFDL Coupled Model. Thus, we implicitly assume that larvae remain within a single horizontal layer of the water column or are well mixed vertically in water of nearly constant depth. The instantaneous rate of larval mortality and settlement is represented by $\lambda = M + S$ where *M* and S are the natural mortality and settlement rates of larvae, respectively. The default larval survival and larvae retention rate are 0.15 day⁻¹ and 0.2 day⁻¹, respectively. Alternative values were used to test for the sensitivity of simulation results to these parameters.

We employed a numerical solution of the partial differential equation (eq. 9) provided by Sibert & Fournier (1994). Basically, eq. 9 is solved using implicit alternating direction method (Press *et al.* 1988). This method solves the partial differential equation for each direction (*u* and *v*) after half a time step sequentially (Figure 5). The implicit solution can be expressed as systems of linear equations with tridiagonal matrices of coefficients. Therefore, the 30' x 30' grid world map was firstly segregated into horizontal and vertical segments with consecutive sea cells. Movement of larvae from diffusion and advection was then calculated for each east-west and north-south

segment. The tridiagonal system of equations can be robustly solved by the recursive algorithm (Press *et al.* 1988) (see Appendix 3 and Sibert & Fournier 1993 for details of equations).
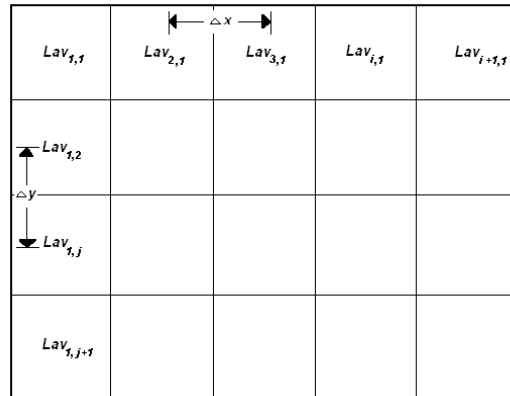
Figure 5. Schematic diagram of a computational grid. The horizontal (*u*) and vertical (*v*) direction movements are solved separately at half a time step sequentially.

A daily time step was used in simulating larval dispersal. The simulation time frame is determined by the calculated *PLD* from eq. 8. Displacement at each time step (Δx and Δy) was assumed to be the distance between two adjacent cells ($Dist_{ij}$), which is calculated by:

$$Dist_{ij} = a\cos(\sin(Lat_j) \cdot \sin(Lat_i) + \cos(Lat_j) \cdot \cos(Lat_i) \cdot \cos(Lon_i - Lon_j)) \cdot Er/2 \quad \ldots 10)$$

where *Lat* and *Lon* are the latitude and longitude of cells *i* and *j*, respectively; *Er* is the radius of the Earth (6378.2 km).

In addition to average larval dispersal as described above, we also modelled extreme dispersal events. Here, extreme dispersal events refer to sporadic dispersal of larvae as a result of ocean advection anomalies. Such events may influence dispersal pattern and meta-population structure (Lockwood *et al.* 2002). In the model, extreme dispersal events are assumed to be random events and are represented by a doubling of the average dispersal distance. We assume that extreme dispersal events occur once every 5 years, but alternative values were used to test the sensitivity of model outputs to this parameter.

Net adult migration (I)
In the model, animals disperse by actively swimming to surrounding areas. Animals were considered to have reached a cell by active dispersal if the dispersal distance in a simulation time-step was greater than the nearest distance between source and destination cells. Distance travelled by active dispersal from a source cell was calculated from a dispersal rate (km·year^{-1}). Generally, species that are pelagic, large-bodied, fusiform-shaped and metabolically more active have higher dispersal rate. The aspect ratio of a fish's caudal fin (i.e., the ratio between the square of the height of fish's caudal fin to the caudal fin area) is a proxy of its 'motility' (Palomares & Pauly 1998). For invertebrates, 'motility' values were estimated from their general shape, and scaled after fishes with similar shapes and habits.

a. Adult dispersal rate
We developed a fuzzy logic expert system that used 'rules-of-thumb' to predict dispersal rate from species' life history, habitats and 'motility'. The 'rules-of-thumb' represented our general understanding of the relationship between some easily-obtainable parameters with dispersal ability of marine animals. These rules are expressed as IF-THEN clauses that link premises (maximum body length, aspect ratio and habitat) to conclusions (dispersal rate) (Appendix 2). Ordinal categories of input attributes were categorized based on pre-defined fuzzy membership functions (Figure 6). For instance, if a fish has a maximum body length of 75 cm, it is classified as small- and medium-sized fish with degrees of membership equal to 0.5 (Figure 6a). Memberships to habitat types (pelagic, demersal and coral reef) are either 0 or 1.

a)

b)

c)
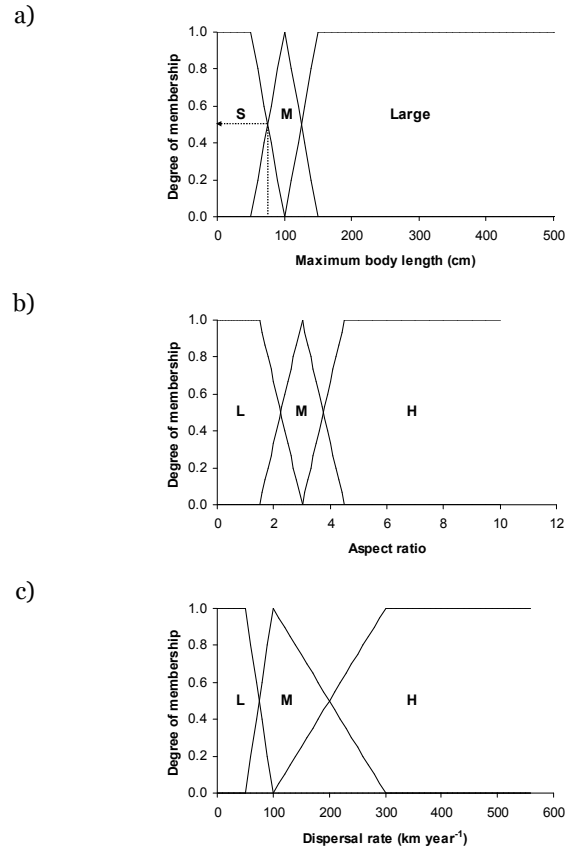
Figure 6. Fuzzy membership functions of the inputs (a. maximum body length and b. aspect ratio) and output (dispersal rate). S – Small, M – Medium, H – High. A fish with maximum body length of 75 cm is calculated to have membership to 'Small' and 'Medium' body size with equal degree of membership of 0.5 (dotted line in 6a).

b. Modelling adult dispersal

Emigration (adult animals moving out of a cell) was calculated from the dispersal or movement rate using an algorithm employed in an Eulerian spatial ecosystem simulation model – Ecospace (Walters *et al.* 1999). Basically, if animals are distributed randomly within a cell (with length of a cell side x and distance from the boundary of a cell y) at the start of a time interval dt, a proportion xdy/x^2 will be a candidate for emigration across each cell boundary (Figure 7). Also, the proportion of average organism within this cell to move a length dy over a short time interval dt, in a completely random direction, is $1/\pi$ (Walters *et al.* 1999). Thus, the instantaneous emigration rate m_i for randomly moving organisms to emigrate across each cell boundary can be calculated by:

$$m_i = \frac{V_i}{\pi \cdot x}$$

...11)

where V_i and x are the adult dispersal rate and length of a cell, respectively (see Walters *et al.* 1999 for details).
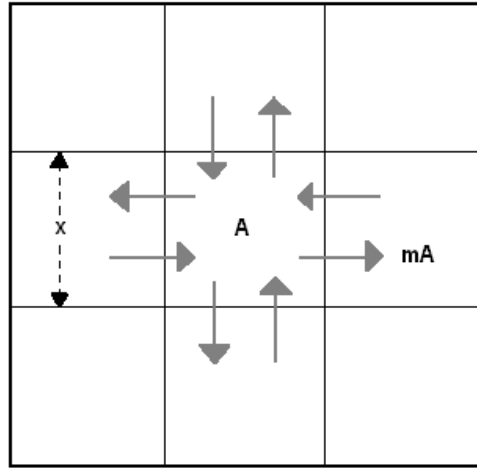
Figure 7. Schematic diagram of emigration and immigration movements by adult on a spatial grid. *A* is the animal abundance in a cell. Emigration rate is inversely proportional to the length of a cell (*x*). Absolute emigration of animals is directly proportional to emigration rate (*m*) and animal abundance.

Animals generally have higher emigration rate towards cells with more preferable environment (e.g., temperature, depth, habitat types). We modelled such behaviour by incorporating a hyperbolic function in calculating the emigration rate m_i:

$$m_i = \frac{m_i^{(base)} \cdot k}{(k + D)} \qquad \ldots 12)$$

where $m_i^{(base)}$ is the movement rate in the absence of any gradient and k is a scaling factor representing the sensitivity of the calculated emigration rate to changes in environmental suitability (as measured by D) (Walters *et al.* 1999). Small values of k (e.g. 0.1) result in high sensitivity to change in D while large values (e.g. 10) render adult dispersal rate insensitive to D. We used an intermediate value of k (= 2), but we also compared model outputs from alternative k values.

D is assumed to be the ratio of habitat suitability (*P*), as defined in eq. 6, between the source (*i*) and destination (*j*) cells. That is,

$$D_{ij} = \frac{P_i}{P_j} \qquad \ldots 13)$$

Thus, animals would have higher emigration rate to cells with higher habitat suitability relative to the source cell. Finally, emigration of animals (*E*) from a cell is calculated by multiplying emigration rate (m_i) by abundance of the cell (A_i) (Figure 7).

Emigrated animals can move back to the source cells. The rate of such re-entry to the source cells (*RE*) is dependent on the abundance relative to its carrying capacity in the destination cells:

$$RE_{ji} = \frac{m_i \cdot A_i \cdot k}{[k + (1 - KR_j)]} \qquad \ldots 14a)$$

$$KR_j = \frac{A_j}{KC_j} \qquad \ldots 14b)$$

where k is the scaling factor in eq. 12, *KR* is the carrying capacity ratio of the destination cell; *A* and *KC* are animal abundance and carrying capacity of a cell, respectively. Thus, we assume that

the re-entry rate of animals is lower from cells with lower abundance relative to carrying capacity. This can also reflect lower density-dependency (e.g., intra-specific competition) in destination cells which favour successful establishment of new migrants. On the other hand, an animal that enter a cell with population abundance at its carrying capacity would return to its original ('source') cell (which is equivalent to stating that cells at carrying capacity cannot accept new animals).

Thus, the net dispersal of adult animals (I_{ij}) to a cell j from cell i is given by:

$$I_{ij} = E_{ij} - RE_{ji} \qquad \qquad \dots 15)$$

However, some of the dispersed animals (larvae and adults) may not establish themselves in the destination cell and die because of density-dependent/independent factors (e.g., increased predation, competition). Dispersed animals that die at cell i and time step t ($Mort_{i,t}$) are calculated in our model.

$$Mort_{i,0} = M^I{}_0 \cdot \sum_{j=1}^{N} \left(I_{i,j,0} + L_{i,j,0} \right) \qquad \qquad \dots 16)$$

where N is the total number of cells from where the dispersed adult animal (I) and settled larvae (L) come. A major assumption of our model is that current species distributions are in equilibrium, i.e., dA/dt = 0. Also, for computation purposes, we have to assume that population in every spatial cell at time-step 0 is at its carrying capacity. These assumptions mean that there is no net emigration or dispersal at time-step 0 and $Mort_{i,o}$.

The 'mortality' of dispersed animals at cell i and time step t ($Mort_{i,t}$) changes as cells' habitat suitability changes with climate. Change in mortality of dispersal animals was modelled by

$$M^I{}_{i,t} = M^I{}_{i,0} \cdot \frac{P_{i,0}}{P_{i,t}} \qquad \qquad \dots 17)$$

where P is the calculated habitat suitability to the species at time step 0 and t. Thus, as habitat suitability changes, spatial dynamics of the modelled species move away from equilibrium and net movement of animals between cells occurs

Predicting changes in species distributions
Using equations 2 to 17, we calculated changes in abundance per time step for each spatial cell for each species. Since we assume that current species distribution is in equilibrium, abundance in each cell remains unchanged if physical conditions (e.g., sea water temperature, habitat types) are constant. However, as global climate changes, habitat suitability in each cell, and thus its carrying capacity, and the growth, net migration and mortality of the organisms therein, change accordingly. For instance, for any cell, if temperature becomes more favourable to a species, its habitat suitability may increase according to eq. 6. Carrying capacity (KC) and population growth (G) at the cell increase according to eqs. 2 and 5. Simultaneously, increase in habitat suitability reduces the mortality rates of larval and adult immigrants. This also allows the successful establishment of larvae and adult migrants in previously un-occupied cells. Thus, abundance in this particular cell would increase. On the other hand, as temperature becomes less favourable to the species, extirpation/emigration increases, and population growth becomes negative (because of reduced carrying capacity), leading to a decrease in relative abundance.

To predict changes in species distribution that are solely a result of global climate change, we subtract from the predicted changes in distribution with climate change scenario a 'baseline' run in which temperature was assumed to change only in the first year, then remain constant throughout the duration of the rest of the simulation. The reason for this is that, in the model, we assume that current (predicted) species distributions are in equilibrium and habitat suitability is

solely dependent on the specified environmental factors (see above). However, the original species distribution was constructed from environmental boundaries such as maximum and minimum depth limits, northern and southern latitudinal limits and habitat associations. Thus 'favourable' habitats, as defined by the specified environmental factors (e.g., temperature, depth) may be available outside these boundaries. In reality, however, there may be other factors unaccounted for in our model that restrict the species from occupying these areas. Therefore, in parallel to simulating changes in relative abundance of a species with changes in sea water temperature, we simulated abundance changes by allowing the system to follow the change in sea water temperature in the first simulation time step (year 1), after which temperature was kept constant. Such procedure 'perturbs' the distribution of the species so it moves out of its equilibrium distribution range (at time step = 0). (Other environmental factors such as ocean advection patterns are treated the same way as temperature changes.) The difference in predicted relative abundance between the two simulations was subtracted from the result of simulation with temperature changes. For example, if relative abundance increased by 3 units under a given climate change scenario and increased by 1 unit without climate change, the predicted change in relative abundance became 3 – 1 units = 2 units. This procedure enables us to minimize the contribution of factors that are not explicitly accounted for in our model to the change in species' relative abundance distribution.

Modelling the dynamics of pelagic species
The model is adapted to represent the seasonal (summer and winter) patterns of distributions for pelagic species. Current summer and winter distributions of pelagic species are predicted based on the algorithm described in Lam *et al.* (this vol.). Also, current and future seasonally-averaged sea water temperatures can be obtained from the NOAA/GFDL Coupled Model. Thus, for pelagic species, the model is initiated with the current summer and winter distributions separately. Subsequently, changes in species distributions in the two seasons are simulated independently using the algorithm described in the above sections. However, instead of sea bottom temperature, predicted sea surface temperature is used to identify the species' thermally-preferred habitats. Moreover, the model does not consider bathymetry in predicting the potential distribution range of pelagic species. Furthermore, seasonality of spawning is considered. Generally, fishes in higher latitudes have stronger seasonality in reproduction than those in lower latitudes. In addition, marine fishes often spawn in spring and fall, with spring being the dominant spawning season (Helfman *et al.* 1997). Thus, we assume that larvae production in the tropics ($0°$ – $10°$ N/S) is similar between seasons, but the proportion of total annual larval production in spring increases linearly with latitude until $50°$ N/S after which the proportion remains constant at 90% in spring (or 10% in fall) (Figure 8).
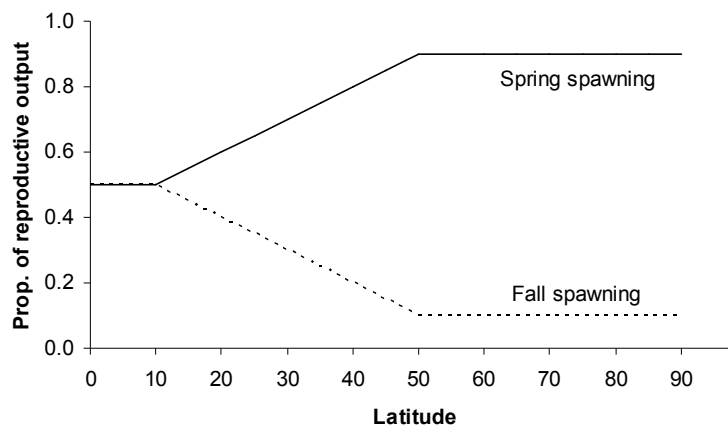
Figure 8. Proportion of total annual reproductive output (larvae production) in spring (solid line) and fall (dotted line) assumed in the dynamic bioclimatic envelope model.

Model implementation

The numerical model to simulate climate change-induced distribution shift is implemented in Visual Basic.net environment. The overall structure of the model is summarized in Figure 9.
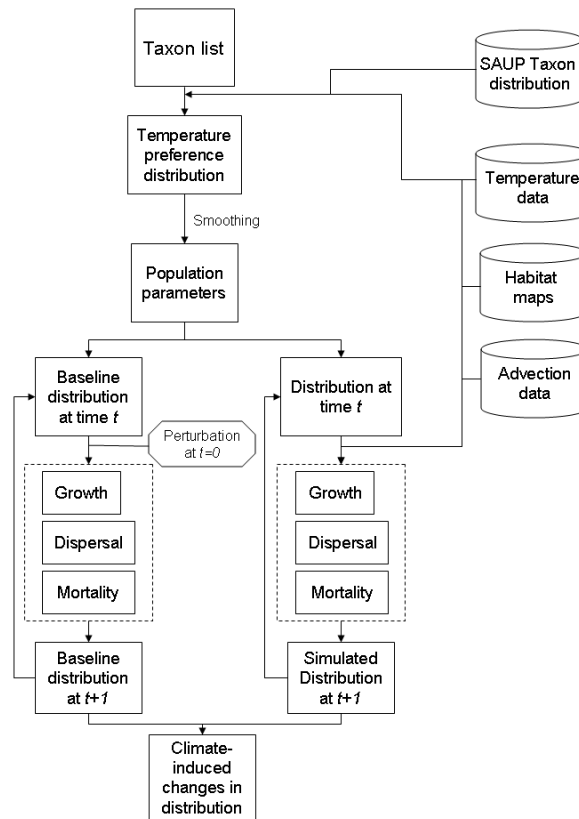
Figure 9. Schematic representation of the structure of the dynamic bioclimate envelope model developed in this study, implemented in Visual Basic.Net environment.

System evaluation

We evaluated the functioning of our model by undertaking model simulation with global sea water temperature generated from simple assumptions on rate of temperature increase in the next 30 years. We considered two scenarios of global increase in sea water (bottom and surface) temperature (Table 2). In each scenario, sea water is warming up slowly near the equator and quickly toward the poles. Ocean advection fields were based on the annual average current velocity data from the Mariano Global Surface Velocity Analysis (Mariano *et al.* 1995). In the test simulations, ocean advection was assumed to be constant throughout the simulation time-frame. However, in the future, ocean advection current data predicted by the NOAA/GFDL Coupled Model will be used in predicting realistic effects of global climate change on species distributions.

Table 2. Parameters used to generate hypothetical scenarios of global sea water temperature increase for model testing.

Scenario	Rate of temperature increase (year^{-1})		Interpolation of temperature in other latitude
	At 0º lat	At 90º N/S lat	
1	0.025	0.075	Linear change in rate of temperature increase from the equator to the poles.
2	0.050	0.150	

To test the performance of our model, we simulated changes in distributions of four commercially exploited species in 30 years under the above two scenarios of global sea temperature change (Table 2). The evaluated species are: Nassau grouper, Small yellow croaker, Polar cod, Atlantic cod, Western Australia rock lobster, Antarctic toothfish and Australian ruff. Their life history parameters (e.g., L_{inf}, W_{inf}, K) were obtained from FishBase and SeaLifeBase (Froese & Pauly

2007; www.sealifebase.org) and from Phillips *et al.* (1992) for the Western Australian rock lobster (Table 3).

Table 3. Input parameters used to simulate changes in distributions of four commercially exploited marine species.

State variables (units)	Nassau grouper	Small yellow croaker	Polar cod	Atlantic cod
L_{inf} (cm)	90	29.2	31.3	129
W_{inf} (g)	13279	403	258	22,300
K (year^{-1})	0.09	0.44	0.22	0.20
R (year^{-1})	0.51	1.58	0.94	0.39
Diffusion coefficient (m^2 s^{-1})	100	100	100	100
Movement rate (km year^{-1})	50	100	100	200
Larval mortality rate (day $^{-1}$)	0.15	0.15	0.15	0.15
Larval settlement rate (day $^{-1}$)	0.20	0.20	0.20	0.20

Table 3. Con't

State variables (units)	Western Australian rock lobster	Antarctic toothfish	Australian ruff
L_{inf} (cm)	10.4*	185	41
W_{inf} (g)	-	75,600	-
K (year^{-1})	0.15	0.06	0.24
R (year^{-1})	0.3	0.02	1.50
Diffusion coefficient (m^2 s^{-1})	100	100	100
Movement rate (km year^{-1})	50	50	100
Larval mortality rate (day $^{-1}$)	0.15	0.15	0.15
Larval settlement rate (day $^{-1}$)	0.20	0.20	0.20

*　　Carapace length

We also evaluated the possible effects of climate change-induced shifting of coral reefs on the distribution of reef-associated species. Coral reefs occur in areas with sea water temperature between 18°C to 30°C (Veron 2000). Instances of increased temperature over the physiological tolerance limits resulting from climate anomalies had led to large-scale coral bleaching events (Glynn 1991, 1993; Hoegh-Guldberg 1999; Bellwood *et al.* 2004). Intensity and frequency of such bleaching events appeared to be increasing since the 1970s (Hoegh-Guldberg 1999; Walther *et al.* 2002). The impacts of large-scale bleaching would be particularly prominent to coral reefs in area at or near the coral's upper temperature limits (Hoegh-Guldberg 1999). Some fishes and invertebrates are obligatorily or strongly dependent on coral reefs (e.g., some species of butterfly fishes, fam. Chaetodontidae). Thus, their distributions may be strongly affected by changes in coral reef distribution (Bellwood *et al.* 2004). On the other hand, the high-latitude limits of coral distribution may not shift much because coral growth at high-latitude is generally limited by factors other than temperature, e.g., light (Hoegh-Guldberg 1999). Also, consistent increase in water temperature from global warming may result in changes in species composition to more heat-resistant species, and acclimation or evolution to higher heat tolerance. Thus, distribution of coral reefs may not change as global sea temperature changes (Polsenberg 2003). These may dampen the effects of global warming on coral reef distribution (Hughes *et al.* 2003).

To test the potential effects of climate-induced changes on coral reef distribution, we attempted to mimic the effects of global warming on coral reefs. Based on a global map of coral reefs (UNEP-World Conservation Monitoring Centre 2005), we plotted the distribution of relative coral reef abundance over latitudinal zones (Figure 10). Relative coral reef abundance was calculated from the ratio of the estimated coral reef area to the area of sea with average depth below 50 m at each latitudinal zone. The latter was calculated from a spatial grid of the world ocean at 30' latitude x 30' longitude resolution, and was used to indicate the availability of waters for potential coral growth. Thus, the calculated relative coral reef abundance is an approximate measure of coral reef density. We assume that relative coral abundance is bimodal and could be approximated by two normal distributions representing relative coral abundance in the northern and southern hemisphere. We fitted the two normal distributions to the observed relative coral reef abundance distribution using least-square methods so that the sum-of-square difference between the observed distribution and the sum of the two predicted distributions was minimized (Figure 10). We then assumed that, under global warming, the mean latitude of each abundance distribution

in the northern and southern hemisphere would shift north and south, respectively, while the higher latitudinal limits and the standard deviations of the distribution remained constant. Future absolute coral abundance at specific area was then calculated from:

$$CA_{i,t} = CA_{i,t-1} \cdot \frac{f(LC_i, \overline{LC}_t, \delta^2)}{f(LC_i \overline{LC}_{t-1}, \delta^2)} \qquad \dots 18)$$

where $CA_{i,t}$ is absolute coral abundance (km²) at grid cell (30' x 30') i and time (year) t. LC_i is the latitude at the centre of grid cell i where the specific area of coral occurs, and δ^2 is the standard deviation of the normal distribution function f (Figure 11).

a)   b)
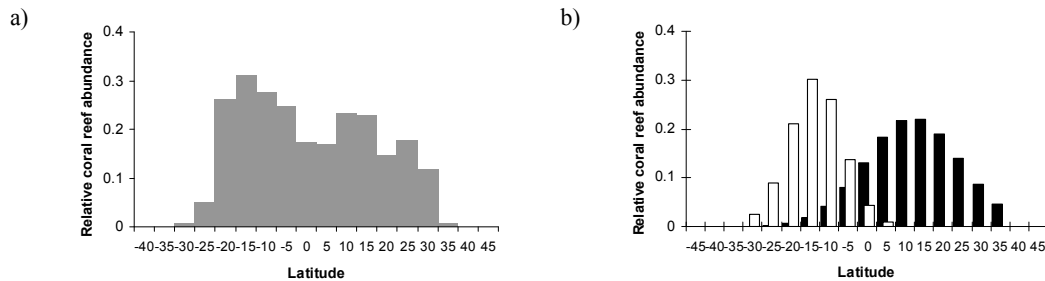
Figure 10. Relative coral reef abundance at different latitudinal zones based on: (a) observed coral reef abundance (UNEP-World Conservation Monitoring Centre 2005); (b) predicted abundance by fitting two normally-distributed relative abundance – latitude relationship with means = 10.4° and -16.4° and standard deviations = 12.36° and 6.88°. The observed northern and southern limits of coral distribution were maintained in the predicted distribution.
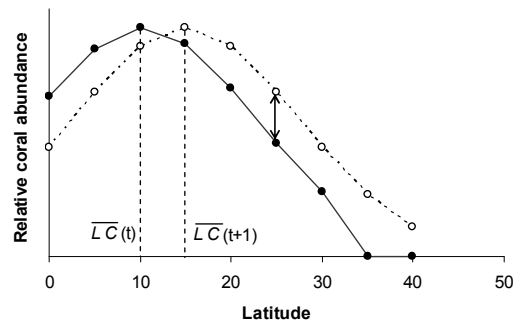
Figure 11. Schematic diagram showing the calculation of the hypothetical effects of global warming on coral abundance in the northern hemisphere. The solid line is a normal distribution obtained from fitting with observed relative coral abundance with a mean of LC(t). Assuming that mean relative coral abundance shift at a rate of (LC(t+1)-LC(t)) per year, the dotted line with open circles represents a predicted distribution of relative coral reef abundance at year t + 1. Predicted absolute coral reef area in a grid cell at latitude of 25°N would increase by a ratio as indicated by the arrows.

We simulated hypothetical changes in distribution of coral reef abundances under three scenarios: (a) no change; (b) mean relative coral reef abundance shifted at a rate of 20 km year⁻¹ (northward and southward in the northern and southern hemisphere, respectively) and (c) mean relative coral reef abundance shifted at 50 km year⁻¹ (Figure 12). We used the Sohal surgeonfish (*Acanthurus sohal*) as a case study to evaluate potential influence of changes in coral abundance under global warming on distributions of coral reef-associated species.
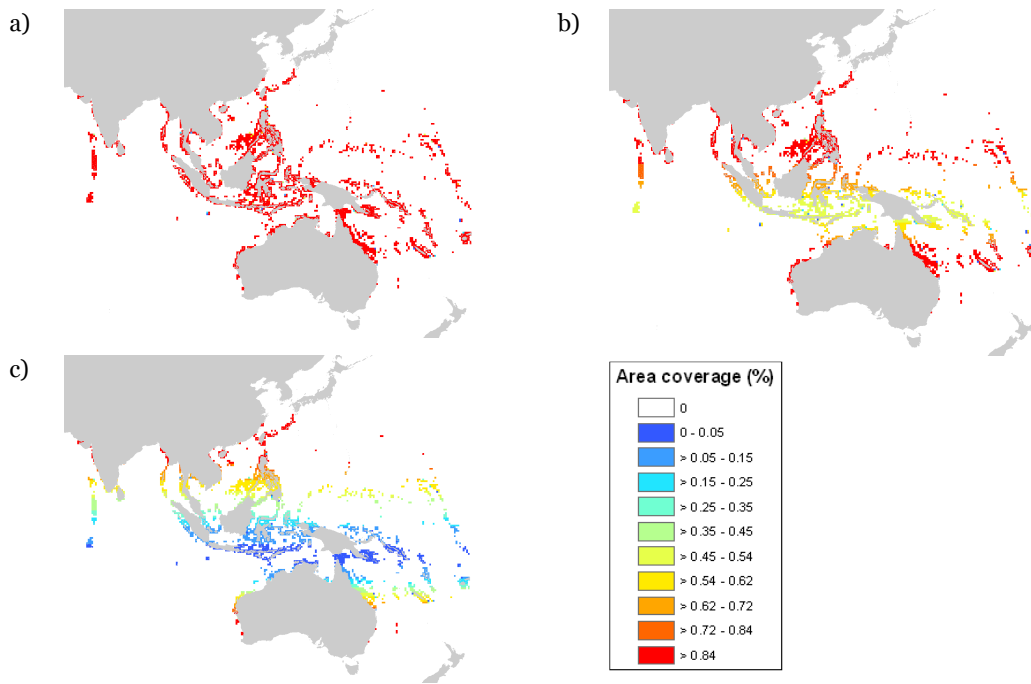
Figure 12. Simulated hypothetical changes in distribution of coral reef abundances in the Indo-Pacific region after 30 years under three scenarios: (a) no change, (b) mean relative coral reef abundance shifted at a rate of 20 km year^{-1} (northward and southward in the northern and southern hemisphere, respectively) and (c) mean relative coral reef abundance shifted at 50 km year^{-1}.

We also tested the effect of change in sea ice coverage on polar species. Both empirical and climate models suggest that sea ice coverage will continue to decrease as global temperature increases as predicted (Johannessen *et al.* 1999, 2004; Vinnikov *et al.* 1999; Flato & Boer 2001; Comiso 2002). Change in sea ice coverage can greatly affect polar ecosystems and the distribution of the associated species (Eicken 1991). For example, the reproductive grounds of krill (*Euphausia superba*), a key food source for higher predators such as penguins and whales, can be affected by reducing the area of sea ice formed near the Antarctic Peninsula (Loeb *et al.* 1997; Walther *et al.* 2002). This may also affect the distributions of the predators that depend on krill. Thus, we evaluated the sensitivity of predicted polar species distributions to changes in sea ice coverage. We assumed that the polar sea ice edges retreat at a rate of 5 km year^{-1}. This is not an attempt to mimic realistic sea ice changes. Instead, the hypothetical scenario allows us to explore the potential effects of sea ice change on distribution of polar species. Realistic changes in sea ice coverage predicted from climate model will be used in the future.

RESULTS

Simulated shift in distribution

Small yellow croaker (Larimichthys polyactis)
Simulations using the two hypothetical scenarios of increase in global sea water temperature predicted that distributions of the Small yellow croaker would shift northward in 30 years (Figure 13, 14). Both the centroid and latitudinal range limits of the distribution shifted in all positive warming scenarios. The original distribution of Small yellow croaker was restricted to the East China Sea. However, as sea water temperature increased, the northern range limit reached into the Bohai Sea and the coast of Japan (main islands), which were not previously occupied by this species. Simultaneously, the southern range limits shifted north from the Taiwan Strait. The degree of range shift also differs between coast and offshore regions. Under a stronger warming scenario (scenario 2), the northern range limit shifted by 5° latitude while the centroid of the distribution shifted by around 3° northward (Figure 14).
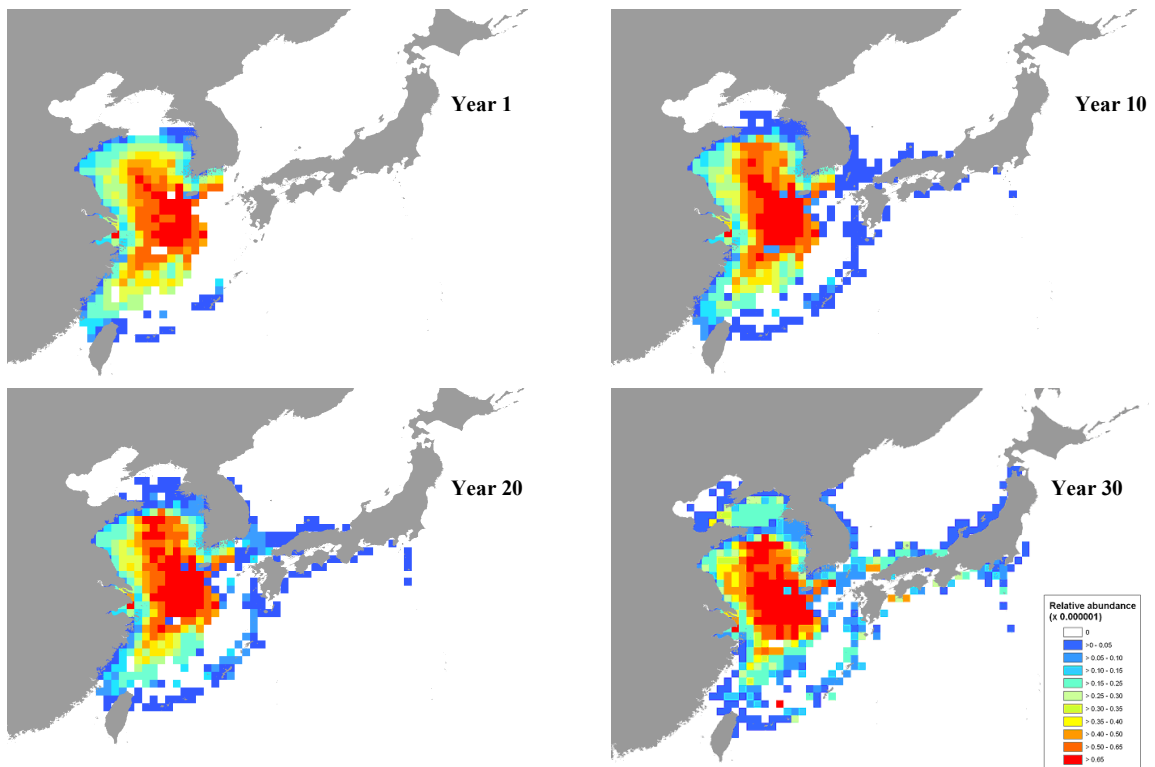
Figure 13. Simulated changes in distribution of Small yellow croaker after 1 year (upper left), 10 years (upper right), 20 years (lower left) and 30 years (lower right) under a hypothetical mild level of ocean warming (scenario 1).
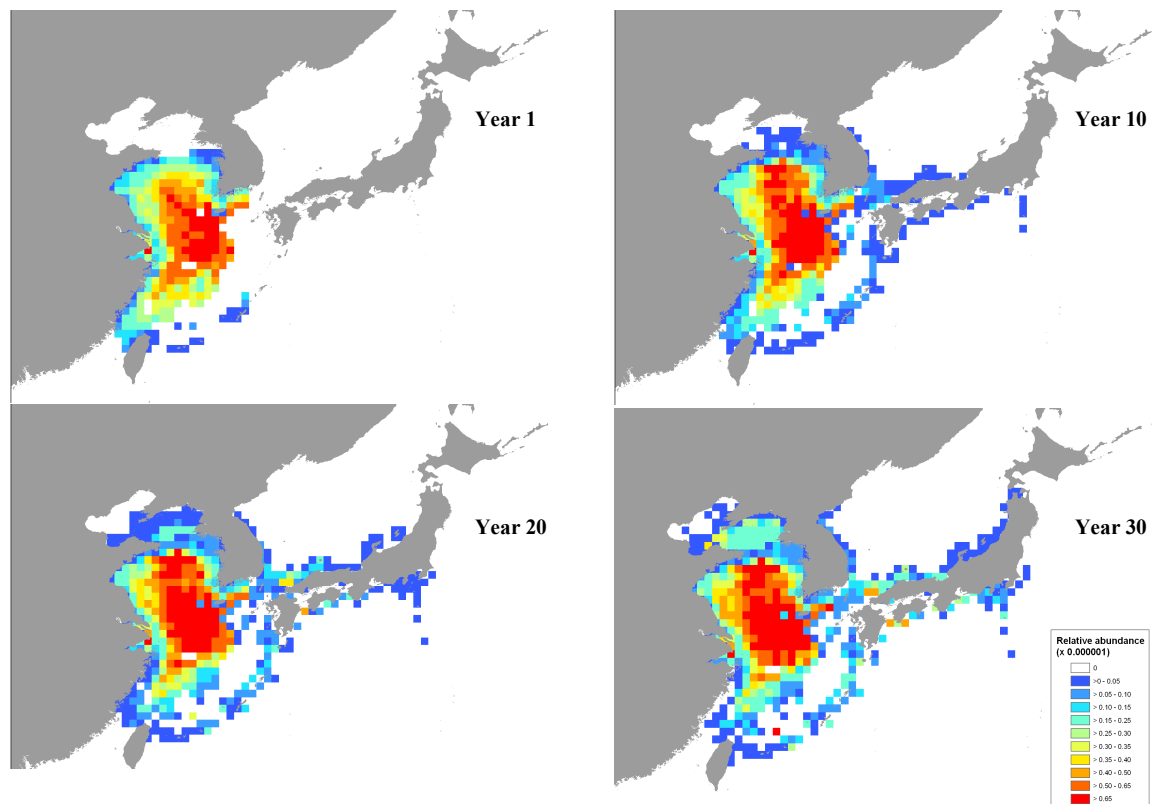
Figure 14. Simulated changes in distribution of Small yellow croaker after 1 year (upper left), 10 years (upper right), 20 years (lower left) and 30 years (lower right) under a hypothetical strong level of ocean warming (scenario 2).

Nassau grouper (Epinephelus striatus)

Similar patterns of range shift were observed for Nassau grouper, which ranges across the equator (Figure 15 & 16). Under both milder and stronger warming scenarios, Nassau grouper generally moved away from the equator after 30 years, while their relative abundance increased in higher latitudes. For example, abundance increased almost five-fold in southern coast of Brazil. Also, the southern range limit extended further into Uruguay. Particularly, in the stronger warming scenario (Figure 16), relative abundance of inshore populations from Venezuela to northern Brazil was much reduced. On the other hand, relative abundance in the southeast and east coast of USA increased.
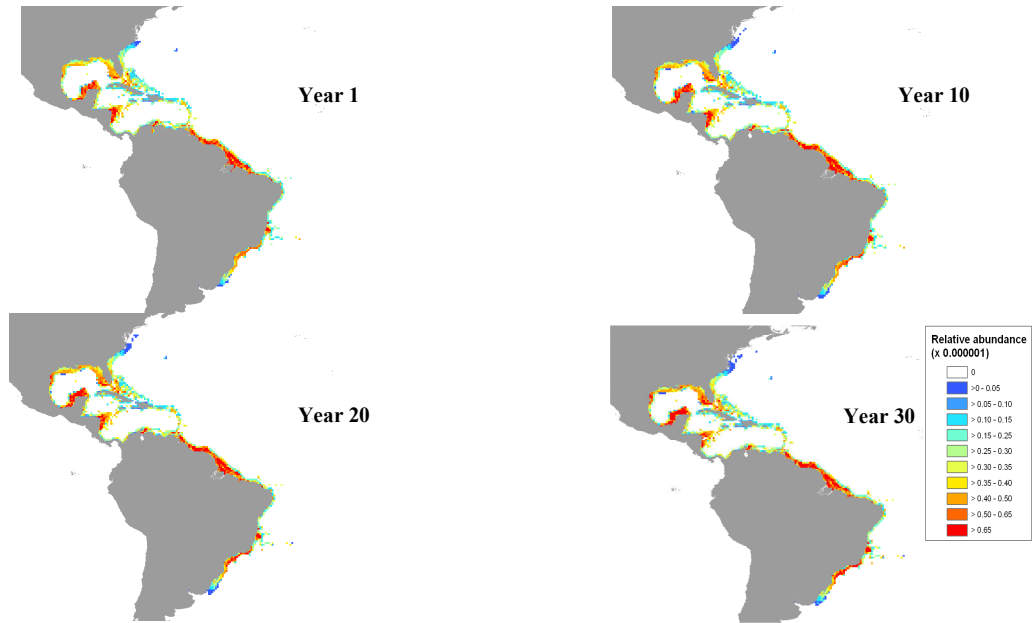
Figure 15. Simulated changes in distribution of Nassau grouper after 1 year (upper left), 10 years (upper right), 20 years (lower left) and 30 years (lower right) under a hypothetical mild level of ocean warming (scenario 1).
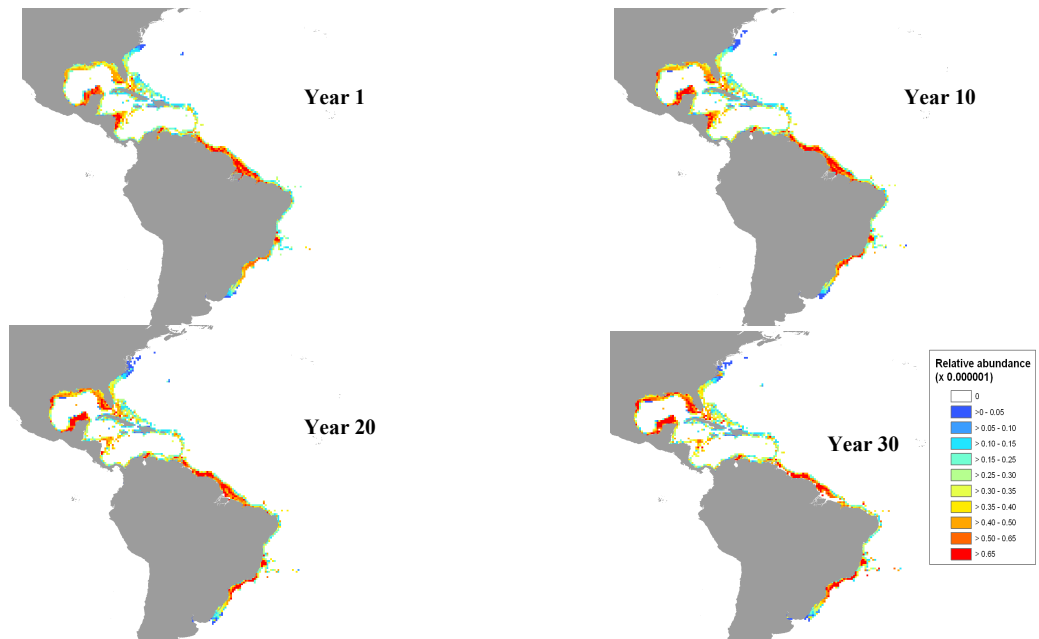
Figure 16. Simulated changes in distribution of Nassau grouper after 1 year (upper left), 10 years (upper right), 20 years (lower left) and 30 years (lower right) under a hypothetical strong level of ocean warming (scenario 2).

Polar cod (Boreogadus saida)
Polar cod was found to be sensitive to the warming scenarios and the model predicted that it would be extirpated in most of its range even under the milder warming scenario (Figure 17). This is due to its occurrence in the Arctic Ocean, which largely precludes it from moving northwards. Polar cod was predicted to be extirpated around Greenland and its abundance was largely reduced in other parts of the Arctic Ocean after 30 years of hypothetical warming.
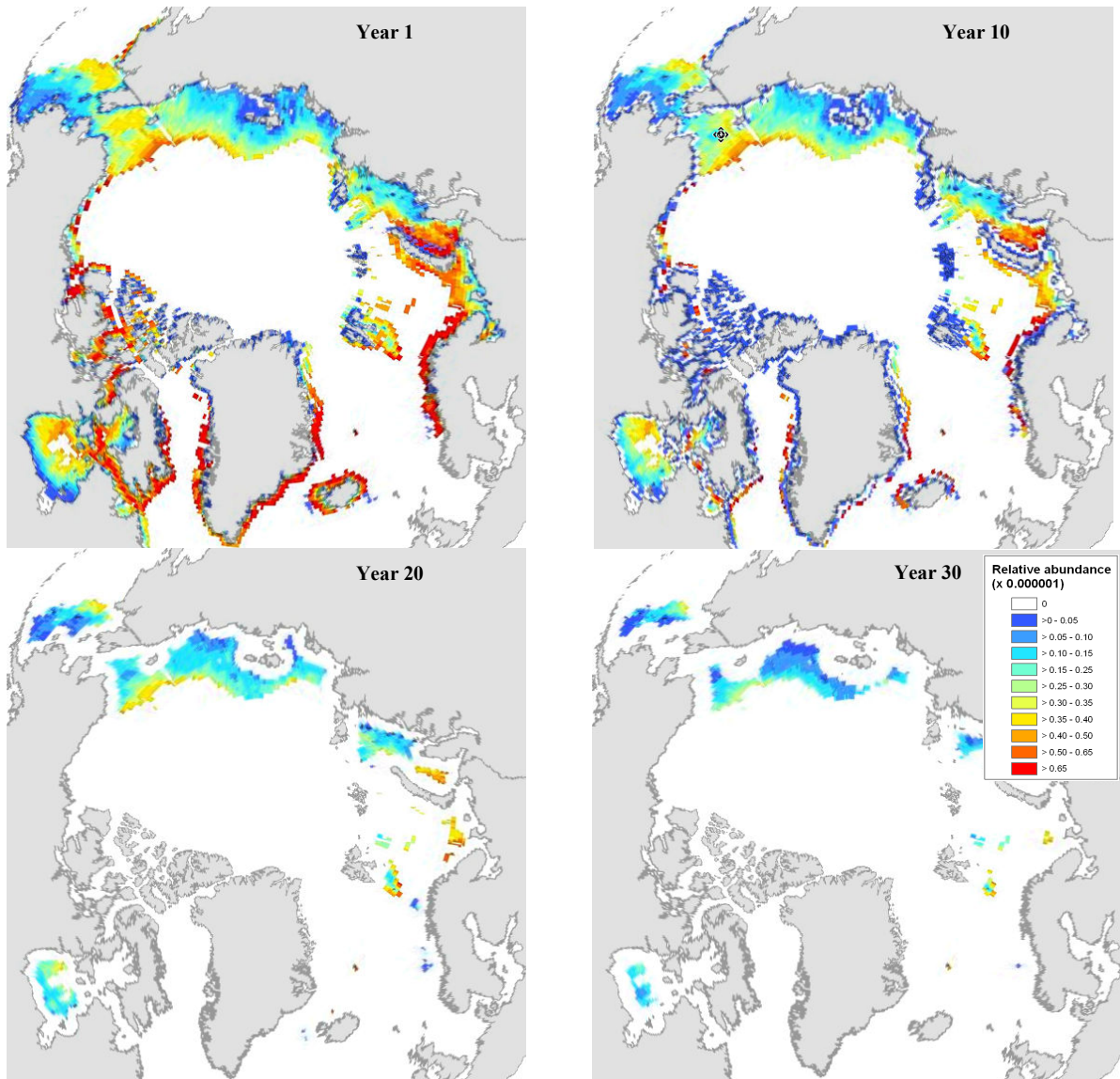
Figure 17. Simulated changes in distribution of Polar cod after 1 year (upper left), 10 years (upper right), 20 years (lower left) and 30 years (lower right) under hypothetical scenarios of ocean warming (scenario 1) and retreating sea ice edge at a rate of 5 km per year. Polar cod is extirpated from most of its range in 30 years.

Antarctic toothfish (Dissostichus mawsoni)
Under a mild ocean warming and with the ice edge retreating at a rate of 5 km per year, the distribution range of Antarctic toothfish was predicted to contract (Figure 18). As this species only occurs around Antarctica, it cannot expand its southern limits when sea water temperature increases. Also, we assume that Antarctic toothfish has an affinity to sea ice edge. The retreating sea ice also contributed to the range contraction. Under the stronger warming scenario, the distribution range of Antarctic toothfish becomes so restricted that it would induce extinction in 30 years.
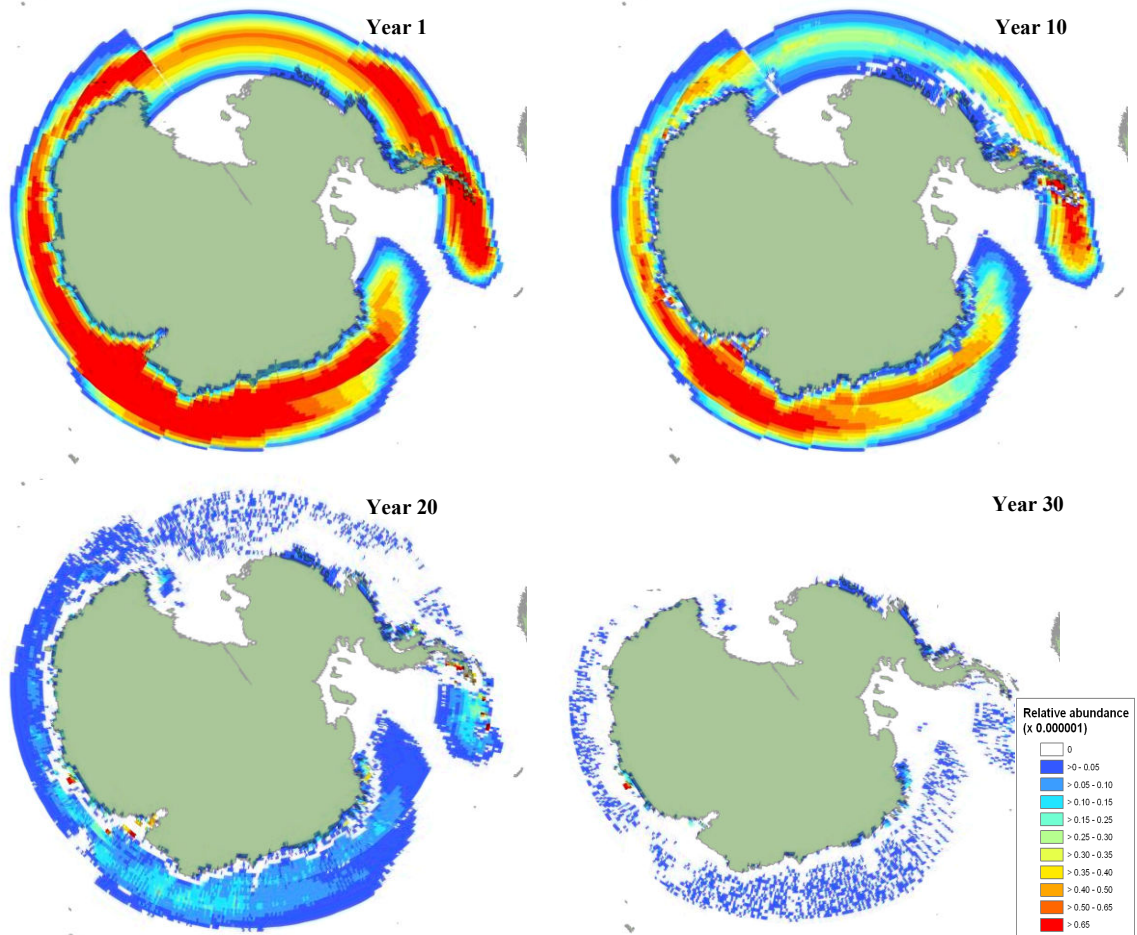
Figure 18. Simulated changes in distribution of Antarctic toothfish after 1 year (upper left), 10 years (upper right), 20 years (lower left) and 30 years (lower right) under hypothetical scenarios of ocean warming (scenario 2) and retreating sea ice edge at a rate of 2 km per year. Antarctic toothfish is predicted to become extinct in 30 years under the specified scenario.

Atlantic cod (Gadus morhua)

A strong global warming scenario (scenario 2) resulted in a general northward shift of distribution of Atlantic cod (Figure 19). In the northwest Atlantic, our model predicted that the abundance of the southern cod stocks (Georges Bank, Gulf of Maine, and Scotian Shelf) would decline. In the northeast Atlantic, relative abundance of cod declines in the North Sea, Irish Sea, Celtic Sea and Norwegian Sea. On the other hand, the relative abundance of the Icelandic, Faroe Island and Barents Sea cod stock increased. Also, the distribution of cod extends further into the Arctic as the ice sheet retreats.
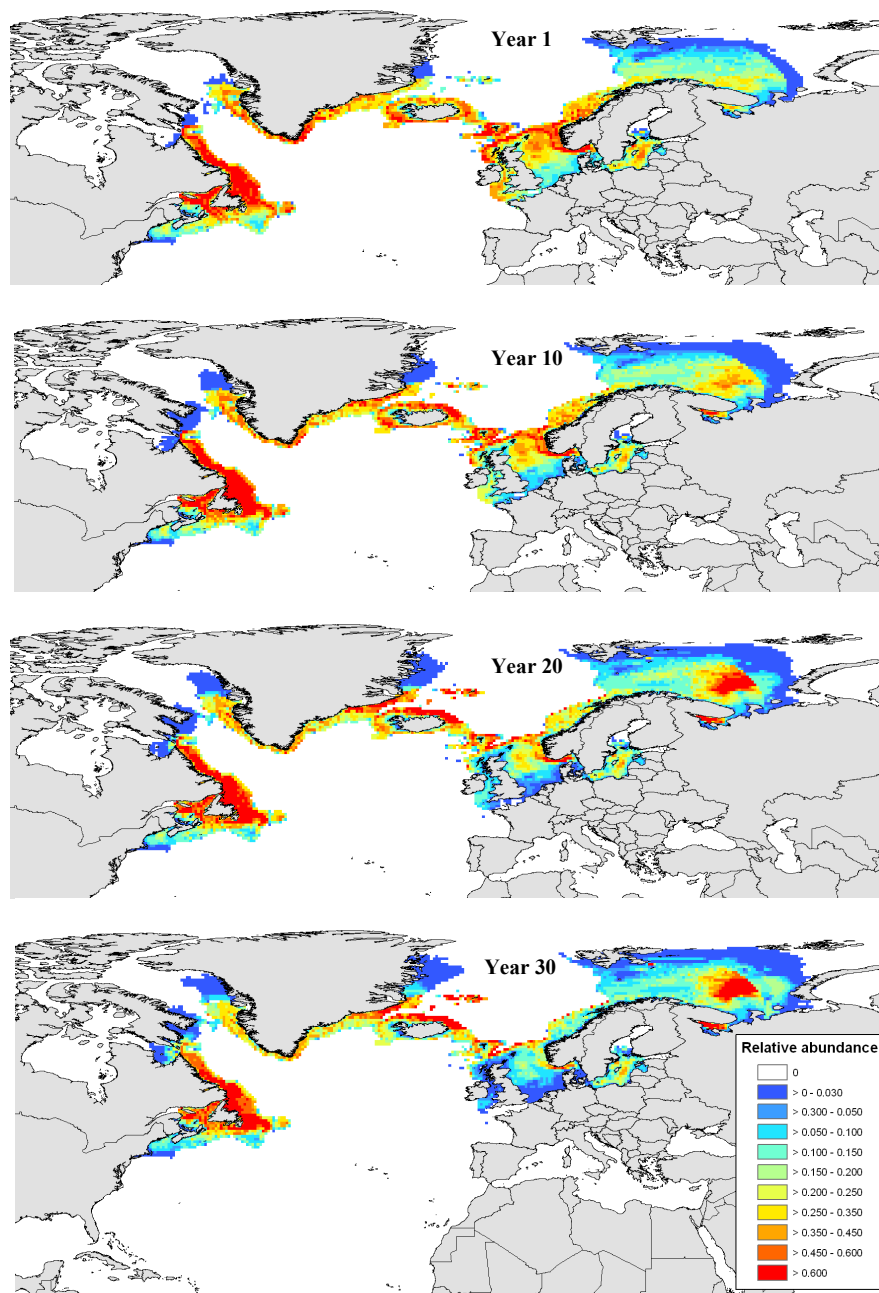
Figure 19. Simulated changes in distribution of Atlantic cod after 1 year (upper left), 10 years (upper right), 20 years (lower left) and 30 years (lower right) under hypothetical scenarios of ocean warming (scenario 2).

Western Australian Rock lobster (Panulirus cygnus)

Distribution range of Western Australian rock lobster was predicted to shift southward under the sea temperature warming scenarios (Figure 20). The centroid of its latitude distribution shifted south by approximately 1º and 3º in 30 years under the milder and stronger warming scenarios, respectively. Moreover, the southern range limit extended further into the southwest of the Australia continent.
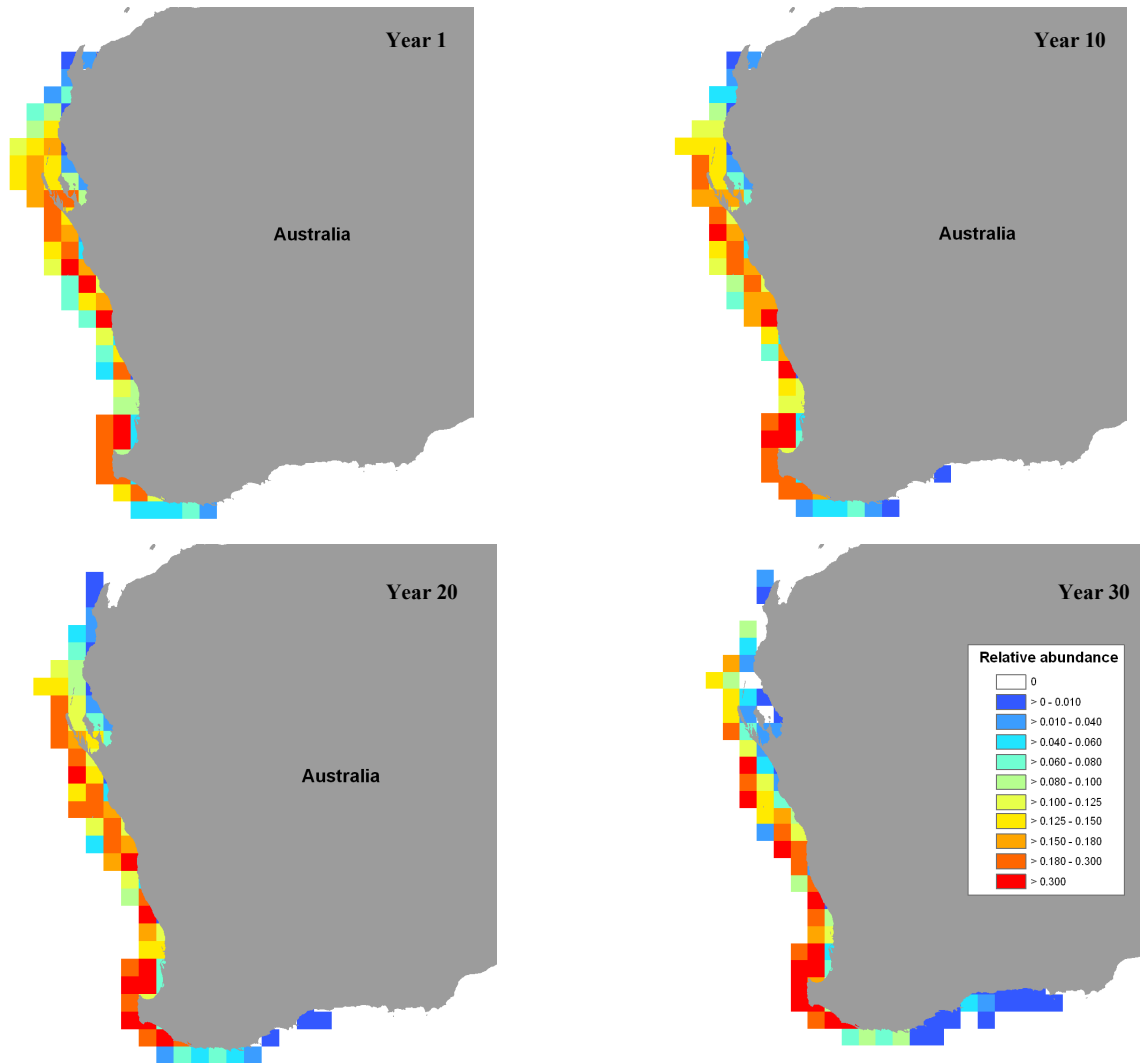
Figure 20. Simulated changes in distribution of Western Australian rock lobster after 1 year (upper left), 10 years (upper right), 20 years (lower left) and 30 years (lower right) under a hypothetical strong ocean warming (scenario 2).

Australian ruff (Arripis georgianus)

Similar to Western Australian rock lobster, when global sea water temperature increases, the distribution range of Australian ruff moves to cooler waters in the south (Figure 21). Australian ruff is a pelagic species and its seasonal movements are accounted for our simulation model. Our results suggest that the summer distribution of Australian ruff is more sensitive to temperature changes in summer (as indicated from the faster rate of southward shift) than in winter.
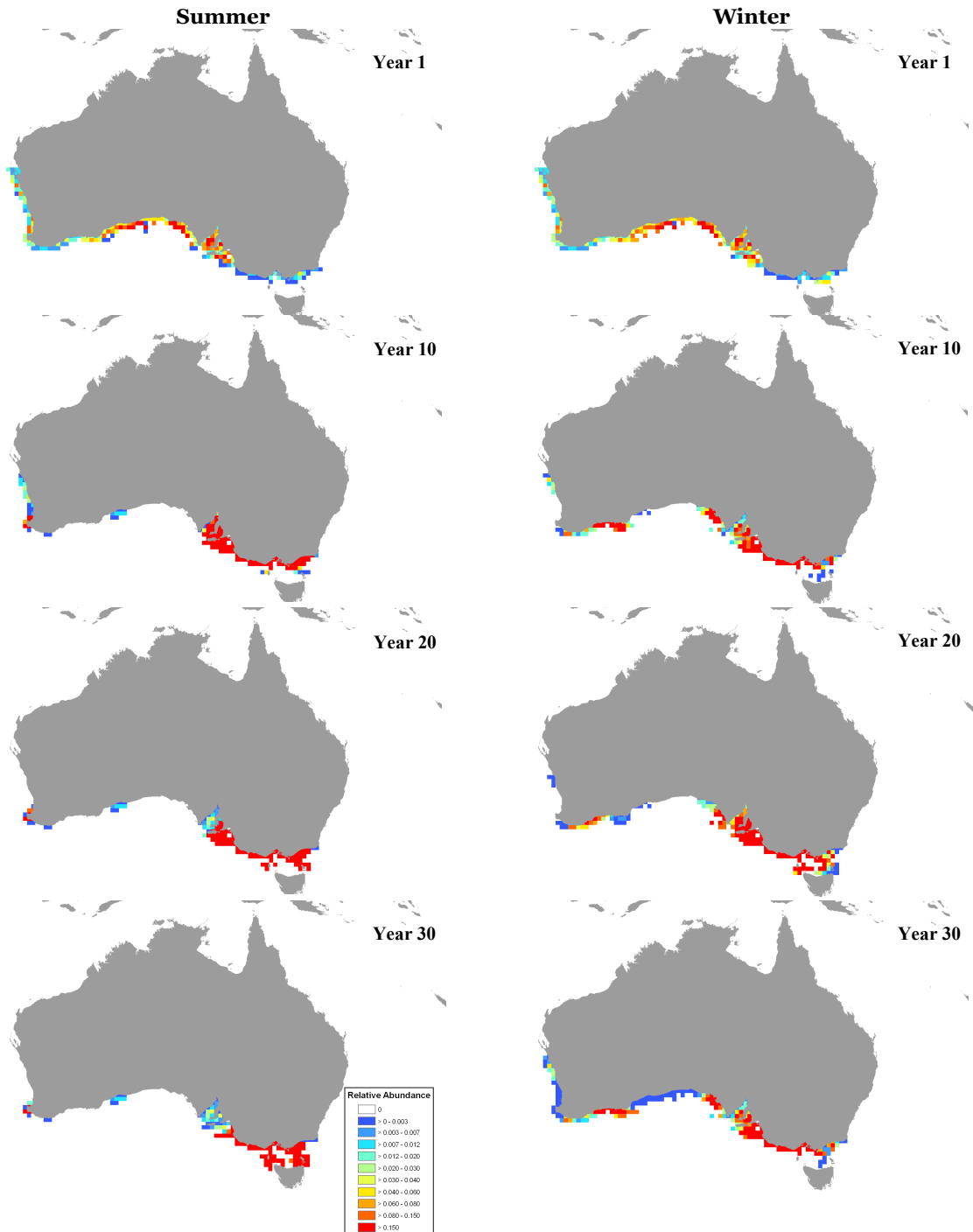
Figure 21. Simulated changes in distribution of Australian ruff in summer (left panel) and winter (right panel) after 1 year, 10 years, 20 years and 30 years under a hypothetical strong ocean warming (scenario 2).

Sensitivity analysis

Larval dispersal

Dispersal and recruitment of fish larvae are sensitive to the larval mortality and settlement rates specified in the larval dispersal model (Figure 22). Again, recruitment is defined here as the settlement of pelagic larvae. Absolute level of total recruitment is controlled by the natural mortality rate of the larvae. Thus, species with extended pelagic larval duration are generally more sensitive to the specified mortality rate. Larval settlement rate strongly affects the distribution of settled larvae. In the case of Small yellow croaker, a high settlement rate (15% day^{-1}) results in strong local recruitment (i.e., recruitment to the adult distribution range), while a low settlement rate (1% day^{-1}) results in wider range of larval dispersal (Figure 22).

a)

b)

c)
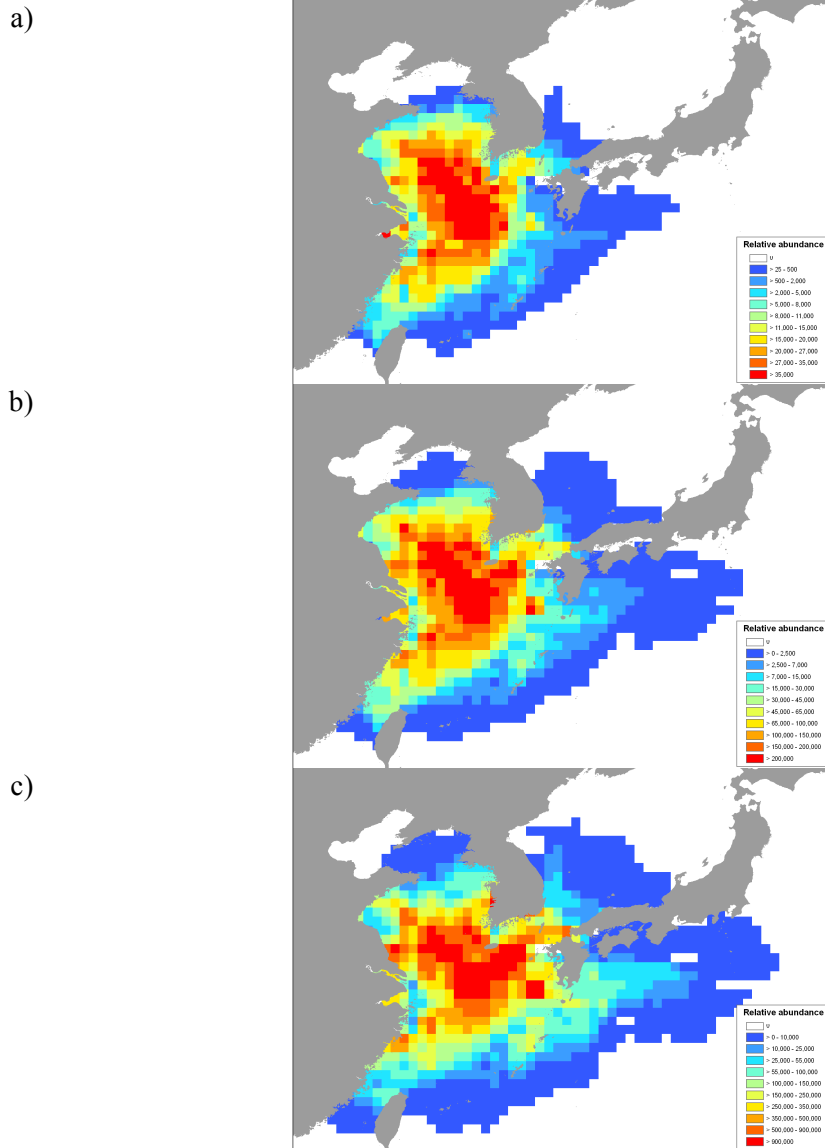
Figure 22. Simulated dispersal of larvae of Small yellow croaker from the current species distribution predicted by Close *et al.* (2006). Alternative larval settlement rates (a) 15% day^{-1}, (b) 7.5% day^{-1} and (c) 1% day^{-1} representing scenarios with strong and weak local larval recruitment, respectively.

Low larval settlement generally accelerates the movement rate and increases the extent of distribution shift (Figure 23). Under a lower larval settlement rate of 0.01 year^{-1} (i.e., larvae were allowed to travel further before settlement), distribution of Small yellow croaker extends further northeast to the coast of Japan after 30 years under a strong warming (scenario 2). The higher dispersal ability enables the fish to occupy such habitat. On the other hand, the general pattern of distribution shift is similar to the scenario with higher larval settlement rate (0.15 year^{-1}).
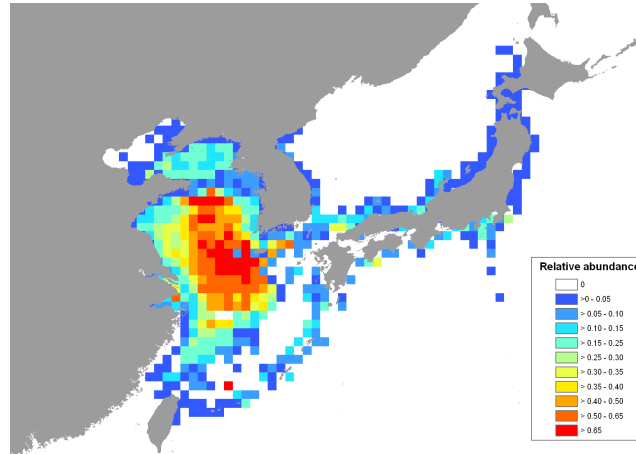
Figure 23. Predicted distribution of Small yellow croaker with low larval dispersal rate (0.01 year^{-1}) after 30 years of strong warming (scenario 2).

A high larval production rate or alternative settings of migration sensitivity parameter (k) results in slight changes in the prediction distribution of Small yellow croaker after 30 years under a strong warming scenario (Figure 24). Relative abundance is slightly higher in the newly-occupied areas in the north. The effect is similar to those obtained from a low larval settlement rate or low larval mortality rate. Alternative settings of migration sensitivity parameter (k) (default = 2, low = 0.5, high = 5) only slightly affect the prediction distributions of Small yellow croaker (Figure 25).
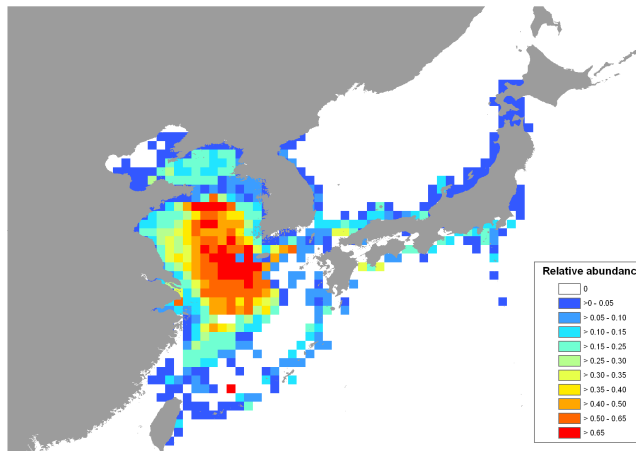
Figure 24. Predicted distribution of Small yellow croaker with high larval production rate (0.5 times parent biomass per year) after 30 years of strong warming (scenario 2).
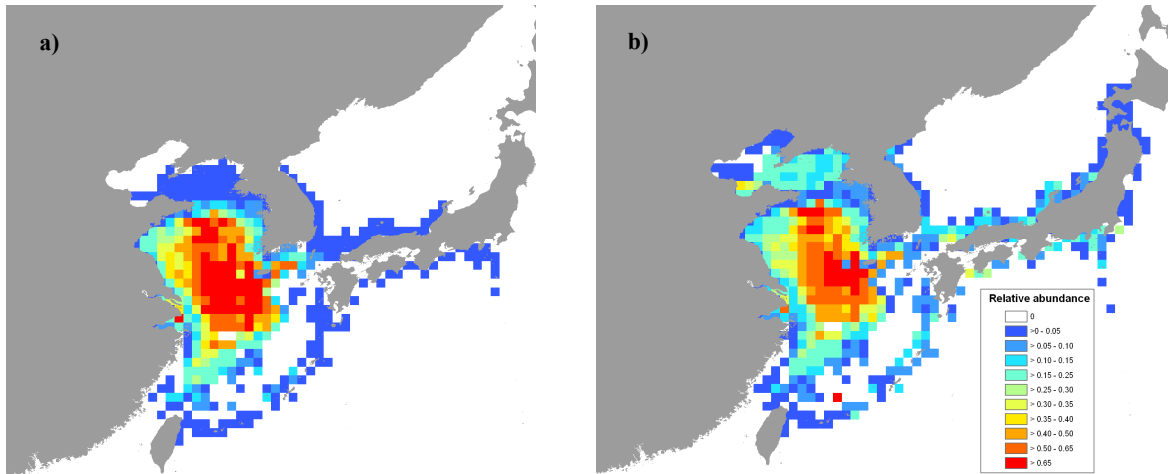
Figure 25. Predicted distribution of Small yellow croaker after 30 years of strong warming (scenario 2) with (a) low migration sensitivity (k = 0.5) and high migration sensitivity (k = 5) (default value of k = 2).

Intrinsic rate of increase

The intrinsic rate of population increase (r) specified in the model does not appear to have strong effects on the predicted change in distribution range of Small yellow croaker (Figure 26). Under both low and high values of r (0.8 and 3 year^{-1}, respectively) and hypothetical strong warming (scenario 2), the extents of range shift after 30 years of simulation are generally the same. However, with lower r, relative abundance in the newly-occupied northern region is lower than predictions with higher r. Predicted relative abundance around the southern limits is similar between simulations with low and high r (Figure 26).
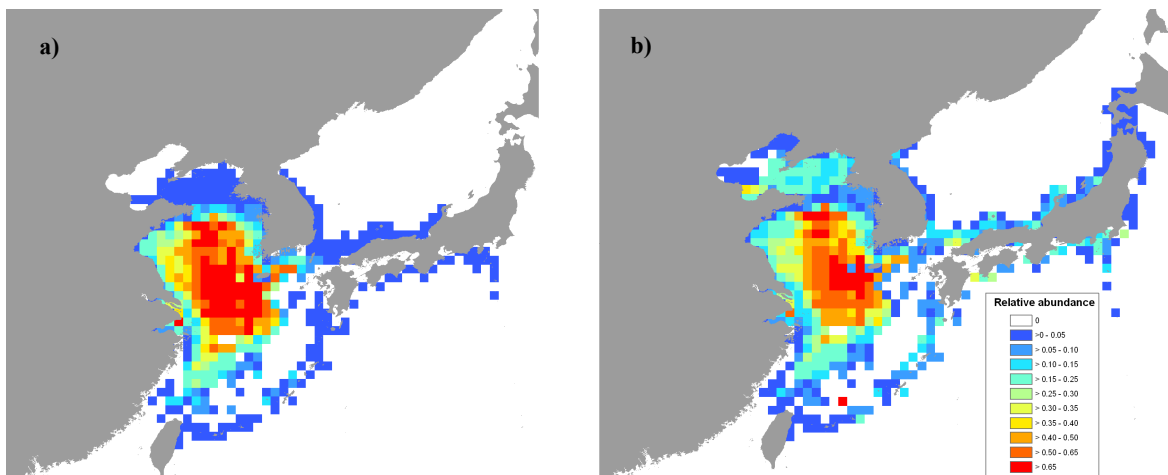
Figure 26. Predicted distribution of Small yellow croaker after 30 years of strong warming (scenario 2) with intrinsic rate of population increase of (a) 0.08 year^{-1} and (b) 3 year^{-1}.

Coral reef shift

A hypothetical shift in coral reef distribution has little effect on the predicted distribution of Sohal surgeonfish (*Acanthurus sohal*) (Figure 27). Sohal surgeonfish is a coral reef fish, although it also occurs in habitats such as rocky bottoms. Under 30 years of hypothetical warming, the relative abundance of inshore populations of Sohal surgeonfish at low latitude is predicted to be much reduced. Conversely, its relative abundance at higher latitude increased. However, coral reefs, overall, had small effects on the simulated distributions.
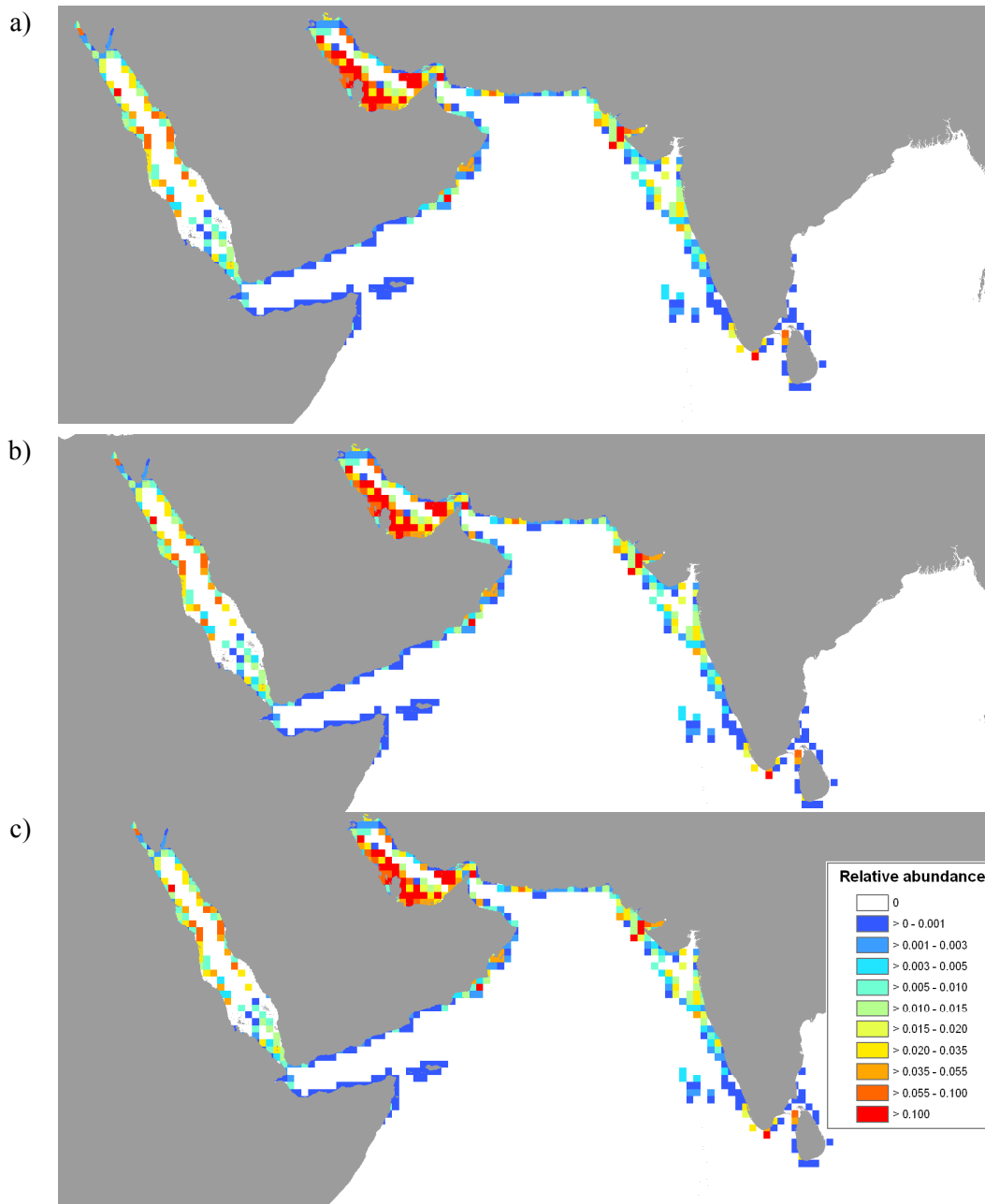
Figure 27. Predicted distribution of Sohal surgeonfish (*Acanthurus sohal*) after 30 years under three hypothetical scenarios (a) no change in coral abundance, (b) coral reef shifts at a rate of 20 km year^{-1}, and (c) coral reef shifts at a rate of 50 km year^{-1}. A mild warming (scenario 2) was used in the simulations.

Discussion

Test simulations

The simulation model presented in this report allows quantitative predictions of the effects of climate change on distributions of all commercially exploited marine species at a global scale. Unlike conventional bioclimate envelope models that predict changes in species distribution only from identified bioclimate envelope (Pearson & Dawson 2003), this model incorporated population and ocean current dynamics in simulating distribution changes. These components are important in shaping distributions of marine organisms (Gaylord & Gaines 2000; Bradbury & Snelgrove 2001). For instance, range limits could be caused largely by oceanographic discontinuities (Gaylord & Gaines 2000). Also, organisms' life history traits may affect their responses (in terms of rate and magnitude) to environmental changes (Perry *et al.* 2005). Thus, their inclusions allowed more realistic simulations of responses to climate change scenarios.

Our model explicitly represents both non-interactive (additive) and interactive (multiplicative) effects of climate influence on population dynamics (Stenseth *et al.* 2002). Example of non-interactive or additive effects included increased net influx of new migrants (through adult movement or larval dispersal) as environmental conditions in an area became more favourable to the species of interest. In the case of Small yellow croaker, increased temperature reduced the mortality of migrants to the previously unoccupied Bohai Sea. Thus, relative abundance of the species increased in Bohai Sea through the addition of new migrants. Simultaneously, carrying capacity of Small yellow croaker increased in the northern range limit and decreased in the southern range limit as temperature increased. These reduced the strength of density dependence in the north, and increased it in the south. Thus, relative abundance of Small yellow croaker shifted gradually towards the north under both (mild and strong) warming scenarios. Responses to the warming scenarios were similar in the case of Nassau grouper.

Some species may be unable to adapt to global warming by range shifting and may be extirpated. Antarctic toothfish occurs around the Antarctic. In our model, as sea temperature increased, the species was unable to shift its range further south, into cooler waters. As sea temperature increased outside the tolerance limits of Antarctic toothfish, suitable habitat that was reachable by the species gradually declined. Eventually, the species was extirpated as suitable habitats disappeared. Thus, if the magnitude of warming is large enough, it is likely that some species will be rendered extinct.

The predicted distribution of Atlantic cod under hypothetical warming scenarios agreed with predictions independently conducted by others (e.g., Drinkwater 2005). Based on observed relationship between recruitment strength and sea-bottom temperature, Drinkwater (2005) predicts that, if sea water temperature increased, the Celtic and Irish Seas stocks of Atlantic cod would disappear, while the southern North Sea and Georges Bank stocks would decline. Cod distribution may also shift northwards along coastal Greenland and Labrador and to the Barents Sea and the Arctic Ocean (Drinkwater 2005). Such predictions generally agree with our simulation results, which provided some support to the validity of our model.

Changes in distribution ranges predicted from climate model generated data will obviously be more complex than the test simulations presented in this study. Here, we assumed a monotonic increase in sea temperature (bottom and surface). However, predictions from climate models are more complex than our hypothetical scenarios. For instance, warming may show hemispheric asymmetry, with more warming in the northern high latitude than in the south, although the evidence is not yet conclusive (Flato & Boer 2001). Also, rate of warming in different ocean basins may vary. Recorded sea water temperature over the last half-century showed different rates of increase in different oceans (Levitus *et al.* 2000). Moreover, we assumed that ocean currents were in a steady-state. However, ocean currents will change with global climate (Rahmstorf & Ganopolski 1999; Vellinga & Wood 2002), which will affect distributions and population dynamics of marine species (Gaylord & Gaines 2000; Walther *et al.* 2002).

In the future, predicted changes in physical attributes (e.g., sea bottom and surface temperature, ocean advection fields) from year 2000 to 2100 will be provided through the kindness of Dr Jorge

Sarmiento and his collaborators at the Atmospheric and Oceanic Sciences Program, Princeton University. The data are simulated from the NOAA's Geophysical Fluid Dynamics Laboratory Coupled Model, version 2.1 (GFDL's CM2.1 model) under three scenarios of future CO_2 emission: (1) drastic reduction of CO_2 from the present, (2) moderate reduction of CO_2 from the present, (3) maintenance at year 2000 level. When we use such data in our simulations, predicted patterns of range-shifting of the studied species should be more realistic.

Model uncertainty

Because of its broad geographic and taxonomic scope, it was unavoidable that we had to make various assumptions in our model, to reduce the number of required parameters and simplify the dynamics of the system to a practical level. Many assumptions are in fact inherent in most bioclimate envelope models developed to study the effects of climate change (Pearson & Dawson 2003). The major assumptions, and the potential implications for predictions from our model, are detailed here.

Biotic interactions

The model did not explicitly account for inter-specific interactions. Species within a community may respond differently to climate change (Walther *et al.* 2002). For instance, distributions of predators and their preys may shift at different rates as climate-linked oceanographic conditions change. This can result in reduced range-overlap and may disrupt existing biotic interactions (e.g., predation) in a community (Murawski 1993; Hughes 2000; McCarty 2001; Walther *et al.* 2002). Thus, a predator with high prey specificity may not find enough food if its prey's range does not shift along with its own. Moreover, food web interactions may affect the rate of climate-induced distribution shift. For example, the rapid expansion of distribution range of the Humboldt squid (*Dosidicus gigas*) in the eastern North Pacific may be linked to changes in climate-related oceanographic conditions and the depletion of their competitors and predators (Zeidberg & Robison 2007). Rapid invasion of predators such as the Humboldt squid may destabilize the ecosystem as potential preys may be exposed to increased predation risk. These trophic dynamics may modify the patterns of range shifts predicted by our model.

Incorporation of biotic interactions in predicting effects of climate change at multi-species or ecosystem levels would be the next step of this modelling exercise. The model developed in this study targets a wide range of exploited marine species at global scale and is aimed to predict general patterns of potential responses of individual species to climate change scenarios. Predictions on individual species can later be incorporated into dynamic multi-species/ecosystem models such as Ecopath with Ecosim and Ecospace (Walters *et al.* 1997, 1999; Pauly *et al.* 2000). The tropho-dynamic models can then evaluate the potential effects of climate changes on biotic interactions and on structure of the ecosystem.

Evolutionary changes

Species with high rates of evolutionary changes may adapt to changing climates and thus affect their patterns of range-shifting. Our model implicitly assumes that rates of adaptation are slower than extinction rates (niche conservatism) (Pearson & Dawson 2003). On the other hand, evolutionary responses to climate changes are shown in some insects (Thomas *et al.* 2001). For instance, two butterfly species have increased the variety of habitat types that they can colonize. Also, fractions of longer-winged (dispersive) individuals of two bush cricket species increased (Thomas *et al.* 2001). In these examples, the dispersal ability of the species was enhanced by evolutionary changes. Although evidence on genetic changes in marine species that are directly related to climate change is scarce, changes in life history traits in response to extrinsic factors (e.g. fishing) that may be phenotypic or genetic are more common (Law 2000). Phenotypic changes in response to fishing included increased somatic growth, reduced age at first maturity and decreased body size (Rijnsdorp 1993; Law 2000; Kraak 2007). However, these changes most likely affect the rate of range-shifting, but not the magnitude of the shift. On the other hand, evidence from Pleistocene glaciation indicates that species more often responded to climate change ecologically, by shifting their ranges, rather than evolutionarily, through local adaptation (Parmesan *et al.* 2000). Thus, although our model may underestimate the rate of range shift by

ignoring potential evolutionary changes that may increase species' dispersal ability, model results can be considered conservative predictions of responses to climate change.

Population dynamics

The complexity of population dynamics may affect species' responses to climate change. The incorporation of population dynamics in our bioclimate envelope model is an advance from previous attempts to predict climate change-induced distribution shift (Pearson & Dawson 2003). However, considering the resolution of the model, the scale of the study and the limited availability of model parameters, simplifications were made to the population dynamic models. Firstly, we modelled populations as homogenous biomass pools. Thus the model did not explicitly represent population and age structures. Populations of a species may have different life history and show different adaptations to environmental changes. For instance, in some species, individuals with bigger body size tend to have a more unstable range limit and to be more likely to shift in range than those with a smaller body size (Roy *et al.* 2001). Secondly, we represented larval production and recruitment by a linear relationship with biomass-pool and a constant larval survival and settlement rate. However, dynamics of larval production, survival and recruitment are generally non-linear and controlled by complex factors that include climate, oceanography and ecology. Thirdly, except for pelagic species, our model simulated annual averaged dynamics of populations. However, seasonal dynamics may be important in understanding responses to climate change for non-pelagic species as well (Barbraud & Weimerskirch 2003).

Given the uncertainties of the parameters, the predicted range-shifts were generally robust. The magnitude of predicted distribution range-shift was similar under alternative values for the intrinsic rate of population increase, larval dispersal and settlement. The extent of the distribution range in the model is determined primarily by the available bioclimate envelope and is thus less dependent on population dynamics. However, the rate of range-shifting may be more sensitive to the specified population dynamics. Species with higher dispersal ability are able to colonize suitable habitats at a faster rate. Also, higher larval production (or reduced larval mortality) also increases the rate of colonization. On the other hand, climate change (e.g., temperature changes) should generally operate at a much longer time scale (decade) than species' population dynamics (year). Thus, predictions from our model should be largely insensitive to population parameters. This is backed by the results from the sensitivity analysis conducted in this study, which generally showed that simulated changes in distribution ranges in 30 years were insensitive to the specified population parameter values.

Our model did not represent density-dependent changes in environment preferences. Species' preferences for habitats may change with population density. For instance, Atlantic cod in the southern Gulf of St. Lawrence tended to occupy colder water when its abundance was high. Such density-dependent shifts in spatial patterns may be a response to decreased food availability by lowering density-independent energy costs (Swain & Kramer 1995). However, if the current species distribution range has captured the full temperature tolerance range of the species, such density-dependent responses should have small effect on predicted distribution range from our model under various climate change scenarios. On the other hand, should the species be able to move to colder habitats from those depicted by the current range because of density-dependent effects, the prediction from our models will be conservative. Density-dependent movement to colder habitats may increase the distribution range if climate change increases the strength of density-dependent competition for food.

Extrinsic factors

Our model assumes that the current distribution of a species reflects its temperature preference and tolerance limits. However, factors other than those explicitly considered here may determine species distribution (Samways *et al.* 1999). Thus, a species' distribution range may be well within its physiological temperature limits. Then, predictions from our model would over-estimate the responses of the species to temperature changes. On the other hand, sea temperature is shown to be a principal factor determining distributions, abundance and physiology of fish species (Pörtner 2001; Roessig *et al.* 2004). Other climate factors that may potentially affect marine fishes and

invertebrates but which are not explicitly incorporated in our model include productivity, salinity, pH, seawater chemistry, UV radiation and sea level. Productivity is partly dealt with in our model as it is correlated with temperature. Salinity, pH, seawater chemistry and sea level may have stronger influence on intertidal or strongly coastal species. Effects on more oceanic species, which represent the majority of commercially-exploited species, are generally less important than temperature. UV radiation may affect survival of pelagic larvae. However, predicted range-shifts from our model appeared to be largely insensitive to larval survival rate. Thus, although fine-scale predictions from our model may be uncertain, predictions at large (global) scale should be robust to parameter uncertainty.

Potential shifting of habitats

Predictions from our model were generally robust to the potential shift of physical habitats. Physical habitats that marine species may be associated to can shift in space under climate change, e.g. coral reefs (Hoegh-Guldberg 1999; Hughes *et al.* 1999). However, the overwhelming majority of the commercially-exploited species that are included in the UN Food and Agriculture Organization (FAO) fisheries statistics, and hence in the *Sea Around Us* database, do not occur exclusively on coral reefs. They were mostly reef-associated species that could inhabit other complex physical structures such as rocky reefs. Distributions of these alternative physical structures were generally not affected by climate change. Thus, at the scale of our model (30' latitude x 30' longitude grid), effects of shift in physical habitat such as coral reefs on the associated (commercially-exploited) species should not be apparent. On the other hand, such habitat effects on species distribution may be important at local scale.

Future improvements

In the future, the model will account for the effect of changes in salinity on species' distribution ranges. Salinity can determine the distribution of marine fishes and invertebrates (Helfman *et al.* 1997; Edgar and Last 1999; Blaber 2000) and global warming may result in changes in sea water salinity (Munk 2003). For example, regional climate models predict reduction in the salinity of the Baltic Sea following increase in river run-off (Omstedt *et al.* 2000; Meier 2002; Meier & Kauker 2003). Species that are adapted to waters with high salinity may disappear from such regions (Roessig *et al.*, 2005). To incorporate the salinity factor into the model, we will categorize marine fishes and invertebrates into different salinity tolerance levels. We will also generate habitat maps of species' preferred sea water salinity levels based on current and predicted sea water salinity and species' salinity tolerance limits. Then, we can incorporate salinity as a habitat factor in the algorithm that account for species habitat affinity (e.g. coral reef) in simulating future distribution ranges.

Moreover, we will incorporate coastal upwelling as a factor in determining the present and future distributions of marine species. Coastal upwelling is an important factor that determines the productivity and distribution of many marine species (Horn and Allen 1978; Barber and Smith 1981). Some species are solely associated with coastal upwelling systems (e.g., the Peruvian anchoveta), while some may avoid such systems. It is predicted that climate change may lead to acceleration of coastal upwelling (Bakun 1990; McGregor *et al.* 2007). Such changes will affect the physical and biological structure of coastal upwelling systems (Barth *et al.* 2007) and, therefore, may contribute to shifts in distribution ranges of their associated species. To incorporate this factor into the dynamic bioclimate envelope model, we will construct a distribution map of major coastal upwelling regions of the world ocean and calculate their intensity using sea surface temperature anomalies. We will then assign an affinity index of coastal upwelling to marine fishes and invertebrates. Using the affinity index and the present and projected upwelling intensity (calculated from predictions from global circulation models), we will then be able to incorporate coastal upwelling as a factor in predicting distribution shifts of marine fishes and invertebrates given different climate change scenarios.

We will also attempt to predict global distribution maps of kelp forests and simulate how climate change may affect the distribution of kelp forests and their associated fauna. Kelp forests are among the world's most productive ecosystems and are important habitats for a wide variety of species (Mann 1973). Their distribution is sensitive to oceanographic conditions such as sea

temperature (Graham *et al.* 2007). Thus, climate change may have considerable impact on the distributions of kelp forest and their associated fauna. A previous study successfully uses ecophysiological and oceanographic model to predict kelp populations (Graham *et al.* 2007). Our model can adopt a similar approach in predicting the effects of climate change on the distribution of these kelp populations. Moreover, similar to coral reef species, we can assign a kelp-affinity index to species that are associated with kelp forests. Combining this index with a global habitat map of kelp, we can improve our predicted distribution ranges of kelp-associated species. By simulating the changes in distribution of kelp forest under climate change scenarios, we can predict how distribution ranges of kelp-associated species may change.

Our model can also incorporate hypotheses relating to climate-induced changes in physiology and population dynamics. The metabolism of fish is generally limited by the intake and availability of oxygen to body cells. These processes are strongly temperature-dependent. The metabolism affects somatic growth, body size and other life history traits that are closely correlated with each other (Pauly 1980, 1981, 1998). These may then affect population dynamics (e.g., reproduction, mortality, density-dependence etc.). Thus, incorporation of such dynamics in the simulation model may allow the model to make more accurate predictions on the impacts of climate change.

We do not explicitly account for the effects of changes in ocean chemistry in our model; this can be an area for future improvement. Physiology and population dynamics of marine organisms may also be affected by changes in ocean chemistry. Specifically, the potential impacts of ocean acidification by anthropogenic CO_2 on the balance of calcium carbonate system in the Oceans have been raised (Feely *et al.* 2004). Ocean acidification may lead to the dissolution of calcium structure such as shells or coral skeleton and render the maintenance of such structures more difficult (Feely *et al.* 2004; Orr *et al.* 2005). High acidity may also increase the mortality of fish eggs and larvae (Kikkawa *et al.* 2003).Under various projected scenarios of future CO_2 emission, conditions of ocean acidification may have stronger impacts on high-latitude ecosystems and the impacts could develop within decades. In the future, we may potentially include ocean chemistry as a factor that affects the organisms' growth and evaluate its effect on their distribution.

To assess the accuracy of predictions from our model, past climate and species distribution data can be used. Based on these past data, we can use the model to simulate changes in distribution ranges of the species. The accuracy of the model can be assessed by comparing the model-reconstructed changes with empirically-observed data. For instance, detailed climate, abundance and distribution data of many commercially-important species in the North Sea are well-documented (Perry *et al.* 2005). Such data can be used for model validation.

CONCLUSIONS

The dynamic bioclimate envelope model developed in this study provides a tool to quantitatively evaluate the effects of climate scenarios on a wide range of marine species. Using the data from global databases such as FishBase and the *Sea Around Us* Project database, the model can be applied to all commercially-exploited marine species, and indeed to any species for which distribution range maps exist. Given the targeted scale of the model and the trade-off between data availability and model details, the model appears to provide reasonable predictions that are robust to major model assumptions. Used in conjunction with models that translate biogeography to fishery productivity, it can be used to inform policy makers about potential socio-economic implications of climate change for global fisheries.

REFERENCES

Alder, J. 2003. Putting the Coast in the *Sea Around Us* Project. The *Sea Around Us* Newsletter. No. 15: 1-2.

Araújo, M. B. and New, M. 2006. Ensemble forecasting of species distributions. Trends in Ecology and Evolution, 22: 42-47.

Araújo, M. B., Pearson, R. G., Thuiller, W. and Erhard, M. 2005. Validation of species-climate impact models under climate change. Global Change Biology, 11: 1504-1513.

Bakun, A. 1990. Coastal ocean upwelling. Science, 247: 198-201.

Barber, R.T. and Smith, R.L. 1981. Coastal Upwelling Ecosystems. In: Longhurst, A.R. (ed). Analysis of Marine Ecosystems, p. 31-68.

Barbraud, C. and Weimerskirch, H. 2003. Climate and density shape population dynamics of a marine top predator. Proceedings of the Royal Society: Series B, 270: 2111-2116.

Barth, J.A., Menge, B.A., Lubchenco, J., Chan, F., Bane, J.M., Kirincich, A.R., McManus, M.A., Nielsen, K.J., Pierce, S.D. and Washburn, L. 2007. Delayed upwelling alters nearshore coastal ocean ecosystems in the northern California current. PNAS, 104: 3719-3724.

Bellwood, D. R., Hughes, T. P., Folke, C. and Nyström, M. 2004. Confronting the Coral Reef Crisis. Nature, 429: 827-833

Blaber, S.J. 2000. Tropical Estuarine Fishes: Ecology, Exploitation and Conservation. Blackwell Science, Oxford, 372 p.

Bradbury, I. R. and Snelgrove, P. V. R. 2001. Contrasting larval transport in demersal fish and benthic invertebrates: the roles of behaviour and advective processes in determining spatial pattern. Canadian Journal of Fisheries and Aquatic Science, 58: 811-823.

Brierley, A. S., Fernandes, P. G., Brandon, M. A., Armstrong, F., Millard, N. W., McPhail, S. D., Stevenson, P., Pebody, M., Perrett, J., Squires, M., Bone, D. G., Griffiths, G. 2002. Antarctic krill under sea ice: elevated abundance in a narrow band just south of ice edge. Science, 295: 1890-1892.

Cheung, W. W. L., Watson, R., Morato, T., Pitcher, T. J. and Pauly, D. 2007. Intrinsic vulnerability in the global fish catch. Marine Ecology Progress Series, 333: 1-12.

Close, C., Cheung, W. W. L., Hodgson, S., Lam, V., Watson, R., Pauly, D. 2006. Distribution ranges of commercial fishes and invertebrates. In: Palomares, M. L. D., Stergiou, K. I., Pauly, D. (eds). Fishes in Databases and Ecosystems. Fisheries Centre Research Reports 14 (4). Fisheries Centre, University of British Columbia, Vancouver, p 27-37.

Comiso, J. C. 2002. A rapidly declining perennial sea ice cover in the Arctic. Geophysical Research Letters, 29(20), 1956, doi:10.1029/2002GL015650.

Cox E (1999) The fuzzy systems handbook: a practitioner's guide to building, using, and maintaining fuzzy systems. AP Professional, San Diego.

Daly, K. L., and Macaulay, M. C. 1988. Abundance and distribution of krill in the ice edge zone of the Weddell Sea, austral spring 1983. Deep-Sea Research, 35: 21-41.

Drinkwater, K. F. 2005. The response of Atlantic cod (*Gadus morhua*) to future climate change. ICES Journal of Marine Science, 62: 1327-1337.

Edgar, G.J., Barrett, N.S., and Last, P.R. 1999. The distribution of macroinvertebrates and fishes in Tasmanian estuaries. Journal of Biogeography, 26: 1169-1189.

Feely, R.A., Sabine, C.L., Lee, K., Berelson, W., Kleypas, J., Fabry, V., Millero, F.J. 2004. Impact of anthropogenic CO_2 on the $CaCo_3$ system in the oceans. Science 305, 362-366.

Eicken, H. 1992. The role of sea ice in structuring Antarctic ecosystems. Polar Biology, 12: 3-13.

Ekman, S. 1967. Zoogeography of the Sea. Sidgwick and Jackson. London.

Farrell, A. P. and Steffensen, J. F. (eds.) 2005. The Physiology of Polar Fishes. Elsevier Academic Press, London. 396 p.

Flato, G. M. and Boer, G. J. 2001. Warming asymmetry in climate change simulations. Geophysical Research Letters, 28: 195-198.

Frank, K. T., Perry, R. I. and Drinkwater, K. F. 1990. Predicted response of Northwest Atlantic invertebrate and fish stocks to CO_2-induced climate change. Transactions of the American Fisheries Society, 119: 353-365.

Frederich, M. and Pörtner, H. O. 2000. Oxygen limitation of thermal tolerance defined by cardiac and ventilatory performance in the spider crab, *Maja squinado*. American Journal of Physiology, 279: R1521-R1528.

Fuiman, L. A., Davis, R. W., and Williams, T. M. 2002. Behavior of midwater fishes under the Antarctic ice: observations by a predator. Marine Biology, 140: 815-822.

Gaines, S. D., Gaylord, B. and Largier, J. L. 2003. Avoiding current oversights in marine reserve design. Ecological Applications, 13(1) Supplement: S32-S46.

Gaylord, B. and Gaines, S. D. 2000. Temperature or transport? Range limits in marine species mediated solely by flow. The American Naturalist, 155(6): 769-789.

Glynn, P. W. 1991. Coral reef bleaching in the 1980s and possible connections with global warming. Trends in Ecology and Evolution, 6: 175-179.

Glynn, P. W. 1993. Coral reef bleaching: ecological perspectives. Coral Reefs, 12: 1-17.

Graham, M.H., Kinlan, B.P., Druehl, L.D., Garske, L.E., and Banks, S. 2007. Deep-water kelp refugia as potential hotspots of tropical marine diversity and productivity. PNAS, 104: 16576-16580

Hannah, L., Midgley, G. F. and Millar, D. 2002. Climate change-integrated conservation strategies. Global Ecology and Biogeography, 11: 485-495.

Harley, C. D. G., Hughes, A. R., Hultgren, K. M., Miner, B. G., Sorte, C. J. B., Thornber, C. S., Rodriguez, L. F., Tomanek, L. and Williams, S. L. 2006. The impacts of climate change in coastal marine systems. Ecology Letters, 9: 228-241.

Haugen, T. O. and Vøllestad, L. A. 2001. A century of life-history evolution in grayling. Genetica, 475-491.

Helfman, F. S., Collette, B. B. and Facey, D. E. 1997. The Diversity of Fishes. Blackwell Science, London. 528 p.

Hellbery, M. E., Balch, D. P. and Roy, K. 2001. Climate-driven range expansion and morphological evolution in a marine gastropod. Science, 292: 1707-1710.

Hilborn, R., Walters, C.J. 1992. Quantitative fisheries stock assessment: choice, dynamics and uncertainty. Chapman & Hall, New York

Hobday, A. J., Okey, T. A., Poloczanska, E. S., Kunz, T. J. and Richardson, A. J. (eds) 2006. Impacts of climate change on Australian marine life: Part C. Literature Review. Report to the Australian Greenhouse Office, Canberra, Australia. September 2006.

Horn, M.H. and Allen, L.G. 1978. A distributional analysis of California coastal marine fishes. Journal of Biogeography, 5: 23-42.

Hughes, L. 2000. Biological consequences of global warming: is the signal already apparent? Trends in Ecology and Evolution, 15: 56-61.

Hughes, N. F. and Grand, T. C. 2000. Physiological ecology meets the ideal-free distribution: predicting the distribution of size-structured fish populations across temperature gradients. Environmental Biology of Fishes, 59: 285-298.

Hughes, T. P., Baird, A. H., Bellwood, D. R., Card, M., Connolly, S. R., Folke, C., Grosberg, R., Hoegh-Guldberg, O., Jackson, J. B. C., Kleypas, J., Lough, J. M., Marshall, P., Nyström, M., Palumbi, S. R., Pandolfi, J. M., Rosen, B., Roughgarden, J. 2003. Climate change, human impacts and the resilience of coral reefs. Science, 301: 929-933.

Hundsdorfer, W., Verwer, J. G. 2003. Numerical Solution of Time-dependent Advection-Diffusion-Reaction Equations. Springer, Berlin. 500 p.

IPCC 2007. Summary for policymakers. In: (Solomon, S., Qin, D., Manning, M., Chen, Z., Marquis, M., Averyt, K. B., Tignor, M. and Miller, H. L. eds.). Climate Change 2007: The Physical Science Basis. Contributing of Working Group I to the Fourth Assessment Report of the Intergovernmental Panel on Climate Change. Cambridge University Press, Cambridge, United Kingdom and New York, New York.

Johannessen, O. M., Shalina, E. V. and Miles, M. W. 1999. Satellite evidence for an Arctic sea ice cover in transformation. Science, 286: 1937-1939.

Johannessen, O. M., Bengtsson, L., Miles, M. W., Kuzmina, S. I., Semenov, V. A., Alekseev, G. V., Nagurnyi, A. P., Zakharov, V. F., Bobylev, L. P., Pettersson, L. H., Hasselmann, K. and Cattle, H. P. 2004. Arctic climate change: observed and modelled temperature and sea ice variability. Tellus, 56A: 328-341.

Kaschner, K. 1998. Modelling and Mapping Resource Overlap between Marine Mammals and Fisheries on a Global Scale. PhD Thesis, The University of British Columbia, Vancouver. 240 p.

Kraak, S. B. M. 2007. Does the probabilistic maturation reaction norm approach disentangle phenotypic plasticity from genetic change? Marine Ecology Progress Series, 335: 295-300.

Kikkawa, T., Kita, J., Ishimatsu, A. 2003. Comparison of the lethal effect of CO_2 and acidification on red sea bream (*Pagrus major*) during the early developmental stages. Marine Pollution Bulletin 48, 108-110.

Kitchingman, A. and Lai, S. 2004. Inferences of potential seamount locations from mid-resolution bathymetric data. In: T. Morato and D. Pauly (eds.) Seamounts: Biodiversity and Fisheries. Fisheries Centre Research Report, 12(5): 7-12.

Law, R. 2000. Fishing, selection, and phenotypic evolution. ICES Journal of Marine Science, 57: 659-668.

Lawler, J. J., White, D., Neilson, R. P. and Blaustein, A. R. 2006. Predicting climate-induced range shifts: model differences and model reliability. Global Change Biology, 12: 1568-1584.

Legendre, L., Ackley, S. F., Dieckmann, G. S., Gulliksen, B., Horner, R., Hoshiai, T., Melnikov, I. A., Reeburgh, W. S., Spindler, M., and Sullivan, C. W. 1992. Ecology of sea ice biota. Polar Biology, 12: 429-444.

Levitus, S., Antonov, J. I., Boyer, T. P. and Stephens, C. 2000. Warming of the world ocean. Science, 287: 2225-2229.

Lockwood, D. R., Hastings, A. and Botsford, L. W. 2002. The effects of dispersal patterns on marine reserves: does the tail wag the dog? Theoretical Population Biology, 61: 297-309.

Loeb, V., Siegel, B., Holm-Hansen, O., Hewitt, R., Fraser, W., Trivelplece, W., Trivelplece, S. 1997. Effects of sea-ice extent and krill or salp dominance on the Antarctic food web. Nature, 387: 897-900.

Longhurst, A. R. 1981. Analysis of Marine Ecosystems. Academic Press, San Diego. 741 p.

Luoto, M., Pöyry, J., Heikkinen, R. K. and Saarinen, K. 2005. Uncertainty of bioclimate envelope models based on the geographical distribution of species. Global Ecology and Biogeography, 14: 575-584.

Mann, K.H. 1973. Seaweeds: their productivity and strategy for growth: The role of large marine algae in coastal productivity is far more important than has been suspected. Science, 182: 975-981.

Mariano, A. J., Ryan, E. H., Smithers, S. and Perkins, B. 1995. The Mariano Global Surface Velocity Analysis. U.S. Coast Guard Technical Report, CG-D-34-95.

Matthews, W. J., Hill, L. G. and Schellhaass, S. M. 1985. Depth distribution of striped bass and other fish in lake texoma (Oklahoma-Texas) during summer stratification. Transactions of the American Fisheries Society, 114: 84-91.

McCarty, J. P. 2001. Ecological consequences of recent climate change. Conservation Biology, 15: 320-331.

McGregor, H.V., Dima, M., Fischer, H.W., and Mulitza, S. 2007. Rapid 20th-century increase in coastal upwelling off northwest Africa. Science, 315: 637-639.

Meier, H.E.M. 2002. Regional ocean climate simulations with a 3D ice-ocean model for the Baltic Sea. Part 1: Model experiments and results for temperature and salinity. Clim Dyn, 19: 237-253.

Meier, H.E.M. and Kauker, F. 2003. Sensitivity of the Baltic Sea salinity to the freshwater supply. Climate Research, 24: 231-242.

Møller, P. R., Nielsen, J. G., and Anderson, M. E. 2005. Systematics of polar fishes. In: p. 25-78 (Farrell, A. P. & Steffensen, J. F. eds.), The Physiology of Polar Fishes. Elsevier Academic Press, London.

Munk, W. 2003. Ocean freshening, sea level rising. Science, 27: 2041-2043.

Murawski, S. A. 1993. Climate change and marine fish distributions: forecasting from historical analogy. Transactions of the American Fisheries Society, 122: 647-658.

Nahas, E. L., Jackson, G., Pattiaratchi, C. B., and Ivey, G. N. 2003. Hydrodynamic modelling of snapper *Parus auratus* etgg and larval dispersal in Shark Bay, Western Australia: reproductive isolation at a fine spatial scale. Marine Ecology Progress Series, 265: 213-226.

Omstedt, A., Gustafsson, B., Rodhe, J., and Walin, G. 2000. Use of Baltic Sea modeling to investigate the water cycle and the heat balance in GCM and regional climate models. Climate Research, 15: 95-108.

Orlowski, A. 1999. Acoustic studies of spatial gradients in the Baltic: implications for fish distribution. ICES Journal of Marine Science, 56: 561-570.

Orr, J.C., Fabry, V.J., Aumont, O., Bopp, L., Doney, S.C., Feely, R.A., Gnanadesikan, A., Gruber, N., Ishida, A., Joos, F., Key, R.M., Lindsay, K., Maier-Reimer, E., Matear, R., Monfray, P., Mouchet, A., Najjar, R.G., Plattner, G.K., Rodgers, K.B., Sabine, C.L., Sarmiento, J.L., Schlitzer, R., Slater, R.D., Totterdell, I.J., Weirig, M.F., Yamanaka, Y., Yool, A. 2005. Anthropogenic ocean acidification over the twenty-first century and its impact on calcifying organisms. Nature 437, 681-686.

Palomares, M. L. D., Pauly, D. 1998. Predicting food consumption of fish populations as functions of mortality, food type, morphometrics, temperature and salinity. Marine and Freshwater Research, 49: 447-453.

Parmesan, C. and Yohe, G. 2003. A globally coherent fingerprint of climate change impacts across natural systems. Nature, 421:37-42.

Parmesan, C., Root, T. L. and Willig, M. R. 2000. Impacts of extreme weather and climate on terrestrial biota. Bulletin of the American Meteorological Society, 81: 443-450.

Pauly, D. 1980. On the interrelationships between natural mortality, growth parameters and mean environmental temperature in 175 fish stocks. J. Cons. CIEM 39(3):175-192.

Pauly, D. 1981. The relationships between gill surface area and growth performance in fish: a generalization of von Bertalanffy's theory of growth. Meeresforschung 28, 251-282.

Pauly, D. 1998. Tropical fishes: patterns and propensities. Journal of Fish Biology 53, 1-17.

Pauly, D., Christensen, V., Walters, C. 2000. Ecopath, Ecosim, and Ecospace as tools for evaluating ecosystem impact of fisheries. ICES Journal of Marine Science, 57: 697-706.

Pearson, R. G. and Dawson, T. P. 2003. Predicting the impacts of climate change on the distribution of species: are bioclimate envelope models useful? Global Ecology & Biogeography, 12: 361-371.

Perry, A. L., Low, P. J., Ellis, J. R., Reynolds, J. D. 2005. Climate change and distribution shifts in marine fishes. Nature, 308:1912-1915.

Peterson, A. T., Ortega-Huerta, M. A., Bartley, J., Sánchez-Cordero, V., Soberón, J., Buddemeier, R. H. and Stockwell, D. R. B. 2002. Future projections for Mexican faunas under global climate change scenarios. Nature, 416: 626-629.

Phillips, B.F., Palmer, M.J., Cruz, R. and Trendall, J.T. 1992. Estimating growth of the spiny lobsters *Panulirus Cygnus*, *P. argus* and *P. ornatus*. Australian Journal of Marine and Freshwater Research, 43: 1177-1188.

Pihl, L., Baden, S. P., and Diaz, R. J. 1991. Effects of periodic hypoxia on distribution of demersal fish and crustaceans. Marine Biology, 108: 349-360.

Polsenberg, J. 2003. Coral may be moving north. Frontiers in Ecology and the Environment, 1: 512.

Possingham, H. P. and Roughgarden, J. 1990. Spatial population dynamics of a marine organism with a complex life cycle. Ecology, 71: 973-985.

Pounds, J. A. 2001. Climate and amphibian declines. Nature, 410: 639-640.

Press, W. H., Flannery, B. P., Teukolsky, S. A. and Vetterling, W. T. 1988. Numerical recipes in C. Cambridge University Press, New York.

Pörtner, H. O. 2001. Climate change and temperature-dependent biogeography: oxygen limitation of thermal tolerance in animals. Naturwissenschaften, 88(4): 137-146.

Pörtner, H. O., Berdal, B., Blust, R., Brix, O., Colosimo, A., Wachter, B. D., Giuliani, A., Johansen, T., Fischer, T., Knust, R., Lannig, G., Naevdal, G., Nedenes, A., Nyhammer, G., Sartoris, F. J., Serendero, I., Sirabella, P., Thorkildsen, S., Zakhartsev, M. 2001. Climate induced temperature effects on growth performance, fecundity and recruitment in marine fish: developing a hypothesis for cause and effect relationships in Atlantic cod (*Gadus morhua*) and common eelpout (*Zoarces viviparus*). Continental Shelf Research, 21: 1975-1997.

Rahmstorf, S. and Ganopolski, A. 1999. Long-term global warming scenarios computed with an efficient coupled climate model. Climate Change, 43: 353-367.

Regier, H.A., Holmes, J.A. and Pauly, D. 1990. Influence of temperature changes on aquatic ecosystems: an interpretation of empirical data. Transactions of the American Fisheries Society, 119: 374-389.

Rijnsdorp, A. D. 1993. Fisheries as a large-scale experiment on life-history evolution: disentangling phenotypic and genetic effects in changes in maturation and reproduction of North Sea plaice, *Pleuronectes platessa* L. Oecologia, 96: 391-401.

Roessig, J. M., Woodley, C. M., Cech, J. J. and Hansen, L. J. 2004. Effects of global climate change on marine and estuarine fishes and fisheries. Reviews in Fish Biology and Fisheries, 14: 251-275.

Roy, K. Joblonski, D. and Valentine, J. W. 2001. Climate change, species range limits and body size in marine bivalves. Ecology Letters, 4: 366-370.

Samways, M. J., Osborn, R., Hastings, H. and Hattingh, V. 1999. Global climate change and accuracy of prediction of species' geographical ranges: establishment success of introduced ladybirds (Coccinellidae, *Chilocorus* spp.) worldwide. Journal of Biogeography, 26: 795-812.

Sibert, J. R. and Fournier, D. A. 1993. Evaluation of advection-diffusion equations for estimation of movements patterns from tag recapture data, p. 108-121. In: (Shomura, R., Majkowski, J. and Langi, S., eds.). Interactions of Pacific Tuna

Fisheries. Volume 1: Summary Report and Papers on Interaction. FAO Fisheries Technical Paper, 336, Vol.1. Rome, FAO.

Sibert, J. R., Hampton, J., Fournier, D. A., and Bills, P. J. 1999. An advection-diffusion-reaction model for the estimation of fish movement parameters from tagging data, with application to skipjack tuna (*Katsuwonus pelamis*). Canadian Journal of Fisheries and Aquatic Science, 56: 925-938.

Stenseth, N. C., Mysterud, A., Ottersen, G., Hurrell, J. W., Chan, K. and Lima, m. 2002. Ecological Effects of Climate Fluctuations. Science, 297: 1292-1296.

Swain, D. P. and Kramer, D. L. 1995. Annual variation in temperature selection by Atlantic cod *Gadus morhua* in the southern Gulf of St. Lawrence, Canada, and its relation to population size. Marine Ecology Progress Series, 116: 11-23.

Thomas, C. D., Bodsworth, E. J., Wilson, R. J., Simmons, A. D., Davies, Z. G., Musche, M. and Conradt, L. 2001. Ecological and evolutionary processes at expanding range margins. Nature, 411: 577-581.

Thomas, C. D., Cameron, A., Green, R. E., Bakkenes, M., Beaumont, L. J., Collingham, Y. C., Erasmus, B. F. N., de Siqueira, M. F., Grainger, A., Hannah, L., Hughes, L., Huntley, B., van Jaarsveld, A. S., Midgley, G. F., Miles, L., Ortega-Huerta, M. A., Peterson, A. T., Phillips, O. L. and Williams, S. E. 2004. Extinction risk from climate change. Nature, 427: 145-148.

Thresher, R. E., Koslow, J. A., Morison, A. K. and Smith, D. C. 2007. Depth-mediated reversal of the effects of climate change on long-term growth rates of exploited marine fish. PNAS, 104: 7461-7465.

Vellinga, M. and Wood, R. A. 2002. Global climatic impacts of a collapse of the Atlantic thermohaline circulation. Climate Change, 54: 251-267.

Veron, J. E. 2000. Corals of the World. Australian Institute of Marine Science, Townsville, Australia, 1382 p.

Vinnikov, K. Y., Robock, A., Stouffer, R. J., Walsh, J. E., Parkinson, C. L., Cavalieri, D. J., Mitchell, J. F. B., Garrett, D. and Zakharov, V. F. 1999. Global warming and northern hemisphere sea ice extent. Science, 286: 1934-1937.

Walters, C., Christensen, V. and Pauly, D. 1997. Structuring dynamic models of exploited ecosystem from trophic mass-balance assessment. Reviews in Fish Biology and Fisheries, 7: 139-172.

Walters, C, Pauly, D. and Christensen, V. 1999. Ecospace: Prediction of mesoscale spatial patterns in trophic relationships of exploited ecosystems, with emphasis on the impacts of marine protected areas. Ecosystems, 2: 539-554.

Walther, G., Post, E., Convey, P. Menzel, A., Camille, P., Beebee, T. J. C., Fromentin, J., Hoegh-Guldberg, O. and Bairlein, F. 2002. Ecological responses to recent climate change. Nature, 416: 389-395.

Watson, R., Kitchingman, A., Gelchu, A., Pauly, D. 2004. Mapping global fisheries: sharpening our focus. Fish and Fisheries, 5(2):168-177.

Zadeh, L. 1965. Fuzzy sets. Information and Control, 8:338-353.

Zeidberg, L. D., Robison, B. H. 2007. Invasive range expansion by the Humboldt squid, *Dosidicus gigas*, in the eastern North Pacific. PNAS, 104: 12948-12950.

Appendix 1

List of exploited polar species identified based on biogeography of the species (see text).

Common name	Scientific name	Region
Antarctic krill	*Euphausia superba*	Antarctic
Antarctic silverfish	*Pleuragramma antarcticum*	Antarctic
Antarctic stone crab	*Paralomis spinosissima*	Arctic
Antarctic toothfish	*Dissostichus mawsoni*	Antarctic
Bible icefish	*Neopagetopsis ionah*	Antarctic
Black rockcod	*Notothenia coriiceps*	Antarctic
Blackfin icefish	*Chaenocephalus aceratus*	Antarctic
Blunt scalyhead	*Trematomus eulepidotus*	Antarctic
Carlberg's lanternfish	*Electrona carlsbergi*	Antarctic
Charr	*Salvelinus alpinus*	Antarctic
Eatons skate	*Bathyraja eatonii*	Antarctic
Formosan snow crab	*Paralomis formosa*	Arctic
Grey rockcod	*Lepidonotothen squamifrons*	Antarctic
Hooked icefish	*Chionodraco hamatus*	Antarctic
Humped rockcod	*Gobionotothen gibberifrons*	Antarctic
Kerguelen sandpaper skate	*Bathyraja irrasa*	Antarctic
Mackerel icefish	*Champsocephalus gunnari*	Antarctic
Navaga	*Eleginus navaga*	Antarctic
Ocellated icefish	*Chionodraco rastrospinosus*	Antarctic
Polar cod	*Boreogadus saida*	Antarctic
Smalleye moray cod	*Muraenolepis microps*	Antarctic
South Georgia icefish	*Pseudochaenichthys georgianus*	Antarctic
Spiny icefish	*Chaenodraco wilsoni*	Antarctic
Striped rockcod	*Trematomus hansoni*	Antarctic
Striped-eye notothen	*Lepidonotothen kempi*	Arctic
Unicorn icefish	*Channichthys rhinoceratus*	Antarctic
Whitson's grenadier	*Macrourus whitsoni*	Antarctic

Appendix 2

Rules that determine the level of dispersal rate of a species based on its maximum body length, aspect ratio and associated habitat.

No.	Premises			Conclusions (Dispersal rate)
1	IF Maximum body length is	Large	AND	
	Aspect ratio is	High	AND	
	Habitat is	Pelagic	THEN	Very high
2	IF Maximum body length is	Large	AND	
	Aspect ratio is	Medium	AND	
	Habitat is	Pelagic	THEN	High
3	IF Maximum body length is	Large	AND	
	Aspect ratio is	Low	AND	
	Habitat is	Pelagic	THEN	Low
4	IF Maximum body length is	Medium	AND	
	Aspect ratio is	High	AND	
	Habitat is	Pelagic	THEN	High
5	IF Maximum body length is	Medium	AND	
	Aspect ratio is	Medium	AND	
	Habitat is	Pelagic	THEN	Moderate
6	IF Maximum body length is	Medium	AND	
	Aspect ratio is	Low	AND	
	Habitat is	Pelagic	THEN	Low
7	IF Maximum body length is	Small	AND	
	Aspect ratio is	High	AND	
	Habitat is	Pelagic	THEN	Low
8	IF Maximum body length is	Small	AND	
	Aspect ratio is	Medium	AND	
	Habitat is	Pelagic	THEN	Low
9	IF Maximum body length is	Small	AND	
	Aspect ratio is	Low	AND	
	Habitat is	Pelagic	THEN	Low
10	IF Maximum body length is	Large	AND	
	Aspect ratio is	High	AND	
	Habitat is	Demersal	THEN	High
11	IF Maximum body length is	Large	AND	
	Aspect ratio is	Medium	AND	
	Habitat is	Demersal	THEN	Moderate
12	IF Maximum body length is	Large	AND	
	Aspect ratio is	Low	AND	
	Habitat is	Demersal	THEN	Low

Appendix 2 (cont.)

No.	Premises			Conclusions (Dispersal rate)
13	IF Maximum body length is	Medium	AND	
	Aspect ratio is	High	AND	
	Habitat is	Demersal	THEN	Moderate
14	IF Maximum body length is	Medium	AND	
	Aspect ratio is	Medium	AND	
	Habitat is	Demersal	THEN	Low
15	IF Maximum body length is	Medium	AND	
	Aspect ratio is	Low	AND	
	Habitat is	Demersal	THEN	Low
16	IF Maximum body length is	Small	AND	
	Aspect ratio is	High	AND	
	Habitat is	Demersal	THEN	Low
17	IF Maximum body length is	Small	AND	
	Aspect ratio is	Medium	AND	
	Habitat is	Demersal	THEN	Low
18	IF Maximum body length is	Small	AND	
	Aspect ratio is	Low	AND	
	Habitat is	Demersal	THEN	Low
19	IF Maximum body length is	any set	AND	
	Aspect ratio is	any set	AND	
	Habitat is	Reef-associated	THEN	Low
20	IF Maximum body length is	any set	AND	
	Aspect ratio is	any set	AND	
	Habitat is	any set	AND	
	Life style is	Sedentary	THEN	Zero

Appendix 3

Numerical solution of the diffusion-advection partial differential equation (based on Sibert & Fournier 1993).

Larval dispersal through diffusion and advection processes is modelled by:

$$\frac{\partial Lav}{\partial t} = \frac{\partial}{\partial x}\left(D\frac{\partial Lav}{\partial x}\right) + \frac{\partial}{\partial y}\left(D\frac{\partial Lav}{\partial y}\right) - \frac{\partial}{\partial x}(u \cdot Lav) - \frac{\partial}{\partial y}(v \cdot Lav) - \lambda \cdot Lav \qquad \ldots A1)$$

where Lav is relative abundance of larvae, t is time step, u and v are east-west and north-south current velocity parameters, respectively. x and y are displacement in east-west and north-south directions, respectively. D is the diffusion coefficient. The instantaneous rate of larval mortality and settlement is represented by $\lambda = M + S$, where M and S are the natural mortality and settlement (thus leaving the pelagic water layer) rates of larvae respectively.

Equation A1 can be approximated by:

$$\frac{\partial Lav}{\partial t} \approx \frac{Lav_{i,j,t+1} - Lav_{i,j,t}}{\Delta t} \qquad \ldots A2.1)$$

$$\frac{\partial^2 Lav}{\partial x^2} \approx \frac{Lav_{i-1,j,t+1} - 2 \cdot Lav_{i,j,t+1} + Lav_{i+1,j,t+1}}{(\Delta x)^2} \qquad \ldots A2.2)$$

$$\frac{\partial^2 Lav}{\partial y^2} \approx \frac{Lav_{i,j-1,t+1} - 2 \cdot Lav_{i,j,t+1} + Lav_{i,j+1,t+1}}{(\Delta y)^2} \qquad \ldots A2.3)$$

$$\frac{\partial}{\partial x}(u \cdot Lav) \approx \begin{cases} u_{i,j}\dfrac{Lav_{i,j,t+1} - Lav_{i-1,j,t+1}}{\Delta x} + Lav_{i-1,j,t} \cdot \dfrac{u_{i,j} - u_{i-1,j}}{\Delta x}, & u_{ij} > 0 \\[2mm] u_{i,j}\dfrac{Lav_{i+1,j,t+1} - Lav_{i,j,t+1}}{\Delta x} + Lav_{i+1,j,t} \cdot \dfrac{u_{i+1,j} - u_{i,j}}{\Delta x}, & u_{ij} < 0 \end{cases} \qquad \ldots A2.4)$$

$$\frac{\partial}{\partial y}(v \cdot Lav) \approx \begin{cases} v_{i,j}\dfrac{Lav_{i,j,t+1} - Lav_{i,j-1,t+1}}{\Delta y} + Lav_{i,j-1,t} \cdot \dfrac{v_{i,j} - v_{i,j-1}}{\Delta y}, & u_{ij} > 0 \\[2mm] v_{i,j}\dfrac{Lav_{i,j+1,t+1} - Lav_{i,j,t+1}}{\Delta y} + Lav_{i,j+1,t} \cdot \dfrac{v_{i,j+1} - v_{i,j}}{\Delta y}, & u_{ij} < 0 \end{cases} \qquad \ldots A2.5)$$

Solving equations with implicit alternating direction method (Press *et al.* 1988), the east-west movement at the first half time-step $(t + 1/2)$ is expressed as:

$$\left(-\frac{D}{(\Delta x)^2} - \frac{u_{i-1,j}}{\Delta x}\right) \cdot Lav_{i-1,j,t+1/2} + \left(\frac{2}{\Delta t} + \frac{2D}{(\Delta x)^2} + \frac{u_{i,j}}{\Delta x} + \lambda\right) \cdot Lav_{i,j,t+1/2} + \left(-\frac{D}{(\Delta x)^2}\right) \cdot Lav_{i+1,j,t+1/2} =$$

$$\left[\left(-\frac{D}{(\Delta y)^2} - \frac{v_{i,j-1}}{\Delta y}\right) \cdot Lav_{i,j-1,t} + \left(-\frac{2}{\Delta t} + \frac{2D}{(\Delta y)^2} + \frac{v_{i,j}}{\Delta y}\right) \cdot Lav_{i,j,t} + \left(-\frac{D}{(\Delta y)^2}\right) \cdot Lav_{i,j+1,t}\right] \qquad \ldots A3)$$

The north-south movement at the next half time-step (t + 1) is expressed as:

$$\left(-\frac{D}{(\Delta y)^2}-\frac{v_{i,j-1}}{\Delta y}\right)\cdot Lav_{i,j-1,t+1}+\left(\frac{2}{\Delta t}+\frac{2D}{(\Delta y)^2}+\frac{v_{i,j}}{\Delta y}\right)\cdot Lav_{i,j,t+1}+\left(-\frac{D}{(\Delta y)^2}\right)\cdot Lav_{i,j+1,t+1}= \quad\quad\ldots A4)$$

$$-\left[\left(-\frac{D}{(\Delta x)^2}-\frac{u_{i-1,j}}{\Delta x}\right)\cdot Lav_{i-1,j,t+1/2}+\left(-\frac{2}{\Delta t}+\frac{2D}{(\Delta x)^2}+\frac{u_{i,j}}{\Delta x}+\lambda\right)\cdot Lav_{i,j,t+1/2}+\left(-\frac{D}{(\Delta x)^2}\right)\cdot Lav_{i+1,j,t+1/2}\right]$$

Equations A3 and A4 can be expressed as tridiagonal matrices in the form:

$$g_{i,j}=\begin{pmatrix} b_{1,j}\cdot Lav_{1,j,k} & c_{1,j}\cdot Lav_{2,j,k} & & & \\ a_{2,j}\cdot Lav_{1,j,k} & b_{2,j}\cdot Lav_{2,j,k} & c_{3,j}\cdot Lav_{3,j,k} & & \\ & & \ddots & \ddots & \\ & & a_{i-2,j}\cdot Lav_{i-2,j,k} & b_{i-1,j}\cdot Lav_{i-1,j,k} & c_{i+1,j}\cdot Lav_{i,j,k} \\ & & & b_{i-1,j}\cdot Lav_{i-1,j,k} & c_{i+1,j}\cdot Lav_{i,j,k} \end{pmatrix} \quad\ldots A5)$$

where k = t + ½; and

$$h_{i,j}=\begin{pmatrix} e_{i,1}\cdot Lav_{i,1,t+1} & f_{i,2}\cdot Lav_{i,2,t+1} & & & \\ d_{i,1}\cdot Lav_{i,1,t+1} & e_{i,2}\cdot Lav_{i,2,t+1} & f_{i,3}\cdot Lav_{i,3,t+1} & & \\ & & \ddots & \ddots & \\ & & d_{i,j-2}\cdot Lav_{i,j-2,t+1} & e_{i,j-1}\cdot Lav_{i,j-1,t+1} & f_{i,j}\cdot Lav_{i,j,t+1} \\ & & & e_{i,j-1}\cdot Lav_{i,j-1,t+1} & f_{i,j}\cdot Lav_{i,j,t+1} \end{pmatrix} \quad\ldots A5)$$

The coefficients *a, b, c, d, e, f* represent the terms in blankets in equations A3 and A4 while coefficients *g* and *h* are the right-hand-sides of eq. A3 and A4. *g* and *h* must be calculated at each time step as they depend on larval abundance ($Lav_{i,j,t}$ and $Lav_{i,j,t+1/2}$). Since our model covers the entire world oceans, all potential marine habitats for the species are covered. Therefore, we assume closed impermeable boundaries around islands and along coastlines. At the boundaries,

$$\frac{\partial Lav}{\partial x}=0 \quad\quad\quad \text{and} \quad\quad\quad u=0 \quad\quad\quad\quad\quad\quad\quad\quad\quad\quad \ldots A6)$$

and

$$\frac{\partial Lav}{\partial y}=0 \quad\quad\quad \text{and} \quad\quad\quad v=0 \quad\quad\quad\quad\quad\quad\quad\quad\quad\quad \ldots A7)$$

(Sibert *et al.* 1999).

Moreover, to allow the potential for transportation of larvae around the world, we assume periodic boundary condition at the limits of the north-south and west-east extends of our maps.

The tridiagonal systems of equations can be solved by the recursive algorithm (Press *et al.* 1988) to obtain $Lav_{i,j}$ at time steps *t* + ½ and *t*.

CHAPTER 2

MODELLING SEASONAL DISTRIBUTION OF PELAGIC MARINE FISHES AND SQUIDS[2]

Vicky W.Y. Lam, William W. L. Cheung, Chris Close, Sally Hodgson, Reg Watson and
Daniel Pauly

Sea Around Us Project, Fisheries Centre, Aquatic Ecosystems Research Laboratory, 2202 Main Mall, The University of British Columbia, Vancouver, British Columbia, Canada. V6T 1Z4.

ABSTRACT

The distribution of pelagic marine fishes and invertebrates varies seasonally. However, information on the seasonal variation of the distribution of most pelagic marine fishes and invertebrates is scarce. In this paper, seasonal changes in distribution ranges of commercially exploited pelagic fishes and invertebrates are predicted based on the existing *Sea Around Us* Project distribution, a prediction algorithm, the correlation between seasonal changes in north-south boundaries and sea surface temperature. In the northern hemisphere, in summer (July to September), mobile pelagic marine species tend to migrate to the northern part of their distribution range to avoid excessive temperature near the equator, while in winter (January to March), the same species will migrate southward to avoid the low temperature at higher latitudes. The converse applies to the southern hemisphere. The resulting distributions can improve the prediction of temperature preference profile of pelagic species which are important in evaluating the effects of global warming on their distribution ranges. However, this method of predicting summer and winter distributions of pelagic species can only be considered as an approximation as other factors such as food availability, salinity, rainfall and current are not included. On the other hand, such approximation appear reasonable, given the global scope of the application of the predicted seasonal distributions and the large number of evaluated species (> 160).

INTRODUCTION

Temperature is a key factor affecting the physiology (e.g., reproduction, growth) and spatial and temporal distributions of marine fishes and invertebrates. For instance, Pörtner *et al.* (2001) shows that growth rates and fecundity decrease with higher latitude in the case of Atlantic cod (*Gadus morhua*) and common eelpout (*Zoarces viviparus*). Thus, marine ectotherms generally inhabit areas where temperature is favorable for their physiological processes. Also, the northern and southern boundaries of a particular species are determined by the water temperatures suitable for survival and reproduction. Such boundaries may fluctuate according to seasonal changes in temperature. Thus, in the northern hemisphere, the northern boundaries may shift southward in winter and northward in summer (Hutchins 1947), and conversely, in the southern hemisphere.

The correlation between distribution ranges and water temperature is a major factor determining the fluctuation in distributions of the highly mobile pelagic fishes and invertebrates. Many pelagic fishes and invertebrates have the ability to migrate over long-distance to find suitable habitats. As sea water temperature fluctuates seasonally and inter-annually, these species migrate to maintain physiologically suitable temperature in their surrounding water. For instance, Sardinella and

other pelagic fishes migrate northward and southward, along the Northwest African coast such that they remain at the same temperature, despite strong seasonal fluctuation (Pauly 1994). Similarly, tuna and billfish migrate according to changes in sea surface temperature (SST) (Buxton & Smale 1989). Higher catch rates of yellowfin tuna (*Thunnus albacares*) and bigeye tuna (*Thunnus obesus*) were found in regions where SST increased during El Niño and La Niña periods (Lu *et al.* 2001). Specifically, yellowfin tuna displayed movements from tropical to higher latitude when temperatures in the tropical regions were low i.e. during La Niña periods.

Given seasonal sea water temperature data, it is possible to predict intra-annual changes in distribution of marine pelagic fishes and invertebrates. The *Sea Around Us* project predicted annual average distributions of over 1,230 commercial marine fishes and invertebrates, of which over 190 were pelagic species (www.seaaroundus.org). Distributions of the species were predicted based on existing knowledge of species' north-south latitudinal ranges, depth ranges, affinities to habitats, and known distribution boundaries from published literature (Close *et al.* 2006). Assuming that species' north-south latitudinal boundaries are correlated with sea water temperature, their geographic ranges should shift northward and southward as sea water temperature fluctuates seasonally.

Predicting seasonal distributions of pelagic marine fishes and invertebrates allows more accurate modelling of climate change impacts on these species. A dynamic bioclimate envelope model was developed to predict changes in geographic range of marine fishes and invertebrates under climate change scenarios (see Cheung *et al.* this vol.). This model is based largely on species temperature preference, as inferred from predicted species distributions. Assuming that highly mobile pelagic fishes and invertebrates migrate seasonally according to water temperature, ignoring such seasonal migration would over-estimate the temperature limits of the species and, thus under-estimate the impacts of sea water warming. Thus, the temperature preference of a species can be more accurately predicted if seasonal distributions are available. However, since data on seasonal distributions of the majority of marine fishes and invertebrates are lacking, predictions of seasonal distributions have to be based on some simple, but sensible, assumptions that allow application to a wide range of species. This is essentially the objective of this study.

This paper documents an algorithm to predict seasonal changes in distributions of mobile marine fishes and invertebrates. The algorithm based on simple assumptions of correlation between seasonally (summer and winter) changes in species' north-south latitudinal boundaries and fluctuation in sea water temperature. We apply the algorithm to predict distributions of commercially-exploited pelagic fishes and invertebrates. We illustrate the results from the algorithm with examples, and we discuss its *pros* and *cons* and its potential applications.

METHODS

We developed an algorithm that can predict the seasonal distribution of marine pelagic fishes and invertebrates. This algorithm was modified from the species distribution prediction model presented in Close *et al.* (2006). The details of the algorithm, together with its theoretical basis and assumptions, are summarized in the followings:

We assume that the north-south latitudinal limits of species' geographic ranges change according to ocean temperature in different seasons. The monthly average sea surface temperature data from 1956 to 2006 was obtained from Met Office Hadley Centre observation datasets (Rayner *et al.* 2007). The average annual sea surface temperature data within this period were computed. Two seasons were considered: summer and winter. In the northern hemisphere, summer includes July to September and winter includes January to March. On the other hand, Austral summer and winter are January to March and July to September, respectively. Globally, average sea water temperature at each latitudinal zone increases in summer and decreases in winter. As highly mobile fishes and invertebrates generally attempt to occupy regions with their preferred sea water temperature, we assume that their southern range boundaries move northward in summer to avoid the excessive temperatures near the southern boundary. In winter, their northern range boundaries move southward to avoid sea water temperature at the northern boundary being under the species' physiological limits. Also, the contrast between summer and winter temperature increases towards higher latitude (Figure 1). Thus, the extent of seasonal shifting in

north-south range boundaries should be higher in higher latitude as species must migrate further in higher latitude to maintain similar temperature in their surrounding water.
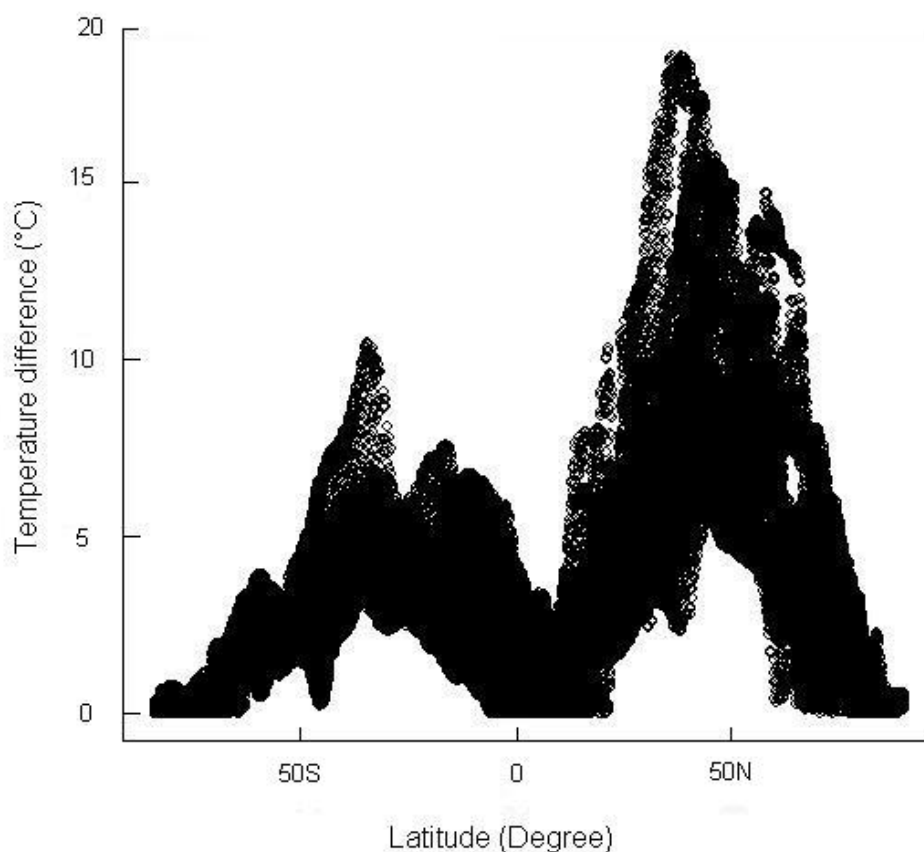
Figure 1. Magnitude of the change in sea surface temperature between summer and winter latitude.

We assume that the centroid of the distribution range also shifts according to temperature. Theoretically, the centroid of a species distribution range generally overlaps with regions where environmental conditions (e.g., sea water temperature) are optimal for the species (MacCall 1990). Thus, we assume that the average temperature at the latitudinal position of the centroid is close to the optimal preferred temperature of the species. We further assume that when latitudinal gradients of sea water temperature shift seasonally, the centroid of the distribution range shifts accordingly. Moreover, the mid-point between the centroid of the distribution range and the north/south range boundary shifts according to temperature. Predicting the seasonal shift in positions of the centroid, range boundaries and the mid-points centroid and range boundaries allow us to calculate seasonal distributions of the species. Longitudinal and vertical movement are not considered here, as these are not generally observed in large-scale seasonal migration patterns of pelagic marine fishes and squids.

We determined the maximum potential shift in centroid and the mid-point based on the annual average distribution of a species, and the annual and seasonal sea surface temperature with such distribution. Firstly, the latitudinal position of the centroid of species' annual average relative distribution, *C* (*Annual*), was calculated from:

$$C(Annual) = \frac{\sum\limits_{i=1}^{n} A_i \cdot L_i}{\sum\limits_{i=1}^{n} A_i} \qquad \qquad \dots 1)$$

where A_i is the species relative abundance in each spatial cell on the map, L_i is the latitudinal coordinate of the cell, and n is the total number of cells within the species' geographic range. When calculating the latitudinal position of the mid-point, we only include the cells lie within the distribution range between the centroid and northern/southern boundary. The latitudinal position of the mid-point, *MP(Annual),* was computed from:

$$MP(Annual) = \frac{\sum\limits_{i=1}^{m} A_i \cdot L_i}{\sum\limits_{i=1}^{m} A_i} \qquad \qquad \dots 2)$$

where m is the total number of cells within the distribution range between the centroid and the northern or southern boundary.

Secondly, we calculated the annual average sea surface temperature at *C(Annual)* and *MP(Annual).* The temperature at *C(Annual)* is assumed to be the optimal (preferred) temperature by the species T_a. Moreover, we calculated the average sea surface temperature within the species range by latitudinal bands (every 30') for each season (summer and winter). The latitudinal positions of the centroid in summer and winter, i.e., C_S' and C_W', respectively, were assumed to be the latitudinal bands with average temperature that was closest to the optimal preferred temperature T_a. Thus, the maximum potential shift in centroid's latitudinal position was calculated from:

$$CS_s' = \left| C_S' - C(Annual) \right|$$
$$CS_w' = \left| C_W' - C(Annual) \right| \qquad \qquad \dots 3)$$

where CS_s ' and CS_w' are the maximum potential shift in centroid's latitudinal positions in summer and winter, respectively. The latitudinal position of the mid-point in summer and winter i.e., MP_S' and MP_W', were assumed to be the latitudinal bands with temperature closest to the temperature at *MP(Annual).* In summer, *MP(Annual)* was calculated from the latitudinal values of the centroid and the southern bound i.e. MP_S. In winter, MP(Annual) was calculated from the latitudinal values of the centroid and the northern bound i.e. MP_W. The maximum potential shift in the latitudinal position of the mid-point was calculated from:

$$MS_S' = \left| MP_S' - MP_S \right|$$
$$MS_W' = \left| MP_W' - MP_W \right| \qquad \qquad \dots 4)$$

where MS_s' and MS_w' are the maximum potential shift in the latitudinal positions of the mid-point in summer and winter, respectively.

The actual shifts in latitudinal positions of the centroid and the mid-point were determined by the motility of the species. Species' motility was represented here by a 'motility index' (*MI*). This index was calculated by using a fuzzy logic expert system that determines species' motility from species' maximum body length and aspect ratio of caudal fin (i.e., the ratio between the square of the height of fish's caudal fin to the caudal fin area) (Cheung *et al.* this vol.). As aspect ratio is not

available for invertebrates, ordinal levels representing the motility (Sedentary = 1; Low motility = 2; motility = 3; motility = 4) was assigned for each species (see Cheung *et al*. this vol. for details). The calculated motility index scales from 0 to 100. Higher index value indicates higher motility, i.e., higher ability to move, and *vice versa*.

Combining the estimated maximum potential centroid shift and the motility index, we determined the actual seasonal shift in centroid of species distribution range:

$$CS' = CS \cdot \frac{MI}{100} \qquad \qquad \dots 5)$$

where CS' is the actual shift in centroid of the distribution range (in degree) and MI is the motility index. Similarly, the actual seasonal shift in the mid-point was calculated by:

$$MS' = MS \cdot \frac{MI}{100} \qquad \qquad \dots 6)$$

where MS' is the actual shift in the latitudinal position of the mid-point (in degree).

Species' latitudinal range limits shifted according to the seasonal shifts in centroid and the mid-point. The latitudinal limits delineated the maximum latitudinal range of the species. Thus, the northern and southern range limits should represent the occurrence limits in summer and winter respectively. We assume that the actual shift in the range boundaries of the species (*AS*) is the average of the actual shift in the latitudinal positions of the centroid and the mid-point. This value was calculated as:

$$AS = \frac{(CS' + MS')}{2} \qquad \qquad \dots 7)$$

For species with motility index equal to 100, the northern and southern boundaries of the species will change by the average latitudinal shift of the centroid and the mid-point. In summer, a species moves northward within its total distribution range.

Thus, in the northern hemisphere, the southern range limits would shift northward in summer and the northern range limits would shift southward in winter. The northward shift in southern range limit in summer is calculated from:

$$SL' = SL + AS \qquad \qquad \dots 8)$$

where SL' is the latitude of the southern bound in summer, SL is the latitude of the original southern bound and *AS* is the actual shift in distribution range in summer.

Similarly, southward shift in winter in the northern range limit was calculated by:

$$NL' = NL + AS \qquad \qquad \dots 9)$$

where NL' is the latitude of the northern bound in winter, NL is the latitude of the original northern bound. A schematic diagram of the simulation of range shifting is illustrated in Figure 2.

The calculated seasonal latitudinal boundaries were then used to generate geographic distribution for pelagic fishes and invertebrates using the method documented in Close *et al*. (2006).
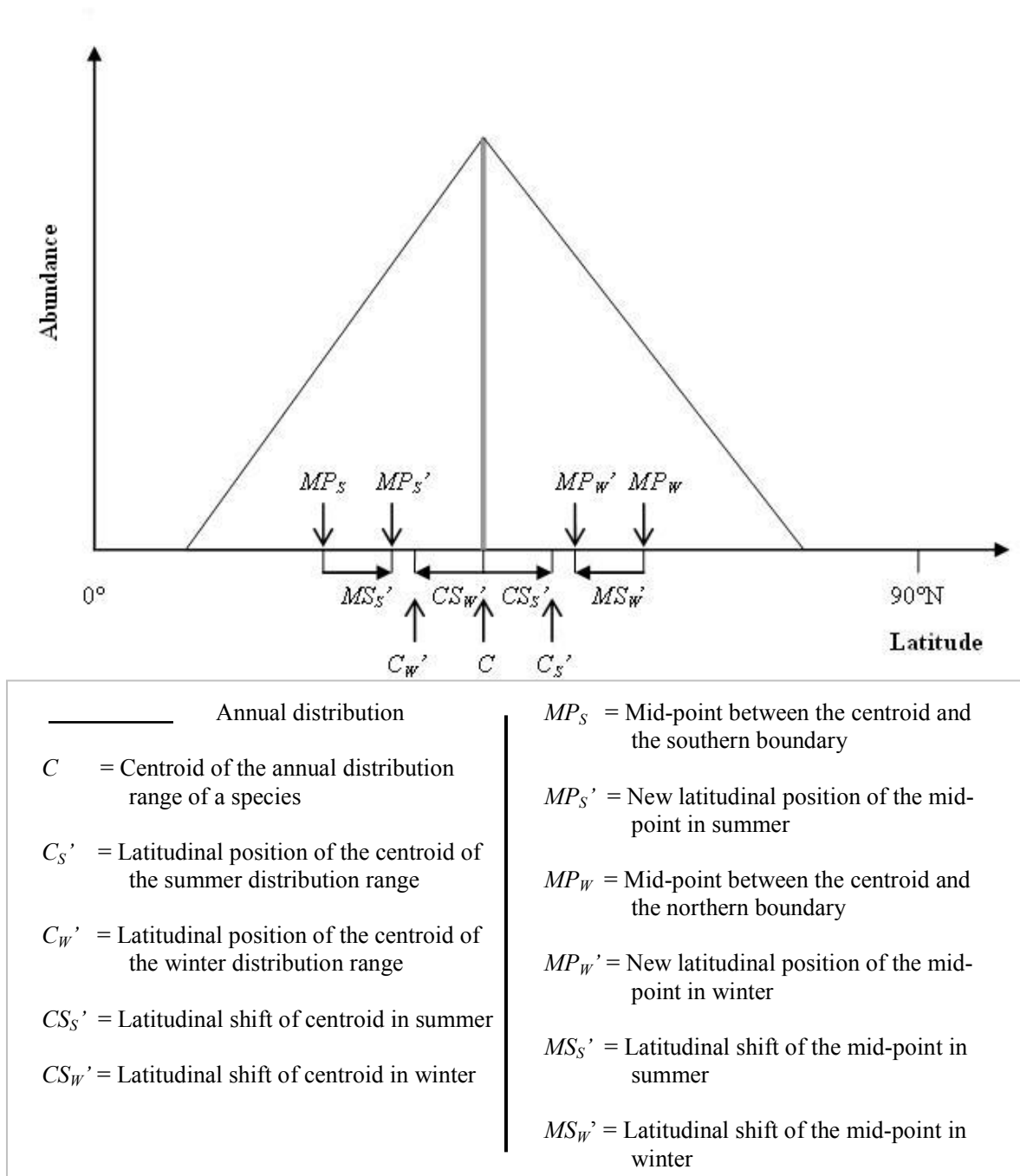
Figure 2a. Schematic diagram showing latitudinal shift in centroid and the mid-point of the distribution range between the centroid and the northern/southern boundary (see text).
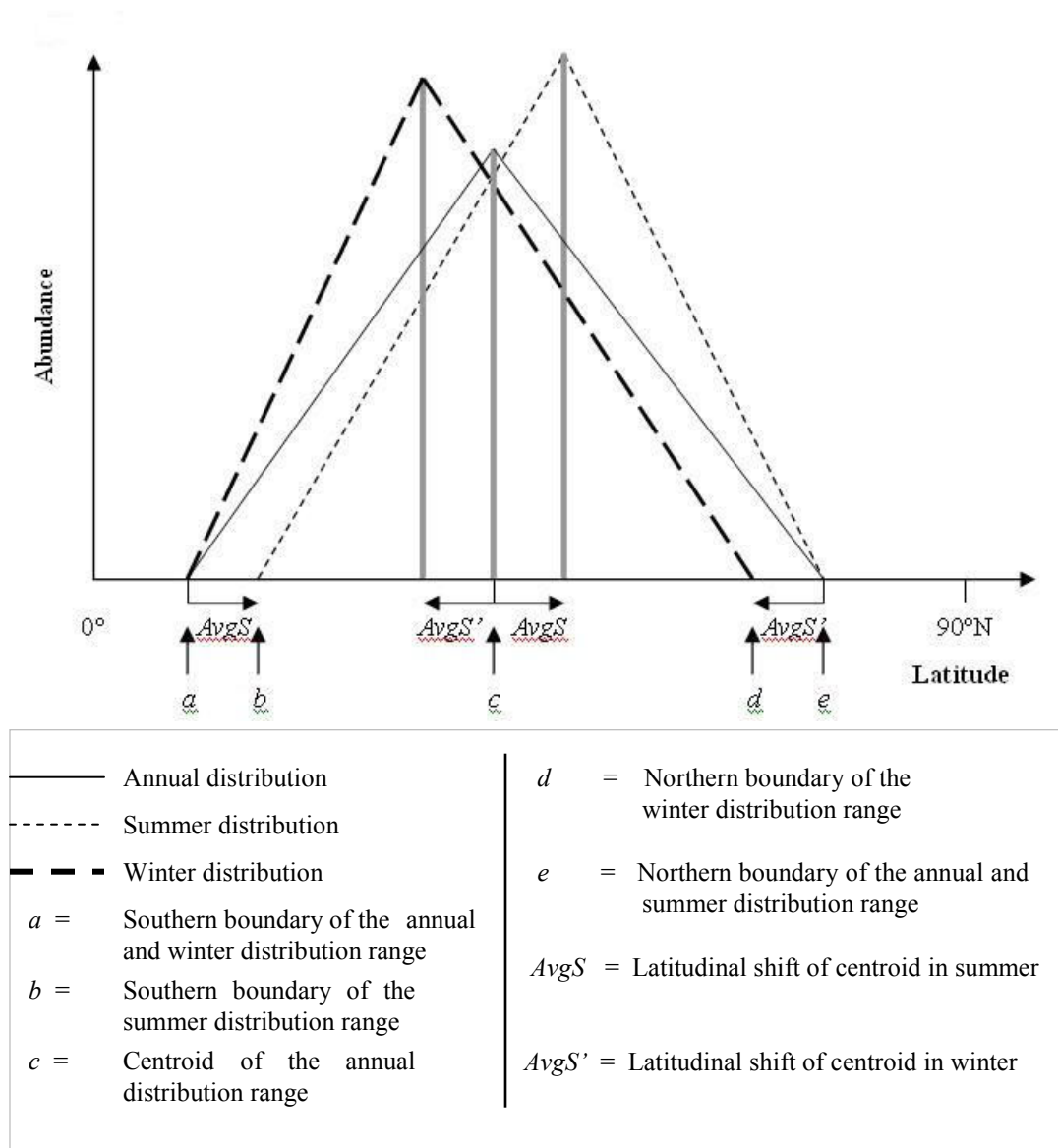
Figure 2b   Schematic diagram showing latitudinal shift in the distribution range (see text).

RESULTS

In the Northern hemisphere, the distribution of species shifts to the northern part of their ranges in the summer, whereas the species move to the southern part of their ranges in the winter (and conversely in the Southern hemisphere). The extent of the summer movement may not be necessarily the same as that of the winter movement. Species with longer bodies and higher aspect ratio have a higher capability of shifting to the extreme ends of their ranges with changes in seasonal temperature. Species with smaller bodies and lower aspect ratio of their caudal fin, have a lower motility and their distribution ranges remain more or less the same in summer and winter. We illustrate these general results in the following case studies.

Common dolphinfish (*Coryphaena hippurus*)

The annual distribution range of common dolphinfish extends from 45°N to 38°S. Our model predicted the northward shift of southern boundary of common dolphinfish from 38°S to 30°S in summer and the southward shift of the northern boundary from 45°N to 41°N in winter (Figure 3). In the northern summer, the species migrates largely to the northern hemisphere. On the other hand, the southern boundary extends back into the southern hemisphere in the northern winter while the northern boundary moves slightly southward, e.g. to avoid the cold temperature of the Adriatic Sea in winter.

Common dolphinfish has a high motility index, (= 100), Thus, the shift in boundaries is equal to the entire latitudinal shift of the centroid.
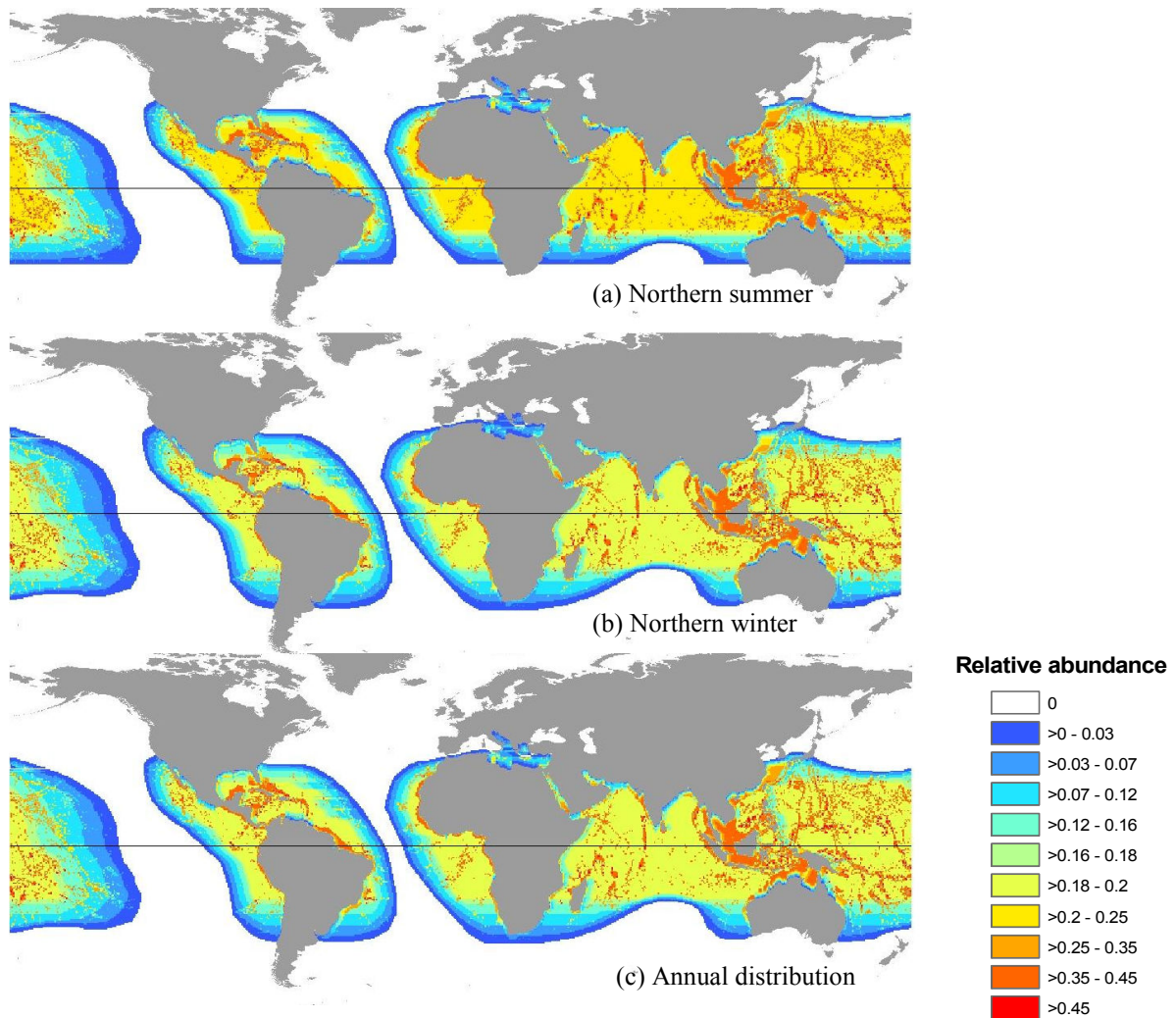
Figure 3. Shift in distribution range of Common dolphinfish in different seasons. (a) Southern boundary shifts northward in summer (b) Northern boundary shifts southward in winter (c) annual distribution range. The straight line on each map marks the equator.

Serra Spanish mackerel (*Scomberomorus brasiliensis*)

This species which has a high motility index (= 77) is distributed along the Caribbean and Atlantic coasts of Central and South America from Belize to Rio Grande do Sul, Brazil. The latitudinal range of its annual distribution extends from 20°N to 35°S. Our model predicts that the southern boundary shifts from Rio Grande do Sul to northern coast of Santa Catarina region, Brazil (28°S) in northern summer (Figure 4). In northern winter, the northern boundary shifts from Belize to Nicaragua (13°N).

(a) Northern summer

(b) Northern winter

(c) Annual distribution

Relative abundance

	0
	>0 - 0.04
	>0.04 - 0.08
	>0.08 - 0.15
	>0.15 - 0.2
	>0.2 - 0.27
	>0.27 - 0.35
	>0.35 - 0.5
	>0.5 - 0.75
	>0.75 - 1.8
	>1.8
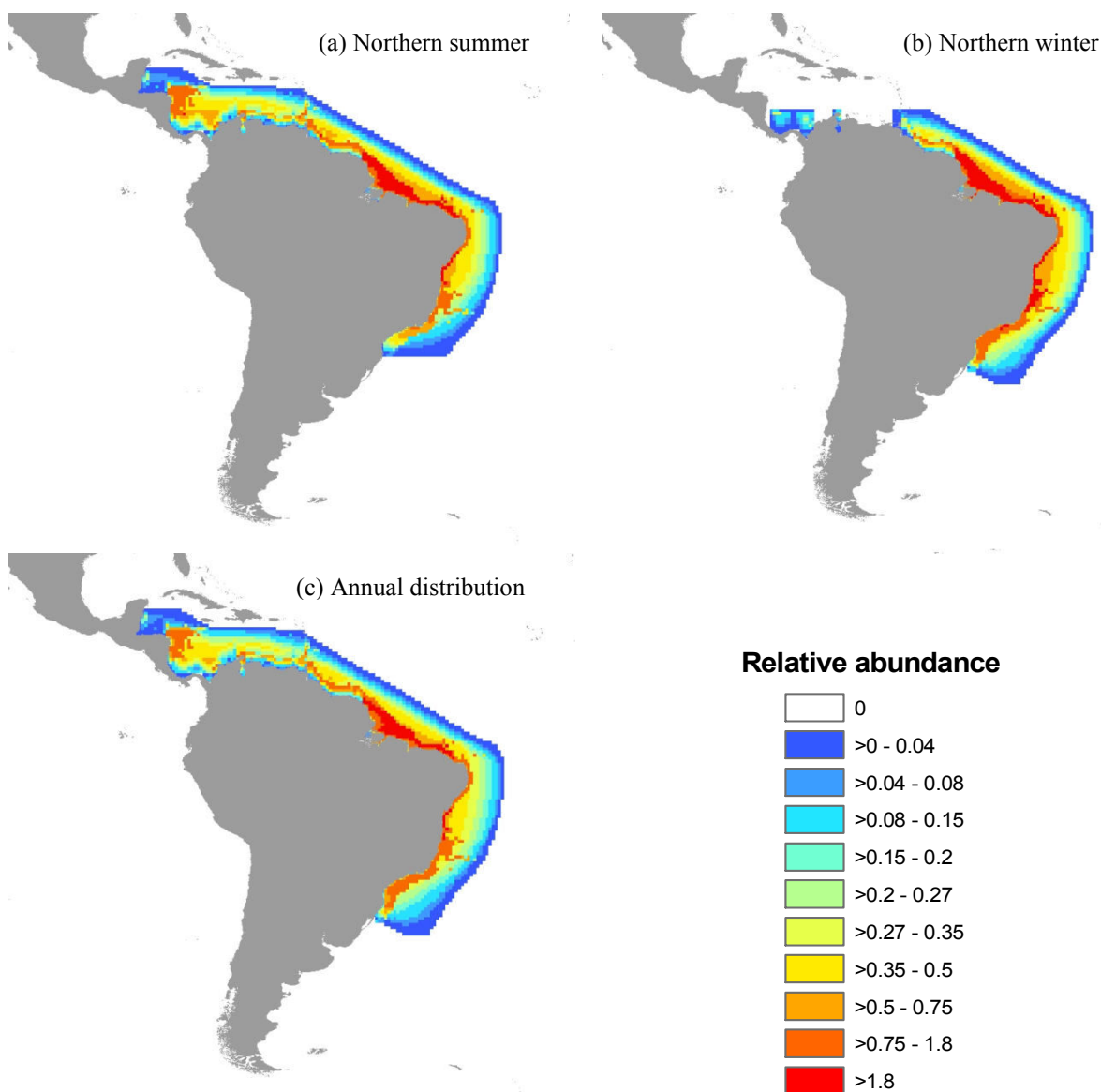
Figure 4. Shift in distribution range of Serra Spanish mackerel in different seasons: (a) southern boundary shifts northward in summer, (b) northern boundary shifts southward in winter, and (c) annual distribution range.

Plain bonito (*Orcynopsis unicolor*)

The plain bonito (motility index = 80) occurs only in the northern hemisphere; its distribution range extends from Bay of Biscay (49°N) to Dakar, Senegal (14°N) (Figure 5). To avoid the excessive summer temperature near the equator in northern summer, the species' southern boundary shifts northward from Dakar (14°N) to the south of Morocco (22°N). In northern winter, the centroid of the distribution shifts southward from south coast of Portugal to the coast of Morocco.
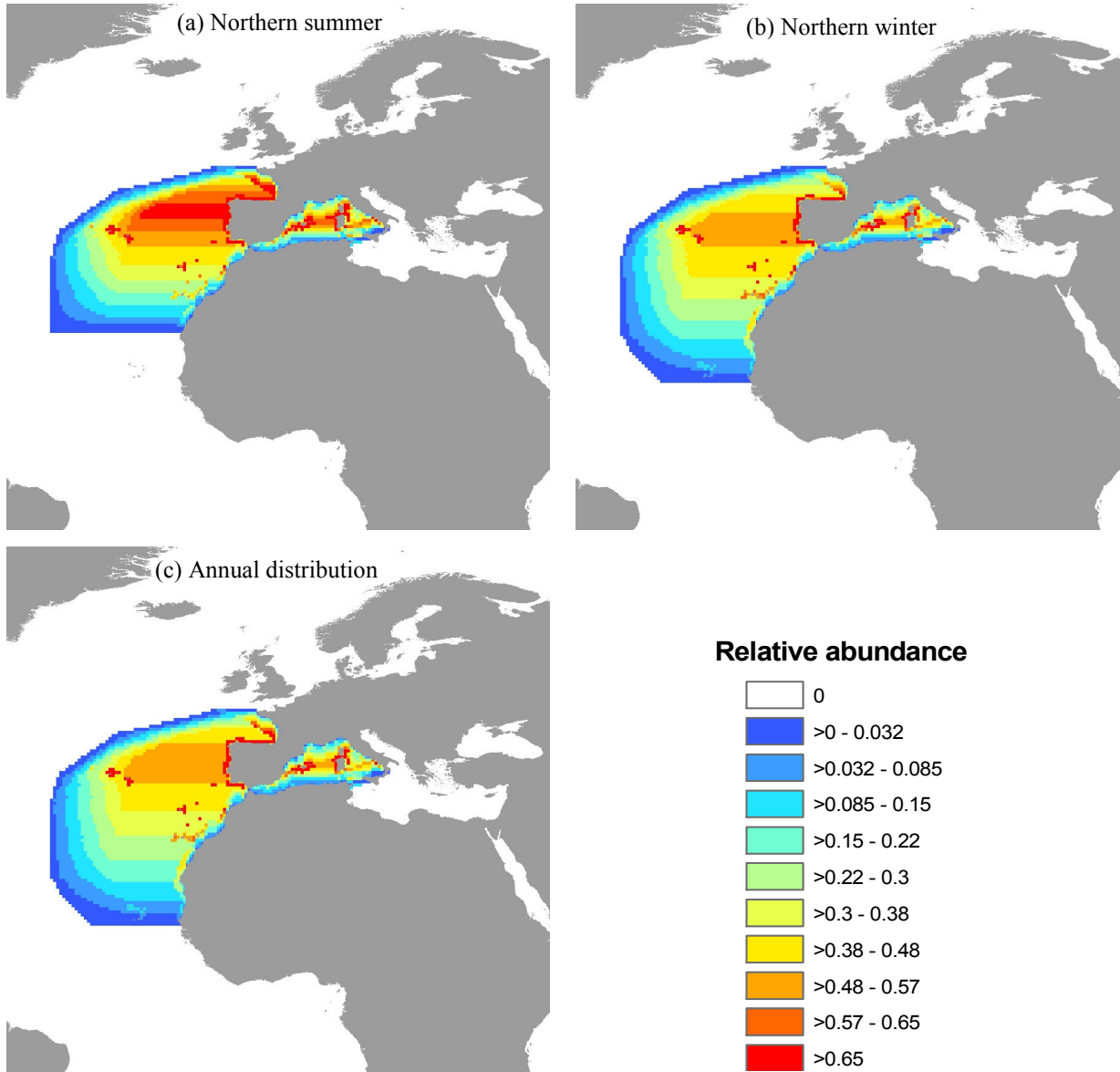
Figure 5. Shift in distribution range of Plain bonito in different seasons: (a) southern boundary shifts northward in summer, (b) northern boundary does not change in winter, and (c) annual distribution range.

DISCUSSION

The distribution ranges of all pelagic fishes and squids are largely dependent on seasonal variations of sea surface temperature (SST). Each species has a specific range of temperature over which the population remains viable. The seasonal migration of these species can be viewed as a strategy to maximize fitness in different seasons (Alerstam *et al.* 2003). Thus, if possible, the species may move to area where water temperature remains within their preferred range. However, long-range migration may not be possible for all species because of limitations in motility. Of the over 1,200 species considered in this study, 116 pelagic species have motility index equal to zero, too low for any seasonal migration to be visible at the scale of this study (i.e., 30' lat. x 30' long.).

The predicted seasonal distributions corroborate with observed seasonal migration patterns of the studied species. Common dolphinfish (*Coryphaena hippurus*) shows seasonal abundance in many tropical and subtropical areas (Massuti & Morales-Nin, 1994, Kraul, 1998). For example, catch records of common dolphinfish show that the adult migrates northward during spring and summer from their wintering grounds in the tropical areas of Atlantic Ocean (Massuti & Morales-Nin, 1994). The species reaches its peak abundance in October in the Mediterranean and decreases again from late November. Many authors suggest that temperature is the controlling factor for the seasonal migration of common dolphinfish and the shift between north and south is correlated with the 23°C isotherm (Kraul, 1998). This 23°C isotherm approaches 36°N in August but goes down to 19°N in February (Kraul, 1998). Some studies also suggest that the peak abundance of Common dolphinfish is found in area with SST of about 25 – 28°C (Massuti & Morales-Nin, 1994). These agree with the temperature preference and migration patterns predicted from our model.

A good match between observed and predicted seasonal migration pattern can also be found in serra (*Scomberomorus brasiliensis*) in northeastern Brazil. The abundance of serra increases along the Brazilian coast in March, but decreases continuously throughout July, August and September (Batista & Fabre, 2001). These observations agree with our model prediction, in which the southern boundary of the distribution range of serra shifts northward in summer. On the other hand, its distribution shifts to the northern part of its range in summer (July to September).

The accuracy of the predicted seasonal distributions of pelagic species can be affected by other factors that can impact on the seasonal migration pattern of the species. A major assumption of our model is the importance of sea water temperature in determining seasonal migration patterns. However, other factors such as food availability, salinity, rainfall and current might also play an important role in the seasonal distribution pattern of species. Williams and Newell (1957) finds that the abundance of Common dolphinfish becomes high when the SST reaches 29°C along with low salinities, while its high abundance may also be due to the seasonal plankton. Moreover, oceanographic condition could affect spawning and migratory patterns of the species (Massuti and Morales-Nin 1995). However, given the global focus of our model, the large number of species from a wide range of groups that the model has to handle, and the limited availability of data for most of these species, the approximations in our model are unavoidable. Furthermore, model predictions appear to agree with the observed patterns of seasonal movement of pelagic species. In addition, the predicted seasonal distributions narrow the Temperature Preference Profiles (TPP) predicted from the maps of distribution range and sea water temperature. These predicted TPP are fundamental to the dynamic bioclimate envelope model developed to study the effects of climate change on distribution ranges of marine fishes and invertebrates (see Cheung *et al.* this vol.).

In conclusion, marine pelagic species and squids shift to the northern or southern parts of their distribution ranges in summer and winter, respectively. These species migrate to areas where SST is optimal (or at least suitable) for their survival and reproduction. Predictions from the model can help us to understand the fluctuation in seasonal catch of marine pelagic species.

REFERENCES

Alerstam, T., Hedenström, A., Åkesson, S. 2003. Long-distance migration: evolution and determinants. *OIKOS* 103, 247 – 260.

Batista, V. da S., Fabré, N. N. 2001. Temporal and spatial patterns on serra, *Scomberomorus brasiliensis* (Teleostei, Scombridae), catches from the fisheries on the Maranhão coast, Brazil. Brazilian Journal of Biology 61(4), 541 – 546.

Buxton, C. D., Smale, M. J. 1989. Abundance and distribution patterns of three temperate marine reef fish (Teleostei: Sparidae) in exploited and unexploited areas off the southern Cape coast. Journal of Applied Ecology 26, 441 – 451.

Close, C., Cheung, W. W. L., Hodgson, S., Lam, V., Watson, R., Pauly, D. 2006. Distribution ranges of commercial fishes and invertebrates. In: Palomares, M. L. D., Stergiou, K. I., Pauly, D. (eds). Fishes in Databases and Ecosystems. Fisheries Centre Research Reports 14 (4). Fisheries Centre, University of British Columbia, Vancouver, p 27 – 37.

Hutchins, L. W. 1947. The bases for temperature zonation in geographical distribution. Ecological Monographs 17(3), 325 – 335.

Kraul, S. 1999. Seasonal abundance of the dolphinfish, *Coryphaena hippurus*, in Hawaii and the tropical Pacific Ocean. Scientia Marina 63(3 – 4), 261 – 266.

Lu, H. J., Lee, K. T., Lin, H. L., Liao, C. H. 2001. Spatio-temporal distribution of yellowfin tuna *Thunnus albacares* and bigeye tuna *Thunnus obesus* in the Tropical Pacific Ocean in relation to large-scale temperature fluctuation during ENSO episodes. Fisheries Science 67, 1046 – 1052.

MacCall, A.D. 1990. Dynamic geography of marine fish populations. University of Washington Press, 153p.

Massuti, E., Morales-Inn, B. 1995. Seasonlity and reproduction of dolphin-fish (*Coryphaena hippurus*) in the Western Mediterranean. Scientia Marina 59(3-4), 357 – 364.

Pauly, D. 1994. Un mécanisme explicatif des migrations des poisons le long des côtes du Nord-Quest africain, p. 235 – 244. In: M. Barry-Gérard, T. Diouf and A. Fonteneau (eds.) L' évaluation des resources exploitables par la pêche artisanale sénégalaise. Tome 2. Documents scientifiques présentés lors du symposium, 8 – 13 février 1993, Dakar, Sénégal. ORSTOM Éditions, Paris, 424 p.

Pörtner, H. O., Berda, B., Blust, R., Brix, O., Colosimo, A., De Wachter, B., Giuliani, A., Johansen, T., Fischer, T., Knust, R., Lannig, G., Naevdal, G., Nedenes, A., Nyhammer, G., Sartoris, F. J., Serendero, I., Sirabella, P., Thorkildsen, Zakhartsev, M. 2001. Climate induced temperature effects on growth performance, fecundity and recruitment in marine fish: developing a hypothesis for cause and effect relationships in Atlantic cod (*Gadus morhua*) and common eelpout (*Zoarces viviparus*). Continental Shelf Research 21, 1975 – 1997.

Rayner, N.A., Parker, D. E., Horton, E. B., Folland, C. K., Alexander, L. V., Rowell, D. P., Kent, E. C., Kaplan, A. 2007. Global analysees of sea surface temperature, sea ice, and night marine air temperature since the late nineteenth century. J. Geophys. Res. Vol. 108, No. D14, 4407 10.1029/2002JD002670 (www.metoffice.gov.uk/hadobs. Accessed on October 16, 2007)

Williams, F., Newwll, B. S. 1957. Notes on the biology of the dorade or dolphin-fish (*Coryphaena hippurus*) in East African waters. East African Agricultural Journal 23(2), 113 – 118.

CHAPTER 3

ASYMMETRY IN LATITUDINAL, LONGITUDINAL AND BATHYMETRIC DISTRIBUTION OF MARINE FISHES AND INVERTEBRATES[3]

Daniel Pauly, William W. L. Cheung, Chris Close, Sally Hodgson, Vicky W.Y. Lam and Reg Watson

Sea Around Us Project, Fisheries Centre, Aquatic Ecosystems Research Laboratory, 2202 Main Mall, The University of British Columbia, Vancouver, British Columbia, Canada. V6T 1Z4.

ABSTRACT

The distribution ranges of organisms, and marine animals in particular, are a manifestation of their environmental requirements, although they are often modified by the dynamics of prey and predators. Distribution range maps can also be used to infer where an activity occurs which requires the presence of a set of species, e.g., a fishery which targets them.

The distribution of marine fishes and invertebrates serves as the basis for the mapping of fisheries by the *Sea Around Us* Project. Thus, accurate range maps are extremely important, and an earlier contribution by Close *et al.* (2006; FCRR 14(4): 27-37) reviews the step-by-step approach, and the assumptions used to predict the distribution of relative abundance of marine fishes and invertebrates from broad geographical limits, e.g., ocean basins, latitudinal limits, depth limits, etc., to relatively narrow polygons surrounding a number of ½ degree lat.-long. cells.

Once established, such distributions, at least those referring to demersal fishes and invertebrates, can be interfaced with a map of sea bottom temperature, and inferred temperature preference profiles (TPP). These can be used, among other things, to verify the distribution ranges as predicted distributions should generate unimodal TPP, with the bulk of the distributions spanning a narrow range of temperature (~10° Celsius).

As a relatively large fraction of the TPP that we obtained at first appeared bimodal, or exhibited a strong kurtosis, the assumption was revisited that the distribution of a species with regard to latitude can be simulated by an equal-sided triangle. It is shown here, for the cod (*Gadus morhua*), and generally for all our over 900 demersal species, that assuming a skewed triangular distribution, whose degree of skew is proportional to the temperature gradient from low to high latitude, generates more realistic distributions when compared to observed species distribution maps, although the narrowing of the uni-modal temperature probability distributions is relatively small. This correction will be implemented in all distribution ranges of demersal fishes and invertebrates in the *Sea Around Us* database, and used for catch allocation, and inferences on climate shifted distributions due to climate change.

---

[3] Cited as: Pauly, D., Cheung, W.W.L., Close, C., Hodgson, S., Lam, V.W.Y. and Watson, R., 2008. Asymmetry in latitudinal, longitudinal and bathymetric distribution of marine fishes and invertebrates, p. 63-72. *In*: Cheung, W.W.L, Lam, V.W.Y., Pauly, D. (eds.) Modelling Present and Climate-shifted Distribution of Marine Fishes and Invertebrates. Fisheries Centre Research Report 16(3). Fisheries Centre, University of British Columbia [ISSN 1198-6727].

INTRODUCTION

The distribution range of organisms is, besides their size, the feature that is most informative about their biology. Size largely determines the kind of prey and predators which that organism can have (Pauly & Christensen 2002). The distribution, on the other hand, informs us of the temperature, depth, seasonality, etc., in which they are equipped to live (Helfman *et al.* 1997).

Distribution ranges are also used for practical purposes. In the *Sea Around Us* Project, predicted distribution ranges are used to map fisheries catches (Watson *et al.* 2004). As fisheries maps can be improved by the underlying fish distribution ranges, the *Sea Around Us* Project has worked continuously at improving these ranges, and the last version of the predicted distribution ranges are all available at (www.seaaroundus.org). In Close *et al. (*2006), we reviewed the methods and assumptions used therein, which can be seen as a set of filters:

1) FAO area: the fish and invertebrates covered in the *Sea Around Us* database are assigned (or were pre-assigned by FishBase, or FAO) to one or several of the 18 FAO area where they occur;

2) Latitudinal range: defined by the northern and southern limits of the distribution, whose relative abundance distribution is assumed to be triangular, with a maximum at the latitude midrange (i.e., symmetry is assumed; see below);

3) Range limiting polygon: originating from various sources, and preventing the range from 'spilling over' into water bodies which satisfy (1) and (2), but which are known to have attributes preventing them from being part of the distribution (e.g., low salinities);

4) Depth range: defined by shallow and deep limits, with the density of the distribution in between represented by an asymmetrical triangular distribution, with a maximum at 30% of the depth range, thus accounting for larger depth-related changes in shallow than in deep water. Also, we correct for some of 'equatorial submergence' (Ekman 1967) not discussed here, except to mention that this effect is also assumed to be asymmetrical with regard to depth;

5) Assignment with regard to habitats (shelves, estuaries, seamounts, etc.). This is not further discussed because this does not concern the point to be made here.

These procedures lead to distribution range maps from which various inferences can be drawn, notably the temperature preference of the fish, since temperature is not used directly in any step in this process. Thus, when distribution ranges are mapped onto a temperature atlas, a temperature preference profile (TPP) can be inferred whose mode should indicate the preferred temperature of the animal in question, while the flanks indicate the normal temperature range of the species (see Figure 1, for an example).
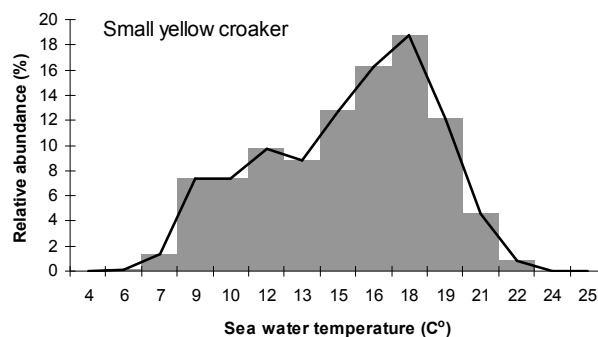
Figure 1. A temperature preference profile (TPP) of the Small yellow croaker (*Larimichthys polyactis*, Sciaenidae) inferred from the predicted species distribution and sea bottom temperature (the latter obtained from Met Office Hadley Centre observations datasets; http://hadobs.metoffice.com/hadisst/).

However, a large number of TPP obtained by this method are bi- or multi-modal, while another set of TPP displays extreme kurtosis. Such patterns are not realistic, because marine fish and

invertebrates usually have one temperature optimum, i.e., one mode in a more or less symmetrical, bell-shaped distribution with regard to temperature (Coutant 1987).

We have examined which of the above steps and assumptions of the method of Close *et al.* (2006) could generate these bi- or multi-modal TPP, and identified Step 2 and 3 above, i.e., the assumptions of symmetrical triangular distribution with respect to relative abundance along latitudes, and abruptly-cut range boundary imposed by polygons, respectively, as the likely culprit.

First, the latitudinal distribution of relative abundance should be asymmetrical (step 2). As the underlying environmental variables which affect distribution range are unevenly distributed, uneven gradients of density of animals should be observed (MacCall 1990). For marine ectotherms, temperature is one of the most important parameters affecting their distributions (Coutant 1987; Pörtner 2001). Thus, the assumption of a symmetrical triangular distribution which is probably correct at low latitudes, where the isotherms are widely spaced, would become incorrect at higher latitudes (around 40° N/S), where the isotherms are close to each other (Figure 2).

To represent such asymmetry in latitudinal-temperate gradient, instead of the symmetrical triangular distribution described in Close *et al.* (2006), we should employ asymmetrical triangular distribution, with the degree of skewness being a function of the closeness of the latitudinal isotherms.

Also, range boundaries should not be abruptly cut (Step 3). This problem arises when portions of the potential distribution ranges are excluded by polygons that are constructed from known distribution range of the species. Thus, relative abundance at the edge of the distribution range may become discontinuous in terms of the environmental gradients. However, such abrupt change in abundance at boundary of a range is rarely observed in the sea. This phenomenon is particularly apparent for pelagic species whose predicted distribution ranges are strongly affected by the polygons. Thus, a gradient of relative abundance should be applied to the polygon boundary to make the predicted distribution range more realistic.
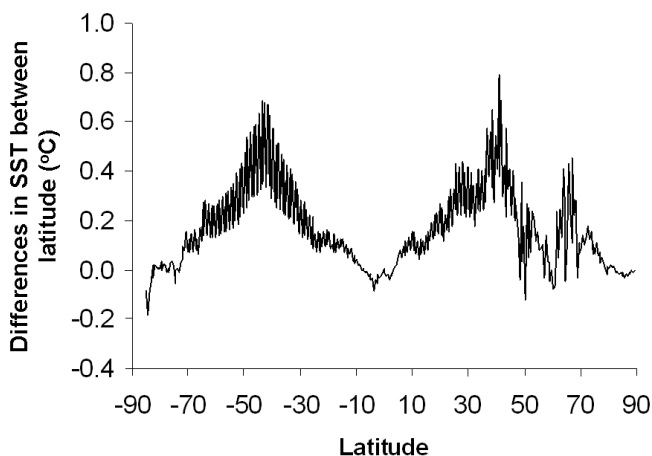
Figure 2. Differences in sea surface temperature between latitudinal zones of the world ocean.

This paper describes the algorithms that improve on the above two assumptions in predicting species distribution range, i.e., latitudinal asymmetry in relative abundance distribution and gradient of relative distribution at range boundaries. We compare the predicted distribution ranges and TPP of selected species to evaluate the effects of implementing the new algorithms.

METHODS

Latitudinal asymmetry

The distribution of relative abundance along latitude was assumed to be triangular-shaped and the mode (peak) of the triangular distribution was assumed to be determined by the steepness of the latitudinal-temperature gradient at range limits. To determine the latitudinal position of the peak, we first constructed a profile of temperature-gradient index (Figure 3a and b for the northern and southern hemispheres, respectively) approximated from the observed sea surface temperature gradients (see Figure 2). The temperature-gradient index represents the marginal changes in temperature by latitude and scales from 0 to 1, with 1 indicating maximum changes in temperature. The profiles are represented by trapezoidal distribution. Latitudinal zones between 40.75° and 42.25° in the northern hemisphere and 42.25° and 43.75° in the southern hemisphere have the maximum temperature-gradient index values of 1, from where the index decreases linearly to the equator and poles (Figure 3). For example, the northern and southern latitudinal limits of Atlantic cod (*Gadus morhua*, Gadidae) are 35° and 78°. Based on the temperature-gradient index profile (Figure 3a), the corresponding temperature-gradient index values are 0.86 and 0.25, respectively.

a)
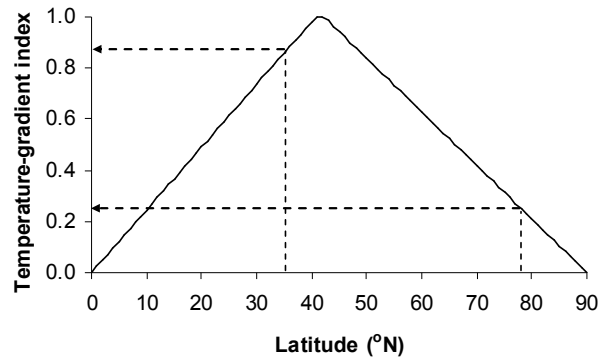
b)
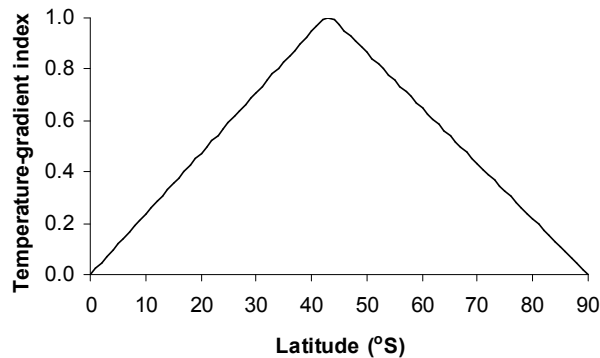
Figure 3. Temperature-gradient index by latitude in (a) northern hemisphere and (b) southern hemisphere. The broken lines on (a) indicate the northern (78°) and southern (35°) latitudinal limits of Atlantic cod.

Secondly, the degree of skewness of the triangular latitudinal-relative abundance distribution is determined by the difference in temperature-gradient index between the north and south latitudinal range margins. We assume that relative abundance declines more rapidly towards the range margin with steeper temperature gradient. The degree of skewness (*Skew*) is calculated from:

$$Skew = a - b \cdot \left[TG(L^U) - TG(L^L) \right] \qquad \text{...1)}$$

and the latitudinal position of the peak of the triangular latitudinal-relative abundance distribution is (L^P):

$$L^P = (L^U - L^L) \cdot (1 - Skew) + L^L \qquad \text{...2)}$$

where a and b are constants that determine the maximum and minimum degree of skewness; TG is a function to calculate the temperature-gradient index at the upper and lower latitudinal limits (L^U and L^L, respectively). The default values of a and b are 0.5 and 0.3, respectively. Since temperature-gradient tends to be steeper at mid-latitude (around 40° N/S), the calculated latitude-relative abundance distributions will also skewed towards the mid-latitudinal zone (Figure 4). For example, given the L^U and L^L of Altantic cod (78° and 35° N), the calculated S is 0.68 and the peak of the triangular distribution is at 48.7° N (see distribution c in Figure 4).
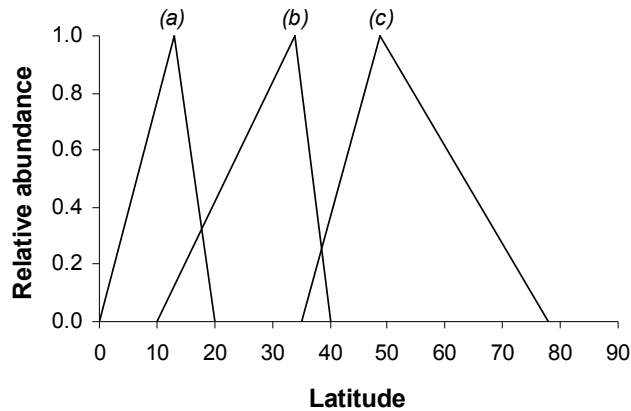
Figure 4. Asymmetric triangular relative abundance – latitudinal distributions generated from three sets of latitudinal range limits: (a) 0° – 20° N, (b) 0° – 40° N, and (c) 35° – 78° N.

This algorithm applies to distribution ranges that cover either the northern or southern hemisphere only, or across the equator with a bimodal latitudinal distribution. The latter is represented by two triangular distributions in each hemisphere which extend from the equator to its northern and southern latitudinal limits. Equatorial species with ranges covering across the equator are assumed to have a symmetrical triangular latitudinal-relative abundance distribution (Close *et al.* 2006).

Abundance gradient at polygon boundaries

We apply a gradient of abundance for distribution range boundaries of a species, as delineated by pre-specified polygons. We assume a trapezoid distribution to each segment of spatial grid within a polygon along the same latitude and longitude (Figure 5). Along a seaward polygon boundary, we assume that relative abundance declines linearly from a maximum at 1/5 of the segment length away from the boundary to zero at the boundary edge. If the polygon boundary is land-bounded, we assume a steeper relative abundance gradient that declines from 1/20 of the segment length away from the boundary edge with relative abundance being half of maximum at the boundary (see Figure 5). In addition, the minimum lengths of the gradient at seaward and landward boundaries are 10 and 5 spatial cells, respectively.

68
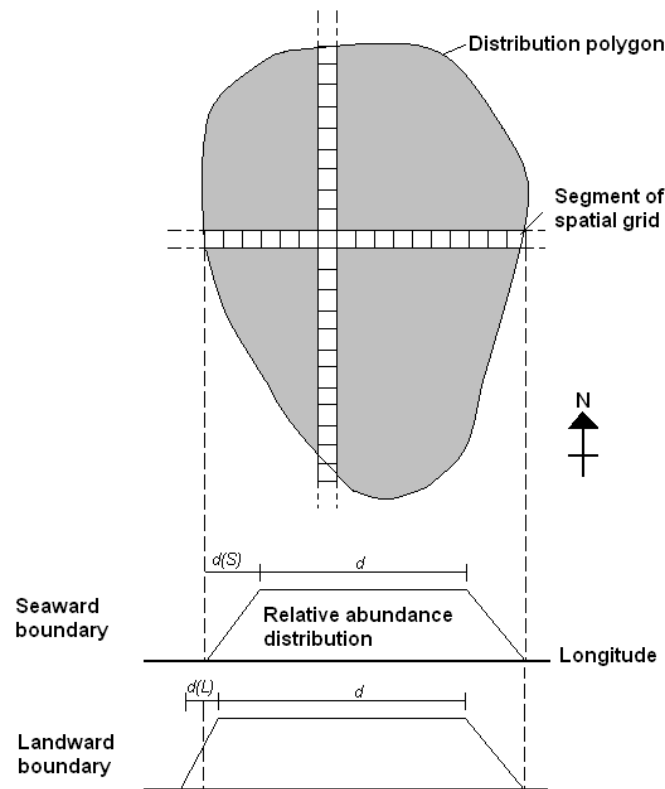
Figure 5. Schematic diagram showing the distribution of relative abundance along the same latitude with a specified polygon. The gradient of relative abundance at the boundary edge is dependent on (1) whether the edge is sea- or land- bounded, and the length of the segment (*d*). The distances *d(S)* and *d(L)* are set as 1/5 and 1/20 of *d*. Also, at the seaward boundary, the relative abundance at the edge is zero while, at the landward boundary, the relative abundance at the edge is half of the maximum relative abundance.

Application examples

To test the effects of these new assumptions, we applied the algorithms on latitudinal asymmetry and abundance gradient at polygon boundary to two species: Atlantic cod (*Gadus morhua*) and Atlantic herring (*Clupea harengus*). We generated predicted distribution maps of the two species with the original routine documented in Close *et al.* (2006) and the routine with the modified assumptions and algorithms as described above. We superimposed the distributions of Atlantic cod and Atlantic herring on maps of sea bottom and sea surface temperature, respectively (Met Office Hadley Centre observations datasets, http://hadobs.metoffice.com/hadisst/). We also constructed TPP from the two sets of maps and compared their validity based on uni-modality and variance of the TPP.

RESULTS

Based on visual inspection, the new algorithms provided a predicted distribution of Atlantic cod that appears to be a closer match to reality (Figure 6). Distribution range of cod predicted from the original Close *et al.* (2006) algorithm centers at higher latitude (Figure 6a and c). The new distribution for cod, predicted from a latitude-abundance distribution that is skewed towards lower latitude (Figure 6b and d), has centers of abundance at the Grand Bank, Newfoundland coast, southern parts of Greenland, Iceland, and around Faroe Island.
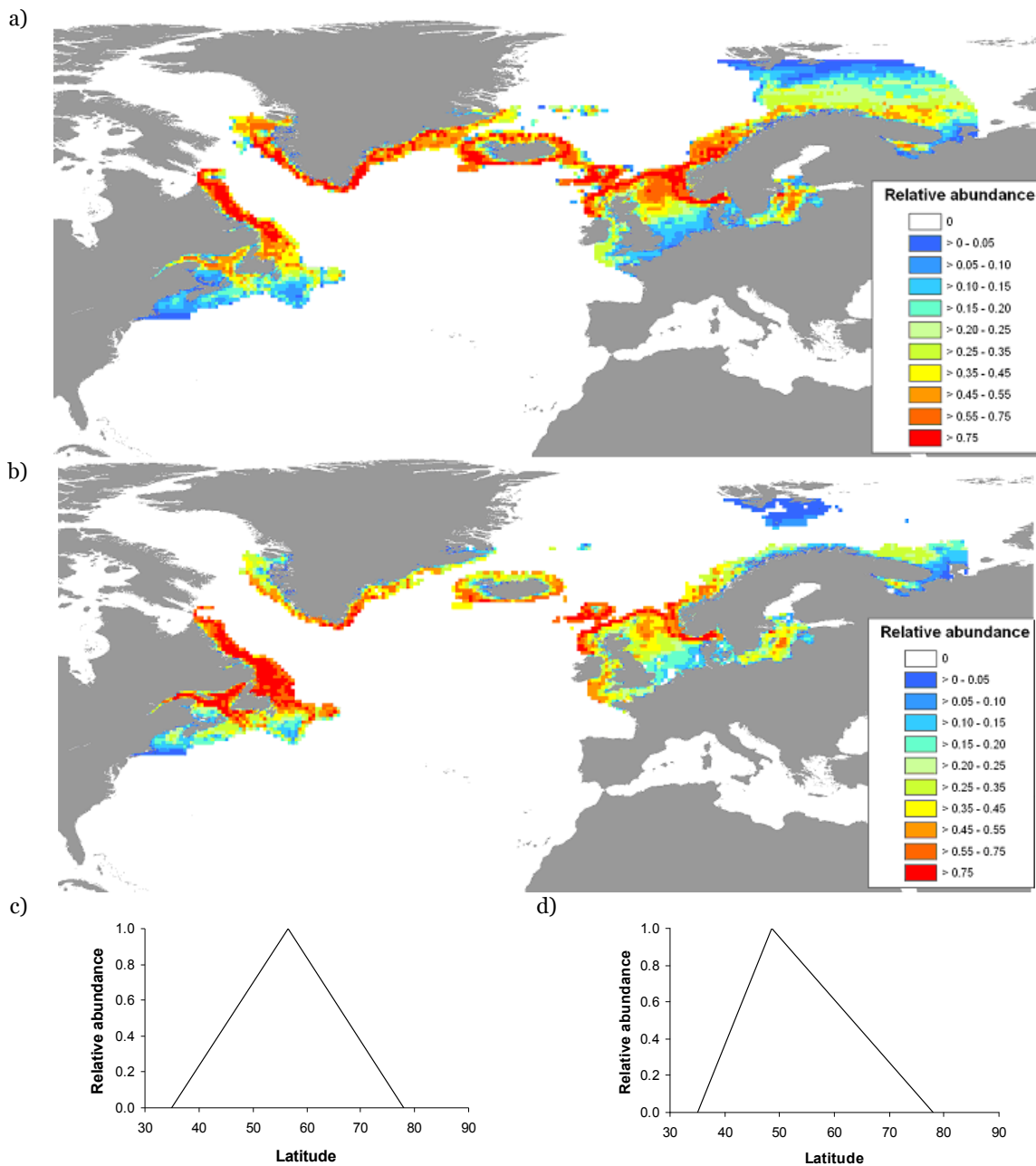
Figure 6. Predicted distribution ranges and the underlying assumptions on the latitudinal gradient of relative abundance of Atlantic cod with (a, c) symmetric triangular distribution and (b, d) asymmetric triangular distribution of relative abundance.
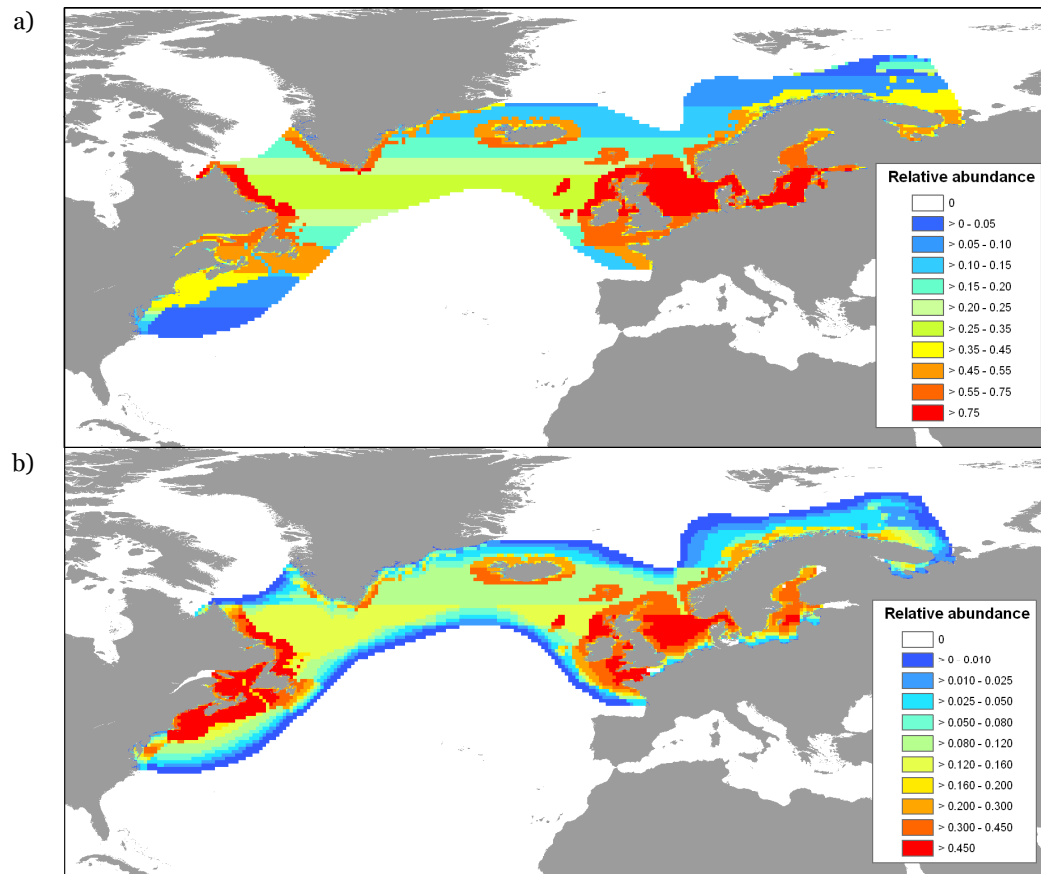
Figure 7. Predicted distribution ranges of Atlantic herring predicted with (a) the original Close *et al.* (2006) algorithm and (b) with additional assumption on abundance gradient at the edge of specified polygons.

Application of the abundance gradient at the edge of polygons eliminated the unrealistic boundary with abrupt drop in relative abundance of Atlantic herring (Figure 7). For example, adjacent to the southern coast of Iceland, the distribution range predicted from the original Close *et al.* (2006) algorithm results in an abrupt drop in relative abundance from medium level to zero at the range boundary (Figure 7a). In the case of the revised algorithm, the predicted distribution shows gradual decline in relative abundance towards the boundary edge (Figure 7b).

Temperature profiles, or TPP, obtained from the revised algorithms appear slightly more uni-modal than TPP obtained from the original Close *et al.* (2006) algorithm (Figure 8). With the revised algorithm, the relative abundance of Atlantic cod is more concentrated near sea bottom temperature of around 2 $^\circ$ C (Figure 8a), while the abundance of Atlantic herring is more concentrated at sea surface temperature of around 9 $^\circ$ C (Figure 8b).

a)

b)
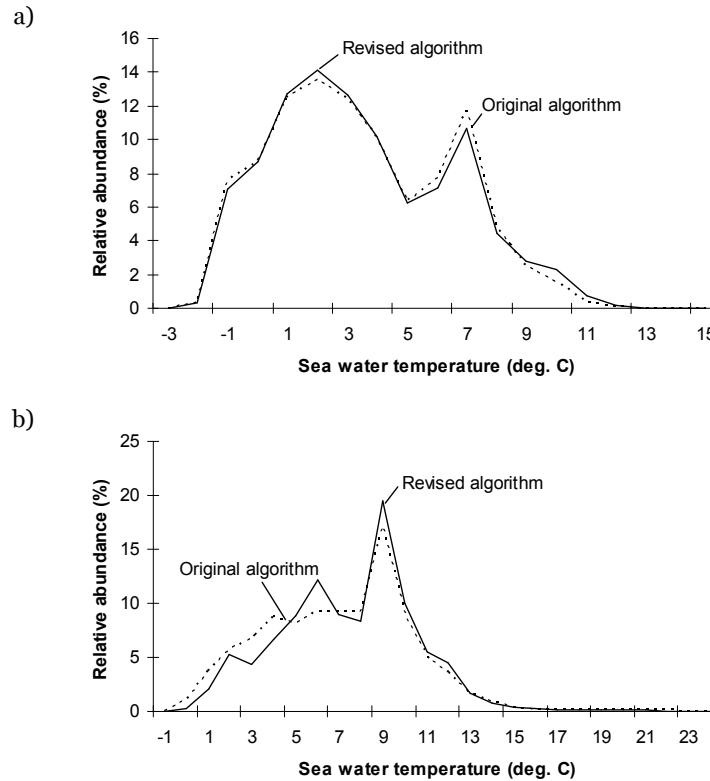
Figure 8. Temperature Preference Profile (TPP) of Atlantic cod calculated based on the distribution ranges that are predicted from the revised algorithm (solid line) and the original algorithm described in Close *et al.* (2006).

DISCUSSION

While the procedure proposed here may seem *ad hoc*, it actually corrects for an inconsistency in our treatment of distribution range maps which we had overlooked earlier. With regard to depth, we had taken asymmetry into account, i.e., we had considered that, e.g., a 10 m depth change has a much stronger effect at shallow than at great depth. The correction suggested here does the same with latitude, as a 1º change of latitude in temperate areas implies a greater change of environmental parameters (especially temperature) than in tropical areas. This correction to our distribution ranges will be fully implemented in our next catch allocation (i.e., the update from time series that end in 2004 to series ending in 2005).

Although the improvement in the predicted TPP in terms of uni-modality and variance of the distribution from considering distributional asymmetry is relatively small, the predicted distributions appear more realistic when compared to observed species distribution maps. Realistic distribution maps are pre-requisites of simulating changes in distribution range under global climate change scenarios (see Cheung *et al.* this vol. for details).

References

Close, C., Cheung, W. W. L., Hodgson, S., Lam, V., Watson, R., Pauly, D. 2006. Distribution ranges of commercial fishes and invertebrates. In: Palomares, M. L. D., Stergiou, K. I., Pauly, D. (eds). Fishes in Databases and Ecosystems. Fisheries Centre Research Reports 14 (4). Fisheries Centre, University of British Columbia, Vancouver, p 27-37.

Coutant, C. C. 1987. Thermal preference: when does an asset become a liability? Environmental Biology of Fishes 18, 161-172.

Helfman, F. S., Collette, B. B. and Facey, D. E. 1997. The Diversity of Fishes. Blackwell Science, London. 528 p.

MacCall, A.D. 1990. Dynamic geography of marine fish populations. University of Washington Press, 153pp.

Pauly, D. and V. Christensen. 2002. Ecosystem Models. Chapter 10, p. 211-227 *In:* P. Hart and J. Reynolds (eds.) *Handbook of Fish and Fisheries*. Blackwell Publishing, Oxford, Volume 2.

Pörtner, H. O. 2001. Climate change and temperature-dependent biogeography: oxygen limitation of thermal tolerance in animals. Naturwissenschaften 88(4), 137-146.